

---

## COMPARISON OF WATER USE BY *PROSOPIS* SPP AND THE CO-OCCURRING *VACHELLIA* KARROO TREES BEFORE AND AFTER CLEARING THE INVASIONS: IMPLICATIONS ON GROUNDWATER

---



REPORT TO THE

**WATER RESEARCH COMMISSION**

PREPARED BY

**Sebinasi Dzikiti<sup>1</sup>, Richard Bugan<sup>1</sup>, David le Maitre<sup>1</sup>, Zanele Ntshidi<sup>1,2</sup>,  
Abel Ramoelo<sup>1</sup>, Mark Gush<sup>1</sup>, Nebo Jovanovic<sup>1</sup>, Klaudia Schachtschneider<sup>3</sup>**

1. Council for Scientific and Industrial Research, Natural Resources and Environment

2. Department of Earth Sciences, University of Western Cape

3. WWF South Africa

WRC Report No 2256/1/18

ISBN 978-1-4312-0974-3

May 2018

**Obtainable from**

Water Research Commission  
Private Bag X03  
Gezina, 0031

[orders@wrc.org.za](mailto:orders@wrc.org.za) or download from [www.wrc.org.za](http://www.wrc.org.za)

**DISCLAIMER**

This report has been reviewed by the Water Research Commission (WRC) and approved for publication. Approval does not signify that the contents necessarily reflect the views and policies of the WRC nor does mention of trade names or commercial products constitute endorsement or recommendation for use.

Printed in the Republic of South Africa  
© **Water Research Commission**

# EXECUTIVE SUMMARY

## Motivation

Invasive alien plants are estimated to have invaded at least 10 million ha of South Africa to some degree and are spreading at about 5% per annum. The deep rooted desert adapted shrub or tree, *Prosopis* spp, is a major invader species in the arid and semi-arid parts of the country. Near the turn of the 19<sup>th</sup> century, six *Prosopis* species from Central America were introduced to Namibia and the arid parts of South Africa for fodder, fuel and shade. Here they have hybridised and spreaded rapidly. Today (2016) extensive stands of this woody weed grow in the North West-, Northern Cape-, Free State-, Western Cape- and parts of the Eastern Cape Provinces. A study by Van den Berg (2010) showed that the average annual rate of spread of *Prosopis* in the Northern Cape, for example, is very high, being approximately 15% in upland areas and up to 30% in riparian areas. The species occupied only 128 000 ha in 1974 in the Province. It then increased rapidly to over 1.5 million ha by 2007, roughly doubling between 2004 and 2007. Given the deep root system of *Prosopis*, its rapid spread poses a serious threat to groundwater and yet no detailed information currently exists on how this species interacts with groundwater in South Africa.

The aims of this study were: 1) to establish the water requirements of *Prosopis* invasions and to quantify the impacts on groundwater levels before and after clearing the invasions, and 2) to develop a remote-sensing-based model for estimating water use by invasive alien plants. The main objectives were:

1. To establish the long-term water use trends by *Prosopis* invasions and co-occurring deep rooted indigenous trees so as to determine impacts on groundwater;
2. To establish the sources of water used by the trees and to quantify the proportion of water they abstract from the saturated zone;
3. To quantify changes in groundwater levels following clearing of *Prosopis* invasions, and;
4. To evaluate and adapt a physically-based model for predicting water use in invaded arid catchments integrating *in situ* and remote sensing data.

## **Methods**

The study was conducted at a site that is densely invaded by *Prosopis* at Brandkop farm near the groundwater-dependent town of Nieuwoudtville in the Northern Cape. The site also had significant amounts of the indigenous deep-rooted *Vachellia karroo* (formerly *Acacia karroo*) trees. An accurate assessment of the impact of *Prosopis* on groundwater requires information on the incremental water use by the invasions over and above that used by the indigenous vegetation such as *V. karroo* that normally replaces *Prosopis* once it has been cleared. The study approach involved quantifying the following biophysical variables before and after *Prosopis* was cleared from the study area:

- Site microclimate;
- Transpiration rates of both *Prosopis* and *V. karroo* trees;
- Root water uptake patterns of both species;
- Stand evapotranspiration rates;
- Sources of water transpired by the trees (i.e. either groundwater or soil water);
- Profile soil water content in the root zone of each species;
- Fluctuations in groundwater levels and estimating recharge rates, and;
- Stand characteristics, e.g. leaf area index, tree density, stem size distribution and tree heights.

The data was used to quantify the vegetation-groundwater interactions at the invaded aquifer. In addition, the data was also used to calibrate and validate the MOD16 evapotranspiration (ET) model (Mu *et al.*, 2011) to establish the spatial variation in water use across the study area.

The novelty of this study resides in the fact that:

- The impact of *Prosopis* invasions on groundwater was, for the first time, assessed in detail in the arid parts of South Africa taking into account the baseline information on water use by the deep rooted indigenous trees that normally replace *Prosopis* once it has been cleared. This approach is critical when estimating potential groundwater savings that can be derived by clearing *Prosopis* invasions since indigenous trees also use groundwater.

- We improved and adapted an ET model using locally measured data from an arid catchment. Besides improvements to the model formulation (see also Dzikiti *et al.*, 2016), the model was also run at the 30 x 30 m spatial resolution for the first time. High spatial resolution is required for monitoring water use in stands of alien plants which often invade narrow riparian zones and flood plains. The original MOD16 product gives ET at 1 km<sup>2</sup> resolution which is too coarse for some applications.

## **Results**

Key results from the study are summarized as follows:

- The annual total grass reference evapotranspiration was more than 10 times higher than the rainfall indicating extremely arid conditions at the study site.
- The leaf area indexes (LAI – m<sup>2</sup> of leaf area per m<sup>2</sup> of ground area) of *Prosopis* and *V. karroo* trees varied from zero in winter when both species shed their leaves to peaks close to 2.0 in summer for the largest trees.
- Transpiration per unit leaf area was higher for *V. karroo* than for *Prosopis*. This was presumably due to a generally deeper sapwood depth in *V. karroo* which led to a high stem hydraulic conductivity thereby allowing the transport of large quantities of water. *Prosopis*, on the other hand, maintained a thin sapwood depth (often a few mm thick), possibly as an adaptation strategy to survive the harsh conditions at the site.
- Though individual *V. karroo* trees had higher transpiration rates than individual *Prosopis* trees of similar size, overall *Prosopis* contributed up to 85% of the total stand transpiration (635 mm/yr). This was because *Prosopis* had a much higher plant density (~ 613 stems per ha) and hence a larger sapwood area index compared to *V. karroo* (~ 100 stems per ha). The adverse impacts of *Prosopis* on groundwater are therefore a result of the ability of the species to form dense stands rather than substantially high transpiration rates by individual trees *per se*.
- Annual total transpiration by *Prosopis* (544 mm) was about four times higher than the rainfall (137 mm) received at the study site. The availability of groundwater to offset the rainfall deficit was therefore crucial to the survival of *Prosopis* at this site.

- The isotopes study showed that both *Prosopis* and *V. karroo* used groundwater. *Prosopis* obtained up to 77% of its water requirements from groundwater compared to around 47% for *V. karroo*. However, these estimates have substantial error margins due to difficulties with the isotopes approach as samples had to be transported over long distances from the study site.
- Based on the above estimates, *Prosopis* consumed at least 4 200 m<sup>3</sup> of groundwater per hectare per year compared to only 420 m<sup>3</sup>/ha/yr for *V. karroo*. The true values are likely higher due to the low rainfall which hardly penetrated the top 5 cm of the soil profile keeping the soil severely depleted.
- Root water uptake patterns showed that *Prosopis* manipulated the soil moisture environment through hydraulic redistribution. *Prosopis* abstracted groundwater via its tap roots and deposited it in the shallow soil layers via the lateral roots. However, this phenomenon was not detected in *V. karroo*. The significance of hydraulic redistribution is that it has significant implications on the population dynamics of the invasions. It facilitates nutrient cycling and avails water to seedlings which cannot access deep water reserves (Dawson, 1993).
- Groundwater levels from four boreholes drilled across the site showed clear seasonal oscillations.
- Groundwater recharge was mainly due to base flow from the Doorn River rather than the rainfall received on site.
- Clearing *Prosopis* slowed down the rate of decline in groundwater levels in summer from a pre-clearing peak of 9.0 mm/d to 5.0 mm/d after clearing. The continued decline in groundwater levels after clearing reflected the continued abstraction by the indigenous trees as well as base flow out of the study area.
- Contrary to the original MOD16 ET model that has widely been reported to under-estimate ET under semi-arid conditions (Ramoelo *et al.*, 2014), the improved model simulated plant transpiration at the arid site with a root mean square error (RMSE) of less than  $\pm 0.49$  mm/d while the RMSE was  $\pm 0.55$  mm/d for the ET before clearing increasing to  $\pm 0.77$  mm/d after including post-clearing ET measurements.

## **Conclusions**

The main outcomes from this study are:

- This study demonstrated that deep rooted indigenous trees growing in arid to semi-arid environments are equally likely to use as much or more water per plant than invasive alien plants. But the pronounced impacts of *Prosopis* invasions on groundwater are a result of the ability of the species to form dense stands as opposed to higher water use rates by individual trees *per se*.
- *Prosopis* has adaptation strategies to survive harsh conditions, e.g. by maintaining a relatively thin sapwood area (which reduces the carbon cost) and manipulating the available water resources when groundwater levels are high, e.g. via hydraulic redistribution. The indigenous *V. karroo* does not have these attributes possibly explaining its high mortality rate in arid environments compared to *Prosopis*.
- Clearing *Prosopis* is an effective strategy to increase the volume of groundwater which is critical in groundwater-dependent communities. However, priority should be stands with a high density of *Prosopis* and few or no deep rooted indigenous trees. Areas where *Prosopis* is less dense should also be prioritized to prevent the invasions from becoming dense.

## **Recommendations**

Further research is needed:

- To understand the hydrological impacts of bush encroachment given that indigenous trees are equally likely to use as much or more water than invasive alien trees.
- To distil the information presented in this and other studies into simple and practical guidelines to assist organizations like the Working for Water, local municipalities or farmers with decision making, e.g. prioritizing areas to clear given that groundwater use increased with increasing plant density, and;
- To validate and further improve the remote sensing ET model that was adapted in this study.

## ACKNOWLEDGEMENTS

We gratefully acknowledge funding for this project from the Water Research Commission (Project no. WRC K5/2256). The Working for Water program in the Department of Environmental Affairs is thanked for co-funding and clearing *Prosopis* at the study site at Brandkop farm. We are sincerely grateful to Mr Pieter Louw for permission to work at his farm. His help with charging and changing batteries for our equipment and providing labour is sincerely appreciated.

We also wish to acknowledge contribution from the following reference group members:

Dr Shafick Adams	Water Research Commission (Chairman)
Mr Andrew Wannenburg	Department of Environmental Affairs (NRM)
Mr Fanus Fourie	Department of Water and Sanitation
Mr John Meig	Western Cape Department of Agriculture
Prof Dominic Mazvimavi	University of Western Cape
Ms Jana Brits	Department of Water and Sanitation
Mr Brian Dyason	Department of Water and Sanitation
Dr Mohamed Abdol Elbasit	University of Johannesburg

We are sincerely grateful to Mrs Shaamileh Davids from the Archaeology Department at the University of Cape Town for processing our isotope samples. Mr Morne De Wee from Namakwa District Municipality in Calvinia is thanked for coordinating the *Prosopis* clearing tasks at Brandkop farm.

# TABLE OF CONTENTS

<b>EXECUTIVE SUMMARY .....</b>	<b>ii</b>
<b>ACKNOWLEDGEMENTS .....</b>	<b>viii</b>
<b>LIST OF TABLES .....</b>	<b>xi</b>
<b>LIST OF FIGURES .....</b>	<b>xii</b>
<b>LIST OF ABBREVIATIONS AND SYMBOLS .....</b>	<b>xvi</b>
<b>1 INTRODUCTION .....</b>	<b>1</b>
1.1 Background .....	1
1.2 Study approach .....	3
1.3 Project objectives .....	3
<b>2 SITE SELECTION .....</b>	<b>5</b>
<b>3 SITE DESCRIPTION .....</b>	<b>8</b>
3.1 Study area .....	8
3.2 Climate .....	8
3.3 Vegetation .....	9
3.4 Overview of site geology and hydrogeology .....	11
3.4.1 <i>Geology</i> .....	11
3.4.2 <i>Hydrogeology</i> .....	13
<b>4 METHODOLOGY .....</b>	<b>15</b>
4.1 Site microclimate .....	15
4.2 Quantifying transpiration rates of dominant tree species .....	16
4.3 Plant water sources .....	21
4.4 Evapotranspiration measurements .....	22
4.5 Characterizing the geology of the Prosopis invaded aquifer .....	25
4.6 Modelling water use by a Prosopis invaded catchment .....	26
4.6.1 <i>Model overview</i> .....	26
4.6.2 <i>Model sensitivity tests</i> .....	29
4.7 Groundwater recharge estimates .....	35
4.7.1 Available groundwater recharge data for the study area .....	35

4.7.2 Simulating groundwater recharge .....	36
4.7.3 HYDRUS-1D .....	37
<b>5 RESULTS AND DISCUSSION .....</b>	<b>43</b>
5.1 Climatic conditions .....	43
5.2 Water use by <i>Prosopis</i> and co-occurring <i>V. karroo</i> trees .....	46
5.2.1 Allometric relations .....	46
5.2.2 Tree transpiration rates.....	50
5.2.3 Root water uptake dynamics .....	55
5.3 Site hydrogeology .....	58
5.3.1 Groundwater levels.....	61
5.3.2 Spatial interpolation of groundwater levels.....	63
5.4 Vegetation-groundwater interactions .....	63
5.4.1 Effect of tree water uptake on groundwater levels.....	63
5.4.2 Sources of water transpired by the trees .....	65
5.5 Groundwater level response to <i>Prosopis</i> removal .....	68
5.6 Modelling evapotranspiration of a <i>Prosopis</i> invaded area .....	71
5.6.1 Site energy balance before clearing <i>Prosopis</i> .....	71
5.6.2 Energy balance after clearing <i>Prosopis</i> .....	72
5.6.3 Validation of the adapted MOD16 ET model .....	74
5.7 Estimating groundwater recharge .....	81
<b>6 CONCLUSIONS .....</b>	<b>89</b>
<b>7 RECOMMENDATIONS FOR FURTHER RESEARCH.....</b>	<b>90</b>
<b>8 REFERENCES .....</b>	<b>91</b>
<b>APPENDIX A. CAPACITY BUILDING AND TECHNOLOGY EXCHANGE.....</b>	<b>100</b>
<b>APPENDIX B. RESISTIVITY INTERPRETATION: BRANDKOP, NIEUWOUDTVILLE ....</b>	<b>103</b>
<b>APPENDIX C. BOREHOLE LOGS. ....</b>	<b>108</b>

## LIST OF TABLES

Table 1. Summary of sites considered for the study. ....	6
Table 2. Stratigraphy of the area (SRK, 2006; DWS 2012). ....	12
Table 3. Summary of plant water use monitoring equipment installed at the <i>Prosopis</i> invaded site at Brandkop farm. ....	20
Table 4. Proposed revisions to the MOD16 evapotranspiration model using data from South African biomes. $\epsilon_s$ and $\epsilon_a$ are the emissivities of the surface and atmosphere, respectively; LAI the leaf area index, $e_a$ the actual vapour pressure of the air, $T_a$ the mean daily air temperature, $A_c$ the available energy at the canopy level, $F_c$ , the fractional vegetation cover (equal to FPAR in Mu <i>et al.</i> , 2011); $A_{soil}$ is the available energy at the soil surface, $k_R$ is the extinction coefficient for net radiation (equal to 0.6 according to Impens & Lemeur, 1969); $G$ is the soil heat flux, $T_{min\_open}$ is the minimum temperature for stomatal opening, $T_{min\_close}$ is the minimum temperature for stomatal closure, $VPD_{open}$ is the minimum vapour pressure deficit required for stomata to open, $VPD_{close}$ is the maximum vapour pressure deficit for stomatal closure, $SWC$ depicts the soil water content, $SWC_{min}$ and $SWC_{max}$ are the minimum soil water content and soil water content at saturation for specific sites and $f_{wet}$ is the relative surface wetness and $T_{opt}$ is the optimum temperature for plant growth (25°C). ....	32
Table 5. The seasonal LAI associated with <i>Prosopis</i> and <i>V. karroo</i> trees. ....	39
Table 6. Parameters and values used in the HYDRUS-1D automatic calibration process. ....	40
Table 7. Summary of HYDRUS-1D inputs. ....	41
Table 8. Summary of the monthly weather conditions at Brandkop farm from August 2013 to January 2016. ....	45
Table 9. Borehole characteristics. ....	58
Table 10. Fraction of <i>Prosopis</i> and <i>V. karroo</i> xylem water derived from soil and groundwater sources, respectively. ....	67
Table 11. Amount of transpiration derived from the soil and groundwater sources by <i>Prosopis</i> and <i>V. karroo</i> , respectively. ....	68
Table 12. New parameters for the adapted MOD16 model applied to the <i>Prosopis</i> invaded site. ....	74

## LIST OF FIGURES

Figure 1. Abundance of <i>Prosopis</i> invasions in South Africa (after Ross Shuttleton, pers. comm.) .....	5
Figure 2. Location of the potential study sites that were considered for this study .....	7
Figure 3. A general overview of the study area at Nieuwoudtville showing the location of the Brandkop farm and the <i>Prosopis</i> invasions in 2007 as mapped by Van den Berg (2010).....	9
Figure 4. A Google Earth image of the study site and vicinity showing the different vegetation states. Dark green shade: nearly pure <i>V. karroo</i> ; turquoise: mixed, <i>V. karroo</i> dominant; yellow: nearly pure <i>Prosopis</i> ; blue: mixed small trees; purple: mixed large trees. The main channel of the Doorn River runs from right to left (south-east to north-west) along the lower edge of the bottom polygons. The red circle depicts the area where data was collected. ....	10
Figure 5. The geology in the immediate vicinity of the study site (CGS, 1997). ....	13
Figure 6. An automatic weather station monitoring the microclimate at Brandkop farm.....	16
Figure 7. Heat pulse velocity sap flow equipment monitoring transpiration by (a) <i>Prosopis</i> invasions and; (b) <i>V. karroo</i> trees.....	18
Figure 8. Locations of the key equipment within the study area at Brandkop farm. The blue line depicts the Doorn River channel.....	19
Figure 9. Eddy covariance flux tower measuring evapotranspiration at the <i>Prosopis</i> invaded site.....	23
Figure 10. Characteristics of the root system of: (a) <i>Prosopis</i> , and; (b) <i>V. karroo</i> . ...	25
Figure 11. Schematic representation of the original MOD16 evapotranspiration model (after Mu <i>et al.</i> , 2011). ....	28
Figure 12. Performance of the original MOD16 model in predicting; (a) evapotranspiration at a semi-arid site, and; (b) the net radiation (Dzikiti <i>et al.</i> , in review). The dashed line represents a 1:1 relationship, while the solid line shows the correlation/relationship between modelled and measured values. ....	28
Figure 13. Sensitivity of MOD16 ET predictions to $\pm 30\%$ changes in key parameters and variables.....	34
Figure 14. The soil water balance. ....	38

Figure 15. Seasonal changes in; a) the daily solar radiation, b) maximum and minimum air temperature, c) maximum and minimum vapour pressure deficit, and; d) daily rainfall and the reference evapotranspiration at Brandkop farm. ....	44
Figure 16. Sapwood-heartwood relationships for a (a) <i>Prosopis</i> and (b) <i>V. karroo</i> tree at Brandkop farm. The blue line in (b) depicts the trace of methylene blue dye indicating the extent of the sapwood depth. ....	47
Figure 17. Allometric relationships between the size of the conducting sap wood area and (a) stem cross sectional area, (b) branch cross sectional area and (c) tap root cross sectional area for <i>Prosopis</i> . Graph (d) shows the tap root to stem cross sectional area relationship. ....	48
Figure 18. Sapwood as a fraction of the stem area for the tap root, stem and branches of <i>Prosopis</i> trees. ....	49
Figure 19. Allometric relations for <i>V. karroo</i> where (a) shows the sapwood area – stem cross sectional area relationship, and (b) sap wood area – tap root cross sectional area relationship. ....	49
Figure 20. Comparison of daily transpiration by a <i>V. karroo</i> (LAI = 0.93) and a <i>Prosopis</i> tree (LAI ~ 1.63). ....	51
Figure 21. (a) Daily reference evapotranspiration from 02 August 2013 to 14 January 2016 at Brandkop farm. (b) Daily transpiration by <i>Prosopis</i> (black line), <i>V. karroo</i> (green line) and the total transpiration ( <i>Prosopis</i> + <i>V. karroo</i> – blue line).....	52
Figure 22. Variation in soil water content in the root zone of: (a) <i>Prosopis</i> and (b) <i>V. karroo</i> trees. ....	53
Figure 23. The basal coefficients of <i>Prosopis</i> (brown circles) and <i>V. karroo</i> (black stars) at Brandkop farm.....	54
Figure 24. Cumulative rainfall (grey dotted line), cumulative transpiration by <i>Prosopis</i> invasions (black line) and the indigenous <i>V. karroo</i> (green line) from 02 August 2013 to 15 January 2016. The blue line depicts the cumulative total transpiration by the two tree species. ....	54
Figure 25. Water uptake patterns by a <i>V. karroo</i> tree when the groundwater level was high (~ 4 mbgl) after flooding on site with (a) showing the course of stem sap flow, and; (b) the tap and lateral root water uptake patterns from 20 to 26 February 2014. Sap flow dynamics of (c) the stem and (d) tap and lateral roots when the groundwater level was low (~ >8 mbgl deep) from 20 to 26 February 2015.....	55

Figure 26. Water uptake patterns by a *Prosopis* tree when the groundwater level was high (~ 4 mbgl) after flooding on site with (a) showing the course of stem sap flow, and; (b) the tap and lateral root water uptake patterns from 20 to 26 February 2014. Sap flow dynamics of; (c) the stem and (d) tap and lateral roots when the groundwater level was low (~ >8 mbgl deep) from 20 to 26 February 2015..... 57

Figure 27. Borehole drilling at Brandkop farm..... 59

Figure 28. Samples collected during borehole drilling (Borehole #2). ..... 60

Figure 29. Geological cross section for the study site. .... 61

Figure 30. Changes in groundwater levels in four boreholes across the study site. Borehole #1 (black line) has the longest record. There was no data logger in Borehole #2 (brown circles), while Borehole #3 (green dotted line) and Borehole #4 (Blue line) started logging in October 2014. The black dotted vertical line shows the period when *Prosopis* was cleared..... 62

Figure 31. Potentiometric surface contours (mamsl) across the study site. BK001 is the code for Borehole #1, BK002, for Borehole #2, BK003 for Borehole #3, BK004 for Borehole #4. The interpreted direction of groundwater flow is also shown. .... 63

Figure 32. Direct impact of (a) *V. karroo* and (b) *Prosopis* on groundwater levels during clear days from 1-7 January 2014..... 64

Figure 33. Comparisons of the O/H isotope signature of xylem water of: (a) *Prosopis*, and; (b) *V. karroo* with that of ground and soil water samples taken during winter, spring and summer seasons, respectively. .... 66

Figure 34. Comparison of the cumulative changes in groundwater levels over a three months period from January to March: a) before, and; b) after *Prosopis* invasions were cleared. Black dotted line depicts the possible trend in groundwater level in 2015 had the invasions not been cleared..... 69

Figure 35. Relationship between cumulative tree water uptake and absolute changes in groundwater levels over a three months period from January to March (a) before (2014), and; (b) after *Prosopis* invasions were cleared in 2015. .... 70

Figure 36. Energy balance of the study site before the invasions were cleared from 20-22 May 2014. .... 71

Figure 37. Effect of the atmospheric evaporative demand on evapotranspiration before *Prosopis* was cleared at Brandkop farm..... 72

Figure 38. Energy balance of the study site after the invasions have been cleared from 14-16 May 2015. .... 73

Figure 39. Effect of the atmospheric evaporative demand on evapotranspiration after <i>Prosopis</i> was cleared at Brandkop farm.....	73
Figure 40. Comparison of the measured and modelled evapotranspiration for data collected during specific window periods before (black dots) and after (blue circles) <i>Prosopis</i> has been cleared.....	76
Figure 41. Comparison of the measured and modelled stand transpiration. Dotted line depicts the 1:1 line.....	76
Figure 42. Partitioning of the modelled evapotranspiration between day time and night time fluxes. Total evaporation (blue line) is the sum of the day time (green) and the night time (black) fluxes.....	77
Figure 43. Partitioning of the modelled evapotranspiration (blue line) into the transpiration (green line) and soil evaporation (brown line) components. ....	78
Figure 44. <i>Prosopis</i> invaded area along the Doorn River near Brandkop and the neighbouring farms. The red circle depicts the area where detailed measurements were taken. Clearing of the <i>Prosopis</i> invasions was also done in the same area in February 2015.....	79
Figure 45. Partitioning of ET between transpiration (a) and evaporation from the forest floor (b) and between day time (c) and night time (d) ET values on 14 April 2014. The x and y-axes values represent the matrix for the remote sensing images. ....	80
Figure 46. Monthly total ET at the <i>Prosopis</i> invaded site from January (a) to December 2014.....	81
Figure 47. Daily rainfall data recorded at Brandkop (top) and simulated fluxes at the atmospheric boundary produced by HYDRUS-1D (bottom).....	82
Figure 48. Volumetric soil water content data recorded at Brandkop (top) and simulated volumetric soil water content produced by HYDRUS-1D at 50 cm(N1), 100 cm (N2) and 150 cm (N3) soil depth (bottom). ....	84
Figure 49. The cumulative measured (top) and simulated (bottom) root water uptake by <i>Prosopis</i> trees. ....	85
Figure 50. The cumulative measured (top) and simulated (bottom) root water uptake by <i>V. karroo</i> trees.....	86
Figure 51. The HYDRUS-1D simulated cumulative fluxes observed at the lower boundary of the soil profile planted with <i>Prosopis</i> trees (top) and <i>V. karroo</i> trees (bottom).....	87

## LIST OF ABBREVIATIONS AND SYMBOLS

### **Roman symbols**

A	Total available energy	MJ m <sup>-2</sup> d <sup>-1</sup>
A <sub>soil</sub>	Available energy at soil surface	MJ m <sup>-2</sup> d <sup>-1</sup>
A <sub>c</sub>	Available energy at canopy	MJ m <sup>-2</sup> d <sup>-1</sup>
C <sub>L</sub>	Mean stomatal conductance per unit leaf area	m s <sup>-1</sup>
C <sub>s</sub>	Stomatal conductance	m s <sup>-1</sup>
C <sub>p</sub>	Specific heat at constant pressure	J kg <sup>-1</sup> K <sup>-1</sup>
e <sub>a</sub>	Actual vapour pressure of the air	kPa
e <sub>sat</sub>	Saturation vapour pressure of the air	kPa
ET <sub>o</sub>	Reference evapotranspiration	mm d <sup>-1</sup>
ET	Actual evapotranspiration	mm d <sup>-1</sup>
F <sub>c</sub>	Fractional vegetation cover	-
f <sub>wet</sub>	Fraction of wetted surface	-
G	Soil heat flux	W m <sup>-2</sup>
g <sub>l_e_ev</sub>	Leaf conductance to evaporated water vapour per unit LAI	m s <sup>-1</sup>
g <sub>l_sh</sub>	Leaf conductance to sensible heat per unit LAI	m s <sup>-1</sup>
K <sub>cmax</sub>	Maximum crop coefficient	-
k <sub>d1</sub>	Parameter for VPD stress factor	kPa <sup>-1</sup>
k <sub>R</sub>	Extinction coefficient	-
k <sub>s1</sub>	Parameter for soil water deficit stress factor	-
k <sub>s2</sub>	Parameter for soil water deficit stress factor	-
LAI	Leaf area index	-
PET	Potential evapotranspiration	mm d <sup>-1</sup>
r <sub>a</sub>	Aerodynamic resistance	s m <sup>-1</sup>
r <sub>bl_min</sub>	Minimum boundary layer resistance	s m <sup>-1</sup>
r <sub>bl_max</sub>	Maximum boundary layer resistance	s m <sup>-1</sup>
RH	Average relative humidity	%
RH <sub>max</sub>	Maximum relative humidity	%
RH <sub>min</sub>	Minimum relative humidity	%
R <sub>n</sub>	Net all wave radiation	W m <sup>-2</sup>

$r_s$	Stomatal resistance	$s\ m^{-1}$
$R_{\text{sample}}$	Ratios of the heavy to light isotope of sample	-
$R_{\text{std}}$	Ratios of the heavy to light isotope of standard	-
SWC	Soil water content	$\text{cm}^3\ \text{cm}^{-3}$
$\text{SWC}_{\text{max}}$	Soil water content at saturation	$\text{cm}^3\ \text{cm}^{-3}$
$\text{SWC}_{\text{min}}$	Soil water content at the wilting point	$\text{cm}^3\ \text{cm}^{-3}$
$T_a$	Average air temperature	$^{\circ}\text{C}$
$T_{\text{max}}$	Maximum air temperature	$^{\circ}\text{C}$
$T_{\text{min}}$	Minimum air temperature	$^{\circ}\text{C}$
$T_{\text{min\_close}}$	Minimum temperature for stomatal closure	$^{\circ}\text{C}$
$T_{\text{min\_open}}$	Minimum temperature for stomata to open	$^{\circ}\text{C}$
$T_{\text{opt}}$	Optimum temperature for plant growth	$^{\circ}\text{C}$
VPD	Vapour pressure deficit of the air	kPa
$\text{VPD}_{\text{open}}$	Vapour pressure deficit for stomata to open	kPa

### **Greek symbols**

$\alpha$	surface albedo	-
$\Delta$	slope of saturation vapour pressure vs temperature	$\text{kPa}\ \text{K}^{-1}$
$\epsilon_a$	emissivity of the air	-
$\epsilon_s$	emissivity of the surface	-
$\gamma$	psychrometric constant	$\text{kPa}\ \text{K}^{-1}$
$\lambda$	latent heat of vaporisation	$\text{Jkg}^{-1}$

This page was deliberately left blank

# 1 INTRODUCTION

## 1.1 Background

A number of local and international studies have assessed the water use by forest plantations and self-established stands of invasive alien plants (IAPs). Focus has mainly been on the woody species which are believed to consume large quantities of water (Le Maitre *et al.*, 1999; Doody *et al.*, 2011; Vila *et al.*, 2011). In South Africa for example, studies have established the water use by *Acacia mearnsii* (Dye and Jarman, 2004; Clulow *et al.*, 2011), pine forests (Dye *et al.*, 1996; Dzikiti *et al.*, 2013a), eucalyptus plantations and invasions (Dye., 1996; Dzikiti *et al.*, 2016), and poplar invasions. A few other studies have sought to quantify the water requirements of non-woody invasions such as *Arundo donax*.

Evidence from paired catchment studies (Bosch and Hewlett., 1982; Scott, 1999) and tree felling experiments (Dye and Poulter, 1995; Prinsloo and Scott., 1999; Clulow *et al.*, 2011) have shown that IAPs use large quantities of water and that they have significant impacts on stream flows. As a result, commercial forestry with alien tree species has been declared a stream flow reduction activity (SFRA) under the South African Water Act. Authorization is required prior to establishing forest plantations in view of their impacts on the water resources.

Clearing is the most common management practice used to eradicate IAPs. The overriding objective of the clearing programmes is to reduce the excess water use by the invasive species so that the water demands of people and the environment can be met through increased stream flows and groundwater yields (Chew *et al.*, 2009). While some studies in relatively humid environments have reported increased stream flows and groundwater levels following the removal of invading vegetation (Prinsloo and Scott, 1999), there are studies in more arid regions where decreases in evapotranspiration due to alien vegetation clearing did not necessarily translate to increased stream flow (Hart *et al.*, 2005; McDonald, 2010) or increased groundwater levels (Hays, 2003).

Doody *et al.* (2011) identified three critical factors that determine the actual volume of water that can be saved following alien plant removal. These include: 1) how the invasions interact with various water sources (i.e. soil water/ river water or groundwater); 2) the geology of the invaded aquifer, and; 3) the water use characteristics of the indigenous vegetation that replace the invasions once they have been cleared. Few studies have investigated the impact of *Prosopis* invasions on groundwater in the drier parts of South Africa (Fourie *et al.*, 2007; Dzikiti *et al.*, 2013b). There is also little information on the recovery of groundwater following clearing. The influence of the deep rooted indigenous vegetation on groundwater recovery after alien plant removal is also unknown.

*Prosopis* is a warm desert shrub that often develops multiple stems that branch close to the ground. They have an extensive root system 90% of which occur in the top few centimetres of the soil profile. The species is well known for its very deep tap root which allows it to survive in harsh arid environments. The average depth of the tap root of fully grown trees is typically in the range 20-30 m although a depth exceeding 50 m was recorded in the USA (Jackson *et al.*, 1996). The Northern Cape Province has seen a sharp increase of approximately 363% in land invaded by *Prosopis* between 1990 and 2007 (van den Berg, 2010). This raises important questions which are critical for the management of the invasions and for the provision of ecosystem goods and services to local communities such as groundwater supply.

Some of the questions that require science based answers are listed below:

- What are the main sources of water used by *Prosopis* invasions in South Africa?
- How much groundwater does *Prosopis* use and what are the impacts on this water source?
- How does the water use by *Prosopis* compare with that by co-occurring indigenous trees?
- What are the main drivers of water use by *Prosopis* invasions and how much groundwater can potentially be saved by clearing this woody weed?
- What are the factors that influence the actual volumes of groundwater that can be recovered by clearing *Prosopis* in the arid parts of South Africa?

## 1.2 Study approach

To answer these questions, this research adopted a multidisciplinary approach involving eco-hydrological, hydrogeological, micrometeorological, ecological and remote sensing inputs. The approach was highly quantitative including the measurement of tree transpiration rates, root water uptake patterns, site microclimatic conditions, stand evapotranspiration rates, vegetation cover, plant water sources (i.e. whether soil water or groundwater), soil water content dynamics, groundwater levels, and satellite imagery.

This data was collected from August 2013 to January 2015 before *Prosopis* was cleared from the study area. Monitoring of only the indigenous vegetation continued from February 2015 to January 2016 after the invasions had been removed. The novelty of this study is that detailed plant water uptake data was collected from both the invasions and the co-occurring indigenous trees that are likely to replace *Prosopis* when it is cleared. This information enabled us to determine the incremental water use by *Prosopis* over and above that used by the indigenous trees and we correlated this directly with the changes in groundwater levels before and after the invasions were cleared.

The data collected was used to calibrate and validate a remote sensing-based evapotranspiration model (MOD16) to provide spatial information on the water requirements of the vegetation in the study area. Estimates of groundwater recharge rates were obtained using the Hydrus-1D model

## 1.3 Project objectives

The study objectives were:

1. To establish the long-term water use trends by *Prosopis* invasions and co-occurring deep rooted indigenous vegetation in order to determine impacts on groundwater;
2. To characterize the hydro geology of a *Prosopis* invaded aquifer;
3. To determine the sources of water used by the vegetation and to quantify the proportion of the total water use that is derived from groundwater;
4. To quantify potential increases in groundwater recharge as a result of clearing *Prosopis* invasions;

5. To evaluate a physically-based model for predicting water use by *Prosopis* invasions integrating *in situ* and remote sensing data, and;
6. To apply the model to scale up estimates of groundwater use by *Prosopis* to selected invaded sites in the country.

## 2 SITE SELECTION

*Prosopis* is widely distributed across many catchments in South Africa and Figure 1 shows the abundance of this species (R. Shuttleton, pers. com). A number of potential study sites were considered for the project as summarized in Table 1. These include sites in the North-West, Free State, Western and Northern Cape Provinces. Some of the sites were visited to physically inspect their condition while we relied on information from local experts (e.g. DWS, North West University, local municipalities and Working for Water) on the other sites.

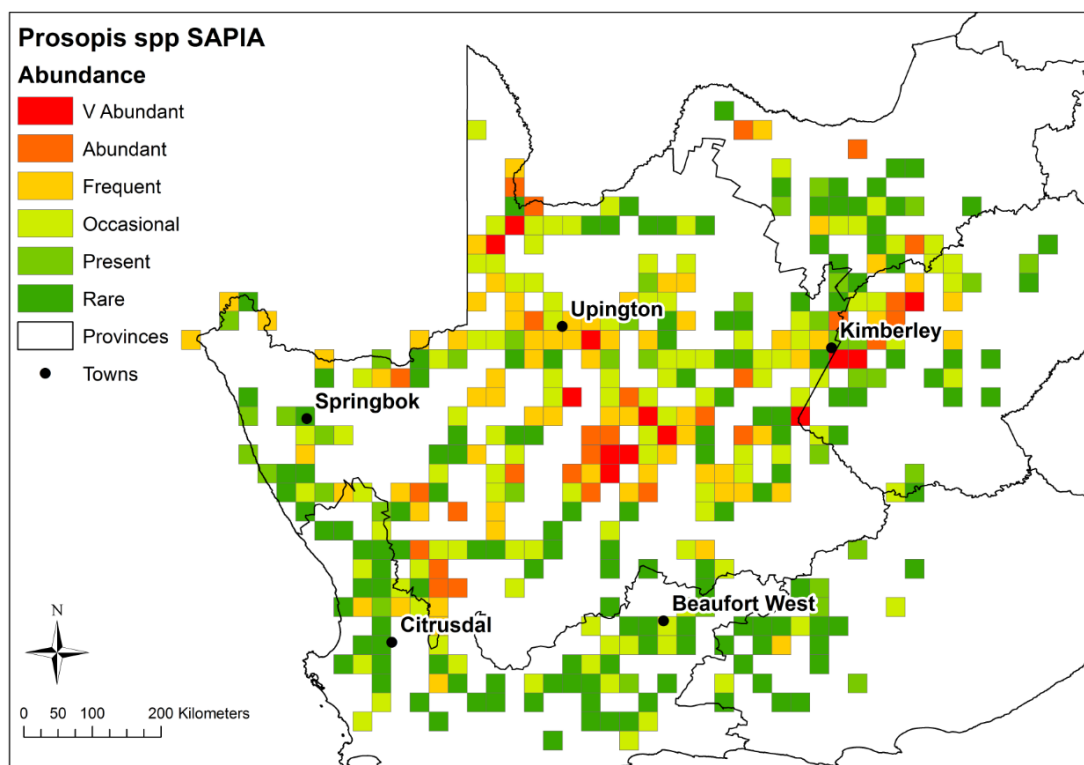


Figure 1. Abundance of *Prosopis* invasions in South Africa (after Ross Shuttleton, pers. comm.)

Our site selection criteria involved finding a site that:

- 1) was moderately to densely invaded by *Prosopis*;
- 2) had co-occurring indigenous plant species that are likely to use groundwater;
- 3) was large in spatial extent (> 1 km<sup>2</sup>);
- 4) was close to a groundwater dependent community;
- 5) was close to a stream or watercourse;
- 6) had monitoring boreholes;
- 7) had good security for our equipment;

- 8) had cell-phone reception for remote data downloads, and;
- 9) had cooperation from the land owner/s.

We developed a scoring system in an attempt to develop an objective method for selecting the site. According to the method, each site attribute listed above was assigned a weight between 1 and 5 with 5 being a highly desirable attribute. The extent to which each attribute was satisfied was then given a score between 0 and 10 during the site visits. The sum of the product of the weight and the score for all the attributes was used to rank the sites with the highest scoring site being the most suitable.

Table 1. Summary of sites considered for the study.

	<b>Site name</b>	<b>Province</b>	<b>Nearest town</b>	<b>Visited</b>
1	Sout Pan	Free State	Bloemfontein	No
2	Tshidilamolomo	North West	Mafikeng	No
3	De Hoop/Brandwag farms	Western Cape	Beaufort West	Yes
4	Rosedale farm	North West	Britstown	Yes
5	Saaipoort farm	Northern Cape	Carnarvon	Yes
6	Clarke Scholtz farm	Northern Cape	Calvinia	No
7	Brandkop farm	Northern Cape	Nieuwoudtville	Yes

Brandkop farm had the highest score because there are dense *Prosopis* invasions co-occurring with the indigenous *Vachellia karroo* (formerly *Acacia karroo*) that also uses groundwater (Schachtschneider and February, 2010). The communities in the neighbourhood of Brandkop are dependent on groundwater for drinking (humans and livestock), and for irrigating wheat and pastures. Security was good as the equipment was away from plain sight and the farm owner (Mr Peter Louw) was very supportive of the project. The only drawback was that there was no cell-phone reception, but we resorted to frequent (two monthly) visits to download the data. The farmer kindly offered to assist with charging and changing the batteries of the equipment.

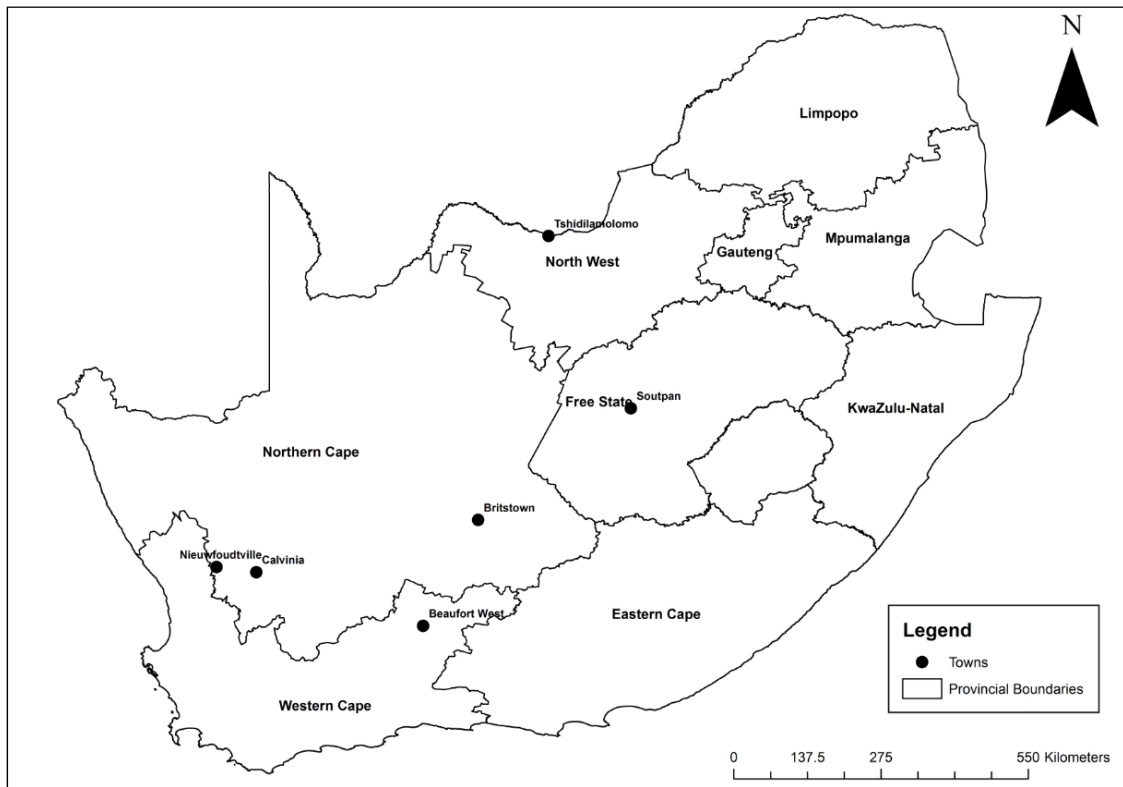


Figure 2. Location of the potential study sites that were considered for this study

## 3 SITE DESCRIPTION

### 3.1 Study area

The size of the *Prosopis* invaded area at Brandkop farm (S31.23254°; E019.20284°; 390.5 masl) and adjacent areas is more than 400 ha. This farm is situated on the Bokkeveld plateau about 22 km to the northwest of the town of Nieuwoudtville on the R 357 to Loeriesfontein. Brandkop farm is located on the floodplain of the Doorn River upstream of its confluence with the Hantam River (Figure 3). The floodplain is broad and flat with numerous braided channels and has been significantly modified by the creation of cultivated lands and irrigation furrows which link to both the Doorn and Hantam Rivers.

### 3.2 Climate

The mean annual rainfall in the vicinity of the study site is about 150 mm with a coefficient of variation of about 32%. The mean annual potential evapotranspiration is more than 2600 mm (Mucina and Rutherford, 2006). The rainfall is strongly seasonal with the peak occurring in June and July and very little or no rainfall from December to February. The mean annual temperature is 15-17°C with maximum temperatures in summer in excess of 40°C in January-February and minimum temperatures in June-July of <1°C with occasional frosts, especially after snowfalls on the escarpment to the west and Hantam mountains to the east. The rainfall record for the Brandkop farm is patchy, with unpatched records from 1925-1950 and 2000-2001. The mean is 119.7 mm, maximum 233.7, minimum 48.0 and the median is 112 mm.

There is a steep rainfall gradient in the Doorn River sub-catchment which forms the southern part of quaternary catchment E32E and drains the northern part of the Nieuwoudtville plateau. The quaternary catchment has an area of about 100 000 ha, a maximum annual rainfall of about 470 mm on the escarpment to the west, and a mean annual runoff of about 30.9 mm (Middleton and Bailey, 2008). There are no flow gauges on the Doorn River but according to the farmer it is seasonal and flows once or twice during most winters with periodic floods.

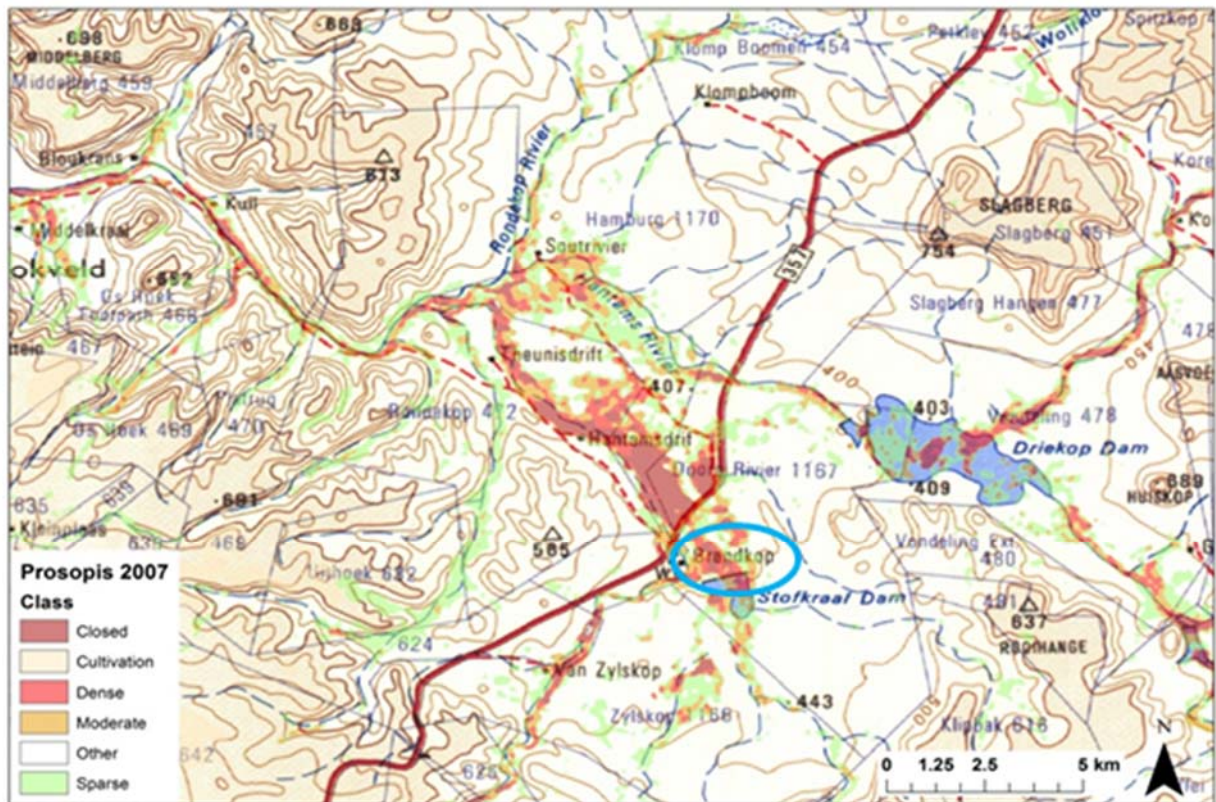


Figure 3. A general overview of the study area at Nieuwoudtville showing the location of the Brandkop farm and the *Prosopis* invasions in 2007 as mapped by Van den Berg (2010).

### 3.3 Vegetation

The dominant dryland vegetation is a Succulent karroo shrubland known as Hantam karroo, dominated by a mixture of succulent-leaved and non-succulent leaved shrubs (Mucina and Rutherford, 2006). The natural floodplain vegetation is called Namaqualand Riviere and is a complex mixture of shrublands and tussock gramioids (grass-like plants) with patches dominated by *Vachellia Karoo* (*V. karroo*) and *Tamarix usneoides* (Figure 4). The soils are typically fine and clayey and saline, with the salinity varying from low to quite high depending on the degree of leaching.

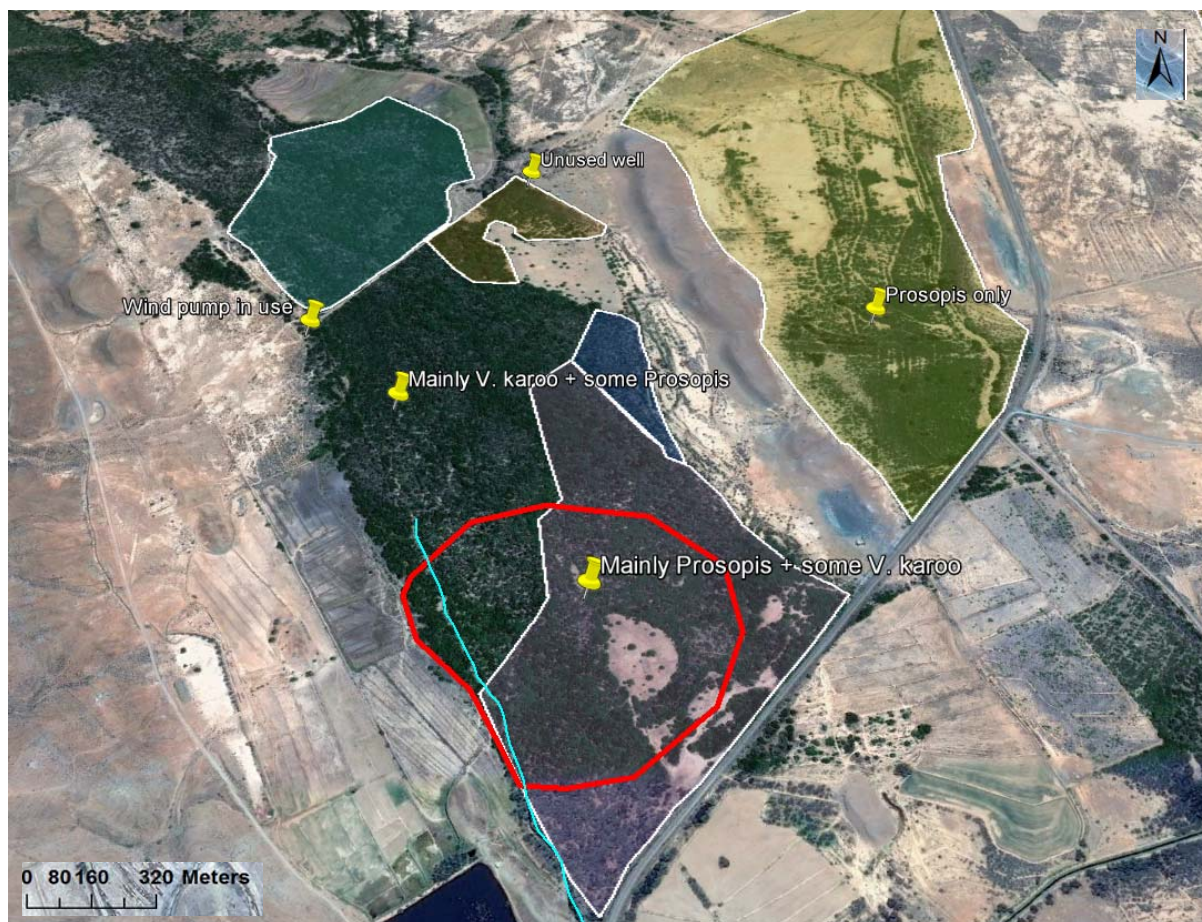


Figure 4. A Google Earth image of the study site and vicinity showing the different vegetation states. Dark green shade: nearly pure *V. karoo*; turquoise: mixed, *V. karoo* dominant; yellow: nearly pure *Prosopis*; blue: mixed small trees; purple: mixed large trees. The main channel of the Doorn River runs from right to left (south-east to north-west) along the lower edge of the bottom polygons. The red circle depicts the area where data was collected.

In the study site, the vegetation is dominated by stands of *V. karoo* which are steadily being replaced by *Prosopis* species which were introduced to the farm in the mid-20<sup>th</sup> century. Parts of the riparian vegetation are dominated by *Prosopis* but along the main channel of the Doorn River there are still stands of nearly pure *V. karoo* (Figure 4). *Prosopis* invasions extend onto the drier parts of the floodplain and the adjacent dryland areas. Much of the invasion is on old lands which were flood irrigated and used for growing wheat when there was sufficient rainfall in the catchment.

*Vachellia karoo* is an important riparian species as it provides nesting sites for bird and a habitat for a range of other fauna. It is a weedy, pioneer species and can form dense stands which open out through self-thinning as it ages. It is not a long-lived tree and has a lifespan of about 30-40 years (Barnes *et al.*, 1996). Stands dominated by

*Prosopis* become very dense, suppressing or displacing other species and unsuitable for many animal species (Steenkamp and Chown, 1996; Dean *et al.*, 2002). The *V. karroo* and *Prosopis* trees in the study site range in height from about 2 m tall in the dryland areas to 5-10 m tall along the banks of the river channel and lowest lying (wetter) parts of the floodplain. *Prosopis* water-use is believed to be higher than that of the native species, including *V. karroo* (Le Maitre, 2009; Wise *et al.*, 2012). This hypothesis was tested in this study.

### 3.4 Overview of site geology and hydrogeology

#### 3.4.1 Geology

The geology of the Olifants-Doorn Water Management Area (WMA) is dominated by metamorphic rocks of the Nama Group in the north and sedimentary rocks of the Cape Supergroup in the southern and south-western parts. In the northern and north-eastern parts, the rocks of the pre-Cape Van Rhynsdorp Group, the sedimentary rocks of the lower Karoo Supergroup and the intrusive Karoo dolerites are dominant (Table 2; Figure 5).

The invasions at Brandkop farm occur in an area underlain by quaternary sediments, which in turn is underlain by shales and siltstones of the Van Rhynsdorp Group (Figure 5).

Table 2. Stratigraphy of the area (SRK, 2006; DWS 2012).

Lithostratigraphic Unit		Era	Characteristics	Hydrogeological Significance	
Sandveld Group		Cenozoic			
Karoo Dolerite		Mesozoic		Fractured contact zones and metamorphic aureoles serve as aquifers. Also barriers to flow.	
Karoo Group	Beaufort Group	Mesozoic	6000 m alternating arenaceous and argillaceous sediments	Localised significance as aquifer systems.	
	Ecca Group	Paleozoic	Dark grey shale and inter-bedded sandstone	Middle to upper thin sandstone strata may have greater hydrogeological significance	
	Dwyka Group		Tillite	Aquiclude	
Cape Supergroup	Wittenberg Group	Paleozoic	Alternating sandstone and shale	Marginal hydrogeological significance	
	Bokkeveld group		Alternating sandstone and shale	Little significance, else regolith aquifer	
	Table Mountain Group		Nardouw Subgroup	1100 m to 810 m alternating sandstone and shale with lenses of quartzite	Top aquifer of TMG. Confined above by lowermost shale unit of Bokkeveld Group
			Cederberg Shale Formation	50 m to 120 m shale	Top confining layer for lower aquifer system
			Pakhuis Formation	40 m	Major fractured rock/secondary aquifer system. Middle aquifer
			Peninsula Formation	1800 m to 2150 m sandstone	
			Graafwater Formation	Sandstone	
			Piekenierskloof Formation	Conglomeratic base, followed by 800 m coarse sandstone	Basal aquifer unit
Klipheuvel Group		Paleozoic	Lower conglomeratic formation and an upper mudstone formation of approx 2000 m	Aquitard of limited hydrogeological significance	
Van Rhynsdorp Group		Paleozoic	A succession of shallow sediments deposited on a tidal plain	Impermeable aquiclude	
Malmesbury Group		Namibian		Impermeable aquiclude	

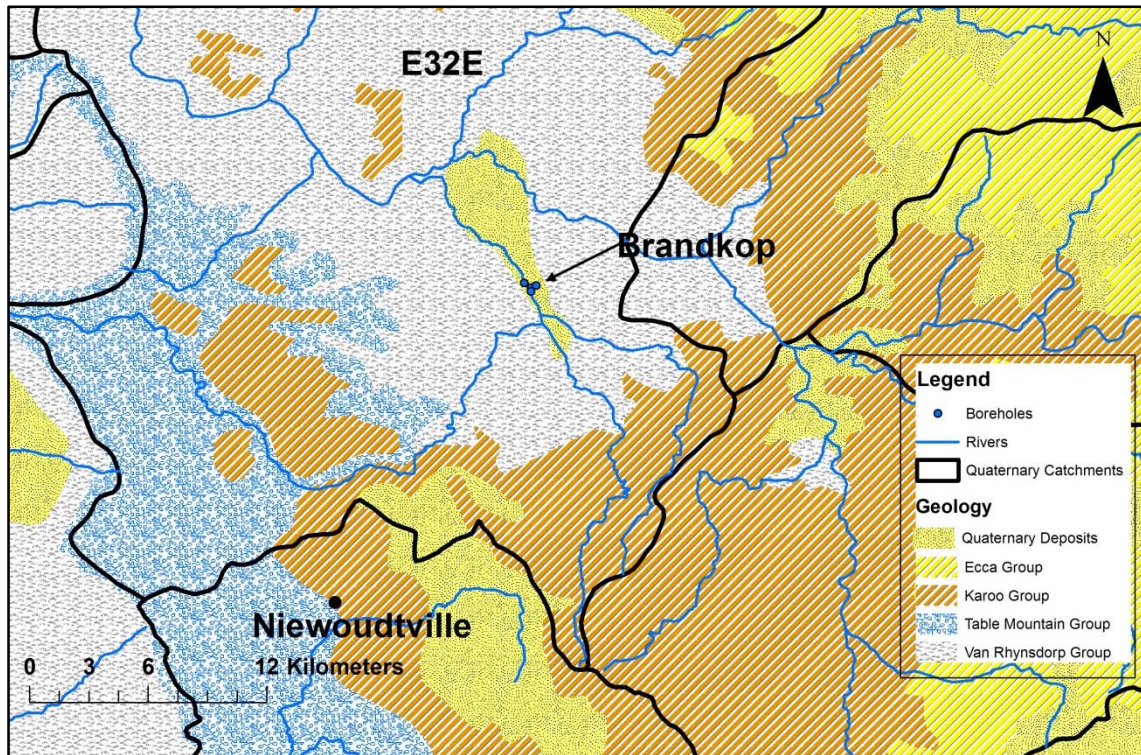


Figure 5. The geology in the immediate vicinity of the study site (CGS, 1997)

### 3.4.2 Hydrogeology

Groundwater is an important component of the water resources of the Olifants-Doorn WMA. The geology and consequently the hydrogeology show considerable variation. The main implications of this variability are that groundwater quantity and quality varies considerably. In certain areas groundwater is an important component of the total water resources budget, whilst in other regions its occurrence is very limited (DWA, 2012). The towns of Calvinia, Nieuwoudtville, Loeriesfontein, etc. are dependent on groundwater.

According to DWA (2012), the aquifer types which occur within the Olifants-Doorn WMA are:

- Fractured
- Intergranular and fractured
- Intergranular
- Karst

The WMA is dominated by fractured, and intergranular and fractured aquifers, with minor occurrences of intergranular and karst aquifers. The typical borehole yields exhibited by fractured aquifers, and by intergranular and fractured aquifers are between 0.1 and 2 L s<sup>-1</sup>. The borehole yields of intergranular aquifers range between 0.1 to > 5 L s<sup>-1</sup> (DWA, 2012).

## 4 METHODOLOGY

### 4.1 Site microclimate

The microclimate at the study site was monitored using an automatic weather station which we installed in the farmer's yard about 1.5 km from the study site (Figure 6). The equipment comprised a pyranometer (Model SP 212 Apogee Instruments, Inc., Logan UT, USA) which measured the solar irradiance and it was installed on a horizontal levelling fixture mounted on a north facing cross arm to prevent self-shading. Air temperature and relative humidity were measured using a temperature and humidity probe (Model CS500, Vaisala, Finland) installed at a height of about 2.0 m above the ground. A wind sentry (Model 03001, R.M. Young; Campbell Scientific, Inc., Logan UT, USA) was used to measure the wind speed and direction at 2.0 meters height while rainfall was monitored using a tipping bucket rain gauge (Model TE525-L; Campbell Scientific, Inc., Logan UT, USA). All the sensors were connected to a data logger (Model CR1000 Campbell Scientific, Inc., Logan UT, USA) programmed with a scan interval of 10 s. The output signals were processed at hourly and daily intervals, respectively.

Ground cover around the weather station had short patchy grass as shown in Figure 6. A location with an ideal reference surface could not be found given the extremely dry conditions and the poor state of the vegetation in the area. Power to the weather station was supplied by two 7 Ah batteries stored in the data logger enclosure. The two batteries were in turn charged by a 50 W solar panel as the entire farming area around Brandkop has no mains electricity. A voltage regulator was fitted to the system to prevent overcharging of the batteries. The weather station was located at least 80 m away from the farm house. Security at the site was good as the area was fenced.

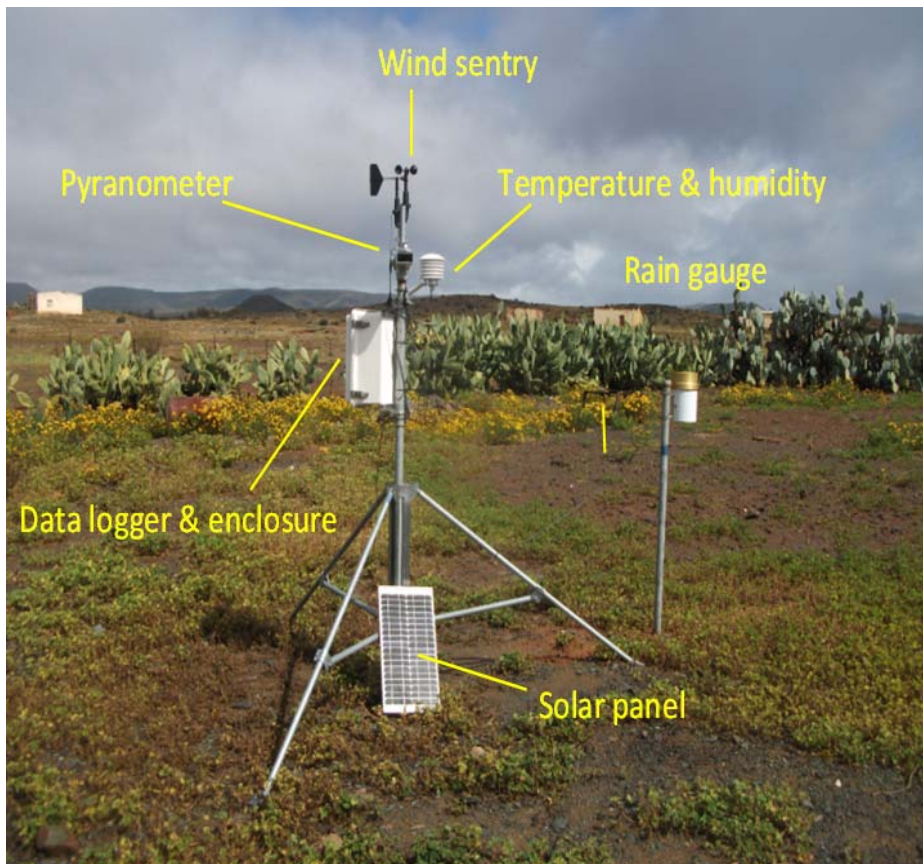


Figure 6. An automatic weather station monitoring the microclimate at Brandkop farm.

#### 4.2 Quantifying transpiration rates of dominant tree species

To quantify the amount of water used by the plants we installed the heat ratio heat pulse velocity (HPV) sap flow system on both *Prosopis* and the co-occurring indigenous *V. karroo* trees. Our selection criteria for the instrumented trees involved first conducting a stem diameter survey on twenty five trees of each species. Stem diameters were measured at approximately 15 cm for *Prosopis* and about 50 cm for the *V. karroo* above the ground just before the main branches. We then categorized the stem diameters into three size classes namely the small (0-10 cm), medium (11-20 cm) and large (> 21 cm). Trees whose stem diameters were close to the median stem sizes in each diameter class were selected taking into account practical limitations such as the heater and thermocouple cable lengths.

The sap flow sensors were installed on five trees for each species and the typical set ups are shown in Figure 7. Three of the instrumented trees (for each species) were located closer to the Doorn River channel (sap flow system # 1) and the other two were further from the river (sap flow system #2) as shown in Figure 8. In addition, to understand the root water uptake patterns of the trees we installed a pair of sap flow sensors on the tap root and another pair on the lateral roots of one tree per species at sap flow system #2. Installation of the roots sap flow sensors was achieved by carefully excavating the soil around the main stem taking care to minimize damage to the roots. Once the sensors were installed, the pits were then backfilled and compacted.

In total, four HPV systems were installed (2 on *Prosopis* and 2 on *V. karroo*) each comprising a CR1000 data logger, a multiplexer (Model AM16/32B; Campbell Scientific, Inc., Logan UT, USA), a custom made relay control module, a 70 Ah battery, 12 heaters and 24 copper-constantan thermocouple pairs. All this equipment was stored in four strong boxes situated at various locations in the invaded area for security reasons and Table 3 summarises the details of each set up. All the equipment was away from plain sight and we experienced no security issues. The farmer changed the batteries once every month.

Destructive sampling of the *Prosopis* trees showed that the conducting sapwood formed a very narrow band a few millimetres wide while much of the stem cross sectional area was occupied by the heartwood. For this reason it was not possible to install the HPV thermocouples at various radial depths into the sapwood. Rather all the sensors were installed at a constant depth between 10 and 15 mm from the bark to avoid sampling the heartwood which would give bad quality data. However, the sensors were distributed equally around the stem to capture the circumferential variations in sap velocity. Installation depths of the thermocouples in the *V. karroo* trees which had a thicker sapwood are as shown in Table 3.



Figure 7. Heat pulse velocity sap flow equipment monitoring transpiration by (a) *Prosopis* invasions and; (b) *V. karroo* trees.



Figure 8. Locations of the key equipment within the study area at Brandkop farm. The blue line depicts the Doorn River channel.

The leaf area index (LAI) of individual trees and that of the stand were measured at regular intervals using the leaf area meter (Model LAI 2000, LI – COR, Inc., Lincoln NE, USA).

Table 3. Summary of plant water use monitoring equipment installed at the *Prosopis* invaded site at Brandkop farm.

Location	Species	No of trees	Equipment	Stem diameters	No. of stem probes	No. of root probes	Installation depth into sapwood	GPS coordinates
Sap flow #2	Prosopis	2	1 x CR 1000 data logger 1 x multiplexer 1 x relay control module 12 x heaters 48 x thermocouples 1 x strong box 1 x battery 3 x soil moisture probes	<u>Tree #1</u> – 21.8 cm  <u>Tree #2</u> – 15.6 cm	<u>Tree #1</u> – 4 probes  <u>Tree #2</u> – 4 probes	  <u>Tree #2</u> – 2 on tap root – 2 on laterals	<u>Tree #1</u> Stem: 10 mm for all probes  <u>Tree #2</u> -Stem: 10 mm all probes; -Roots: 7 mm all roots.	S31.23213° E019.20260° Elev: 393.5 masl
	Acacia	2	1 x CR 1000 data logger 1 x multiplexer 1 x relay control module 12 x heaters 48 x thermocouples 1 x strong box 1 x battery 1 x soil moisture probes	<u>Tree #1</u> – 17.6 cm  <u>Tree #2</u> – 10.8 cm	<u>Tree #1</u> – 4 probes  <u>Tree #2</u> – 4 probes	  <u>Tree #2</u> – 2 on tap root – 2 on laterals	<u>Tree #1</u> Stem: 10, 25, 35, 50 mm  <u>Tree #2</u> Stem: 10, 15, 20, 25 mm Roots: 10 mm	S31.23176° E019.20251° Elev: 392.2 masl
Sap flow #1	Prosopis	3	1 x CR 1000 data logger 1 x multiplexer 1 x relay control module 12 x heaters 48 x thermocouples 1 x strong box 2 x battery 1 x soil moisture probes	<u>Tree #1</u> – 21.4 cm  <u>Tree #2</u> – 9.2 cm  <u>Tree #3</u> – 14.7 cm	<u>Tree #1</u> – 4 probes  <u>Tree #2</u> – 4 probes  <u>Tree #3</u> – 4 probes	Nil	<u>Tree #1</u> Stem: 13 mm for all probes  <u>Tree #2</u> Stem: 13 mm for all probes  <u>Tree #3</u> Stem: 13 mm for all probes	S31°13'45.88" E019°12'02.70" Elev: 391.0 masl
	Acacia	3	1 x CR 1000 data logger 1 x multiplexer 1 x relay control module 12 x heaters 48 x thermocouples 1 x strong box 3 x battery 1 x soil moisture probes	<u>Tree #1</u> – 27.6 cm  <u>Tree #2</u> – 12.7 cm  <u>Tree #3</u> – 10.6 cm	<u>Tree #1</u> – 4 probes  <u>Tree #2</u> – 4 probes  <u>Tree #3</u> – 4 probes	Nil	<u>Tree #1</u> Stem: 10, 25, 38, 50 mm  <u>Tree #2</u> Stem: 10, 25, 35, 45 mm  <u>Tree #3</u> Stem: 10, 15, 22, 27, 32 mm	S31°13'50.22" E019°12'00.54" Elev: 390.3 masl

### 4.3 Plant water sources

To determine the extent to which the trees depended on various water sources (i.e. soil water or groundwater), we collected soil, groundwater and rainwater samples and non-photosynthesizing twigs from both *Prosopis* and *V. karroo* trees. The samples were collected once during each season as follows: August 2013 (spring), February 2014 (summer), April 2014 (autumn) and again in October and November 2014. We were able to collect only one rainfall sample in August 2013. The rainfall sample was collected during a rainfall event while groundwater samples were extracted from the borehole after pumping for at least 30 min.

Rain and groundwater samples were stored in glass vials, sealed and refrigerated. Hand augured soil samples were collected in the depth range 0-50, 50-100 and 100-160 cm. To minimise evaporation the samples were stored into two individually secured air tight polythene bags per sample and frozen. Twig samples (~5-6 cm long) from three sap flow instrumented *Prosopis* trees and three nearby *V. karroo* trees were collected for measurements of the plants' xylem water isotopic signature. Green photosynthesizing material was avoided as these had a higher risk of fractionation. The twig samples were placed into borosilicate tubes and frozen for later insertion onto a cryogenic vacuum extraction line to separate the water for isotope analysis. All extracted tree xylem, soil, rain and groundwater samples were analysed at the University of Cape Town, Archaeology Laboratory.

The twig samples were stored directly into borosilicate tubes (Kimax-Kimble, New Jersey, USA) which were then inserted onto a cryogenic vacuum extraction line to separate the water for isotope analysis. A ten gram sub-sample of the soil was transferred into borosilicate tubes to extract the water for oxygen and hydrogen isotope analysis. A variation of the zinc closed tube reduction method was used to determine  $^2\text{H}/\text{H}$  ratios (Coleman *et al.*, 1982), while  $^{18}\text{O}/^{16}\text{O}$  were obtained using the  $\text{CO}_2$  equilibrium method of Socki *et al.* (1992). Isotopic ratios of both  $^2\text{H}/\text{H}$  in  $\text{H}_2$  and  $^{18}\text{O}/^{16}\text{O}$  in  $\text{CO}_2$  were determined using a Thermo Delta Plus XP Mass Spectrometer (Hamburg, Germany) at the University of Cape Town. Internal standards were run to calibrate results relative to Standard Mean Ocean Water (V-SMOW) and to correct for reference

gas drift. The deviation from V-SMOW is denoted by the symbol  $\delta$  and results are expressed as parts per mil (‰) through the equation:

$$\delta^{xx}E = ((R_{sample} / R_{standard}) - 1) \times 1000 \quad (1)$$

where  $\delta^{xx}E$  is the respective element ( $^2\text{H}$ ,  $^{18}\text{O}$ ),  $^{xx}$  is the mass of the heavier isotope in the abundance ratio, and  $R_{sample}$  and  $R_{standard}$  are the ratios of the heavy to light isotope of sample and standard, respectively (Dawson *et al.*, 2002). The analytical uncertainty is approximately 2 ‰ for  $\delta^2\text{H}$  and 0.2 ‰ for  $\delta^{18}\text{O}$ .

#### 4.4 Evapotranspiration measurements

Equipment installation at the study site was done from 29 July to 2 August 2013. To quantify the stand (area bounded in red in Figure 8) level evapotranspiration (ET), we used an open path eddy covariance system shown in Figure 9. The equipment was mounted on a 10 m lattice mast (S31.23222°; E019.20217°; elev. 393 masl) and the position of the tower is marked in Figure 8. However, because of the high cost of running the eddy covariance system, we collected the ET data during short window periods in summer, autumn, winter and spring before and after the invasions were cleared.

The eddy covariance system comprised a three-dimensional sonic anemometer (Model CSAT3, Campbell Scientific, Inc., Logan UT, USA) and an infrared gas analyser (Model LI – 7500A, LI – COR, Inc., Lincoln NE, USA). The sensors, oriented in a northerly direction, were mounted approximately 1.5 m above the mean canopy height. A net radiometer (Model 240 – 110 NR – Lite, Kipp & Zonnen, Delft, The Netherlands) was mounted at eight and half meters above the ground also pointing northwards to avoid self-shading. The fetch around the tower was approximately 200 m in the easterly direction, more than 300 m in the westerly direction, more than 500 m in the northerly direction and more than 1000 m in the southerly direction. According to a previous study by O'Farrell *et al.* (2009) in the Nieuwoudtville area, the prevailing wind direction is generally south-westerly. Therefore there was adequate fetch around the flux tower to give representative evapotranspiration data.



Figure 9. Eddy covariance flux tower measuring evapotranspiration at the *Prosopis* invaded site.

The soil heat flux was measured at two positions around the flux tower using two clusters of soil heat flux plates (Model Hukseflux, Delft, The Netherlands) installed at an average depth of eight centimetres. Measurements of the rate of change of soil temperature above the soil heat flux plates at two and six centimetre depths were

taken using the soil averaging thermocouples (Campbell Scientific, Inc., Logan UT, USA). This soil temperature and water content data were used to correct the soil heat flux measurements for the energy stored above the plates. A temperature and humidity probe (Model HMP 45 C, Campbell Scientific, Inc., Logan UT, USA) was also installed at canopy height and all the sensors on the flux tower were sampled at 10 Hz frequency by a data logger (Model CR5000, Campbell Scientific, Inc., Logan UT, USA) programmed to process output signals at 30 min intervals. The high frequency eddy covariance data was corrected for air density fluctuations, lack of sensor levelness (coordinate rotation), de-spiking, etc. using the EddyPro v 5.2.1 software (LI-COR, Inc., Lincoln NE, USA)

To establish the variation in soil moisture in the shallow soil layers across the study site, volumetric soil water content was sampled at the flux tower and at the sap flow monitoring stations using soil moisture probes (Model CS616 Campbell Scientific, Inc., Logan UT, USA). The probes at the flux tower sampled the depth range 0-15 cm. A 1.6 m deep profile pit was dug close to *Prosopis* trees at sap flow system #2. Here three CS616 soil moisture probes were installed in the depth ranges 0-50 cm, 50-100 cm and at 160 cm so as to quantify the changes in the profile soil water content in the root zone. Two additional sensors were installed in the depth ranges 0-50 and 100-120 cm close to the *V. karroo* trees. For *Prosopis*, most of the lateral roots were concentrated in the top 0-60 cm depth (Figure 10 a) with a prominent thick tap root extending vertically into the deeper soil layers. *V. karroo* trees on the other hand had a more dispersed root system with the lateral and feeder roots inclined at steep angles with respect to the soil surface and extending deeper into the ground (Figure 10b). *V. karroo* trees also had a prominent tap root extending deep into the soil.



Figure 10. Characteristics of the root system of: (a) *Prosopis*, and; (b) *V. karroo*

#### 4.5 Characterizing the geology of the *Prosopis* invaded aquifer

The first borehole ('Borehole #1', in Figure 8) was drilled at the invaded site close to the sap flow monitoring equipment at the beginning of the experiment on 01/08/2013. The borehole facilitated groundwater level monitoring. It also provided a means to identify relationships between plant water uptake and groundwater level changes. Given the need to interpolate the groundwater level information across the site, geophysical techniques were initially applied. Two resistivity transects were surveyed on 31 July 2013 and 1 August 2013 for the winter season and again on 18 December 2013 for the summer season. The aim of the resistivity measurements was to obtain a general overview of the shallow geology at the site (data was correlated with borehole logs) and also to interpolate the groundwater level across the site. It was also envisaged that additional surveys would be performed to identify changes in the

depth of the water table after the removal of the *Prosopis* invasions (i.e. time lapse analysis).

However, the method was unsuccessful in delineating the water table clearly (see Appendix B). Consequently, a decision was reached to drill additional boreholes, i.e. Boreholes #2, 3 and 4 in Figure 8. The additional boreholes were drilled between 07 and 11 October 2014. These provided additional site-specific groundwater monitoring points and allowed for the water table/potentiometric surface to be interpolated across the site.

Groundwater level was monitored at all boreholes on the site. Automatic water level loggers (Model 3001, Solinst Canada Ltd) collected data at hourly intervals and these were installed in Borehole 1 (02/08/2013), Borehole 3 (10/10/2014) and Borehole 4 (18/12/2014) indicated in Figure 8. A Solinst Baro logger (Model 3001, Solinst Canada Ltd) was installed in Borehole 1 on 02/08/2013 to monitor the atmospheric pressure. The groundwater level was also measured manually using a dip meter at each borehole during field visits.

## 4.6 Modelling water use by a *Prosopis* invaded catchment

### 4.6.1 Model overview

A detailed description of the original MOD16 model (Figure 11) is given by Mu *et al.* (2011). Here we focus only on revisions that have improved the performance of MOD16 at the *Prosopis* invaded site. The current operational MOD16 model (Mu *et al.*, 2011) has been shown to substantially underestimate ET especially in dry ecosystems (Figure 12a) (Ramoelo *et al.*, 2014; Dzikiti *et al.*, in review). For this reason, a model that is specifically parameterized for arid environments is required. However, the strength of the MOD16 algorithm is that it is, to a large extent, based on sound physical principles. In addition, it partitions ET into various components thereby providing information on the relative importance of different ET sources.

According to the Penman-Monteith equation, the latent heat flux ( $\lambda E$ , in  $\text{W m}^{-2}$ ) is calculated as;

$$\lambda E = \frac{\Delta A + \rho C_p (e_{sat} - e_a) / r_a}{\Delta + \gamma(1 + r_s / r_a)} \quad (2)$$

where  $\Delta$  is the slope of the saturation vapour pressure-temperature curve (Pa/K),  $\lambda$  is the latent heat of vaporization (J/kg),  $\rho$  is the density of air ( $\text{kg m}^{-3}$ ),  $C_p$  is the specific heat capacity of air at constant pressure (J/kg/K),  $e_{sat}$  is the saturated vapour pressure of the air (Pa),  $e_a$  is the actual vapour pressure of the air,  $\gamma$  is the psychrometric constant (Pa/K),  $r_s$  is the surface resistance (s/m),  $r_a$  the aerodynamic resistance and  $A$  is the available energy at the given surface. Mu *et al.* (2011) defined  $A$  (in  $\text{MJ m}^{-2} \text{d}^{-1}$ ) as;

$$A = R_n \quad (3)$$

where  $R_n$  is the net radiation absorbed by the surface. The net radiation is calculated using readily available climate data namely the daily solar radiation ( $S$ , in  $\text{MJ m}^{-2} \text{d}^{-1}$ ) and air temperature ( $T_a$  in  $^{\circ}\text{C}$ ) as;

$$R_n = (1 - \alpha)S + (\varepsilon_a - \varepsilon_s)(T_a + 273.15)^4 \quad (4)$$

where  $\alpha$  is the surface albedo,  $\varepsilon_a$  and  $\varepsilon_s$  are the emissivities of the atmosphere and surface, respectively. Comparison between the modelled net radiation and that measured by net radiometers at various flux towers across South Africa (Skukuza, Malopeni and Elandsberg) revealed systematic differences as shown in Figure 12b. Likely sources of error in the modelled net radiation resided with the albedo and emissivity calculations given that  $S$  and  $T_a$  were measured variables. Consequently we adopted alternative expressions to simulate the emissivities (Table 4) which have been used elsewhere in seasonally dry climates (Carrasco and Ortega-Farias *et al.*, 2007; Dzikiti *et al.*, 2014).

In the current MOD16 model, the available energy at the plant canopies ( $A_c$ ) and the soil surface ( $A_{soil}$ ) are calculated as linear functions of the fractional vegetation cover (Mu *et al.*, 2007 & 2011). In this study, we adopted a Beer's law approach (Table 4) in which the net radiation decreases exponentially with LAI from the top of the

canopies to the bottom, consistent with numerous other studies (Fisher *et al.*, 2008; Garcia *et al.*, 2013; Yuan *et al.*, 2010).

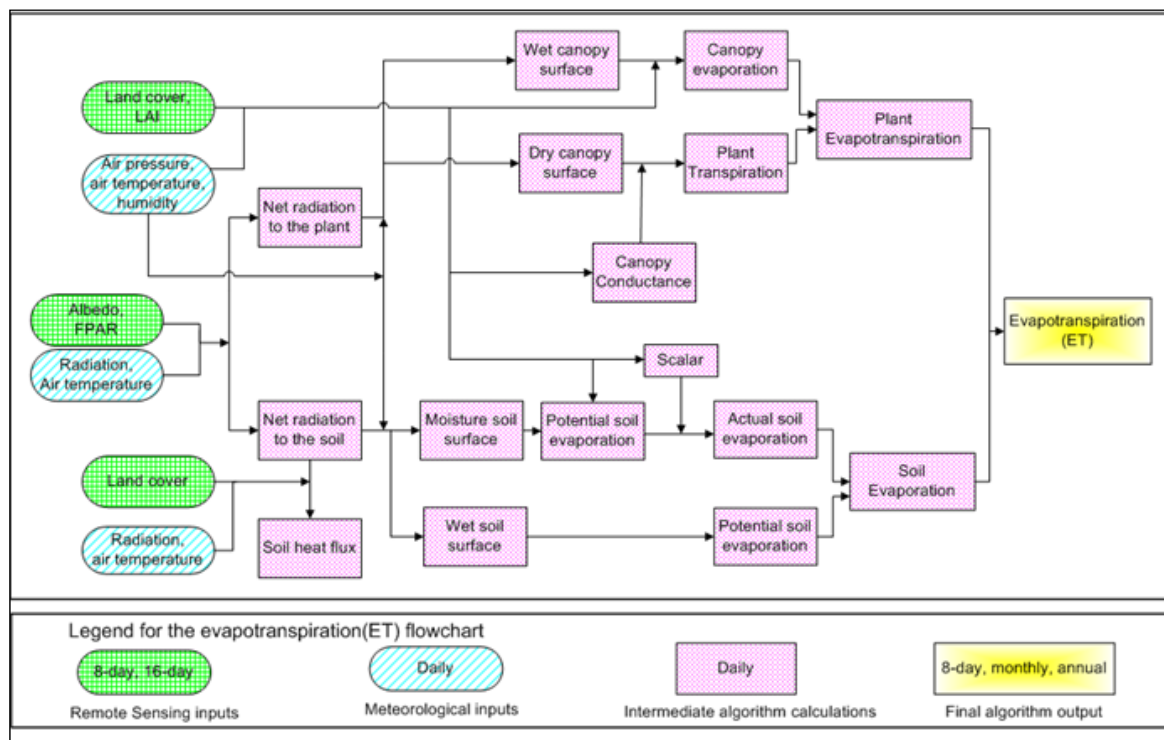


Figure 11. Schematic representation of the original MOD16 evapotranspiration model (after Mu *et al.*, 2011).

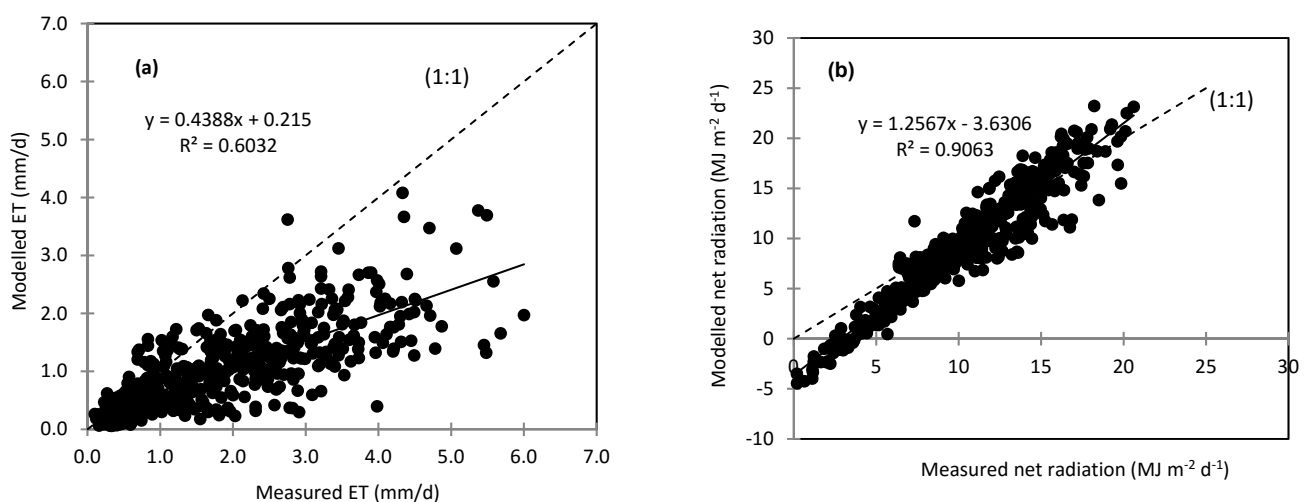


Figure 12. Performance of the original MOD16 model in predicting; (a) evapotranspiration at a semi-arid site, and; (b) the net radiation (Dzikiti *et al.*, in review). The dashed line represents a 1:1 relationship, while the solid line shows the correlation/relationship between modelled and measured values.

#### 4.6.2 Model sensitivity tests

In order to establish the parameters that had the largest influence on ET, a sensitivity test was performed on the original MOD16 model. This was done by varying the parameters one-at-a-time in ten steps over the range  $\pm 30\%$  of the values proposed by Mu *et al.* (2011) for specific biomes. Parameters linked to the transpiration sub-model of MOD16, namely the leaf area index (LAI) and the mean stomatal conductance per unit leaf area ( $C_L$ ), had the largest influence on ET (Figure 13). In the present version of MOD16 (Mu *et al.*, 2011), the surface conductance to transpiration ( $C_s=1/r_s$ ) is constrained only by climatic stress factors namely the minimum air temperature ( $T_{\min}$ ) and the vapour pressure deficit of the air (VPD) according to;

$$C_s = C_L \times f(T_{\min}) \times f(VPD) \quad (5)$$

where  $C_L$  is the mean stomatal conductance per unit leaf area. Full expressions for the stress factors  $f(T_{\min})$  and  $f(VPD)$ , which take values between 0 and 1, are shown in Table 4. Sensitivity tests showed that  $T_{\min}$ , based on the values proposed by Mu *et al.* (2011) did not have a significant effect on ET (Figure 13h). For this reason we replaced the current minimum temperature based stress factor with one that uses the average air temperature (Garcia *et al.*, 2013) (see Table 4) since both the minimum and maximum air temperatures likely have effects on stomatal conductance at the study site. The VPD stress function was replaced by

$$f(VPD) = 1 - kd_1 \times VPD \quad (6)$$

where  $kd_1$  is a parameter obtained by model optimization. Unlike the model by Mu *et al.* (2011) we also included a soil water content stress factor  $f(\delta M)$  according to the original equation by Jarvis (1976), also adopted in the ET Look remote sensing model by Bastiaansen *et al.* (2012) wherein:

$$G_s = C_L \times f(T_a) \times f(VPD) \times f(\delta M) \quad (7)$$

The soil water stress factor whose values also range from 0 to 1 was calculated as:

$$f(\delta M) = 1 - k_{s1} \times e^{-k_{s2} \times \delta M} \quad (8)$$

where  $k_{s1}$  and  $k_{s2}$  are parameters obtained by model optimization.  $\delta M$  is the soil water deficit calculated as

$$\delta M = \frac{SWC - SWC_{\min}}{SWC_{\max} - SWC_{\min}} \quad (9)$$

where SWC is the average soil water content on a given day,  $SWC_{\max}$  is the water content of saturated soils, and  $SWC_{\min}$  is the soil water content at the permanent wilting point.

Given the arid nature of the study site wherein our isotope studies revealed that the trees derived at most 30% of their water from the soil (most of the water derived from groundwater), the effect of the soil water stress factor was minimized by setting soil water deficit ( $\delta M$ ) close to 0 for this site. However, this stress factor could be critical in higher rainfall areas where the vegetation uses substantial amounts of soil stored water as illustrated in Dzikiti *et al.* (in review) for the savannah ecosystems at Skukuza and Malopeni. A biome specific value for the average stomatal conductance per unit leaf area (CL) was derived by inverting equation 2 according to Zhang *et al.* (1997). Measured values of  $R_n$ , transpiration, temperature, relative humidity and wind speed were used for data collected from 30 November to 4 December 2013 when the trees had reached full cover. This data was excluded from the subsequent simulations reported later. An average value of  $0.0057 \text{ m s}^{-1}$  per square metre of leaf area was derived for CL for the *Prosopis* invaded site.

Lastly, a component-by-component inspection of the ET predictions revealed that simulated night time ET was significantly higher than the measured values. We traced this to very high values of the relative surface wetness ( $f_{\text{wet}}$ ) which is calculated as the fractional relative humidity raised to the fourth power (Table 4). According to Fisher *et al.* (2008), the relative surface wetness represents the fraction of time when the

surface is wet. A slight modification to this expression (presented in Table 4) improved the night time ET predictions.

Table 4. Proposed revisions to the MOD16 evapotranspiration model using data from South African biomes.  $\epsilon_s$  and  $\epsilon_a$  are the emissivities of the surface and atmosphere, respectively; LAI the leaf area index,  $e_a$  the actual vapour pressure of the air,  $T_a$  the mean daily air temperature,  $A_c$  the available energy at the canopy level,  $F_c$ , the fractional vegetation cover (equal to FPAR in Mu *et al.*, 2011);  $A_{soil}$  is the available energy at the soil surface,  $k_R$  is the extinction coefficient for net radiation (equal to 0.6 according to Impens & Lemeur, 1969);  $G$  is the soil heat flux,  $T_{min\_open}$  is the minimum temperature for stomatal opening,  $T_{min\_close}$  is the minimum temperature for stomatal closure,  $VPD_{open}$  is the minimum vapour pressure deficit required for stomata to open,  $VPD_{close}$  is the maximum vapour pressure deficit for stomatal closure,  $SWC$  depicts the soil water content,  $SWC_{min}$  and  $SWC_{max}$  are the minimum soil water content and soil water content at saturation for specific sites and  $f_{wet}$  is the relative surface wetness and  $T_{opt}$  is the optimum temperature for plant growth (25°C).

Original equations	Revised equations	References
<b>Mu et al., 2011</b>		
1.0 Net radiation		
a) $\epsilon_s = 0.97$	$\epsilon_s = 0.95 + 0.01 * LAI$ ; $\epsilon_s = 0.98$ for $LAI > 3$	Bastiaansen <i>et al.</i> , 2002
b) $\epsilon_a = 1 - 0.26e^{(-7.77 \times 10^{-4} \times T^2)}$	$\epsilon_a = 1.31 \left[ \frac{e_a}{T_a} \right]^{\frac{1}{7}}$	Brutsaert, 1975; Carrasco and Ortega-Farias., 2007; Dziki <i>et al.</i> , 2014
2.0 Available energy		
a) $A_c = F_c \cdot A$	$A_{soil} = A e^{-k_R \cdot LAI} - G$	Garcia <i>et al.</i> , 2013; Fisher <i>et al.</i> , 2008; Yuan <i>et al.</i> , 2010
b) $A_{soil} = (1 - F_c) A - G$	$A_c = A - A_{soil}$	Yuan <i>et al.</i> , 2010
3.0 Transpiration sub-model		

a)  $f(T_{\min}) = \begin{cases} 1.0 & T_{\min} \geq T_{\min\_open} \\ \frac{T_{\min} - T_{\min\_close}}{T_{\min\_open} - T_{\min\_close}} & T_{\min\_close} < T_{\min} \leq T_{\min\_open} \\ 0.1 & T_{\min} < T_{\min\_close} \end{cases}$   $f(T) = 1.1814 [1 + e^{0.2(T_{opt}-10-T_a)}]^{-1} \cdot [1 + e^{0.3(-T_{opt}-10-T_a)}]^{-1}$  Garcia *et al.*, 2013

b)  $f(VPD) = \begin{cases} 1.0 & VPD \leq VPD\_open \\ \frac{VPD\_close - VPD}{VPD\_close - VPD\_open} & VPD\_open < VPD \leq VPD\_close \\ 0.1 & VPD \geq VPD\_close \end{cases}$   $f(VPD) = 1 - k_{d1} * VPD$  This study

c)  $f(SWC) = 1$   $f(\delta M) = 1 - k_{s1} * e^{-ks2\delta M}$  This study

d)  $f_{WET} = RH^4$   $f_{WET} = RH^{10}$  Marsh *et al.*, 2013; This study

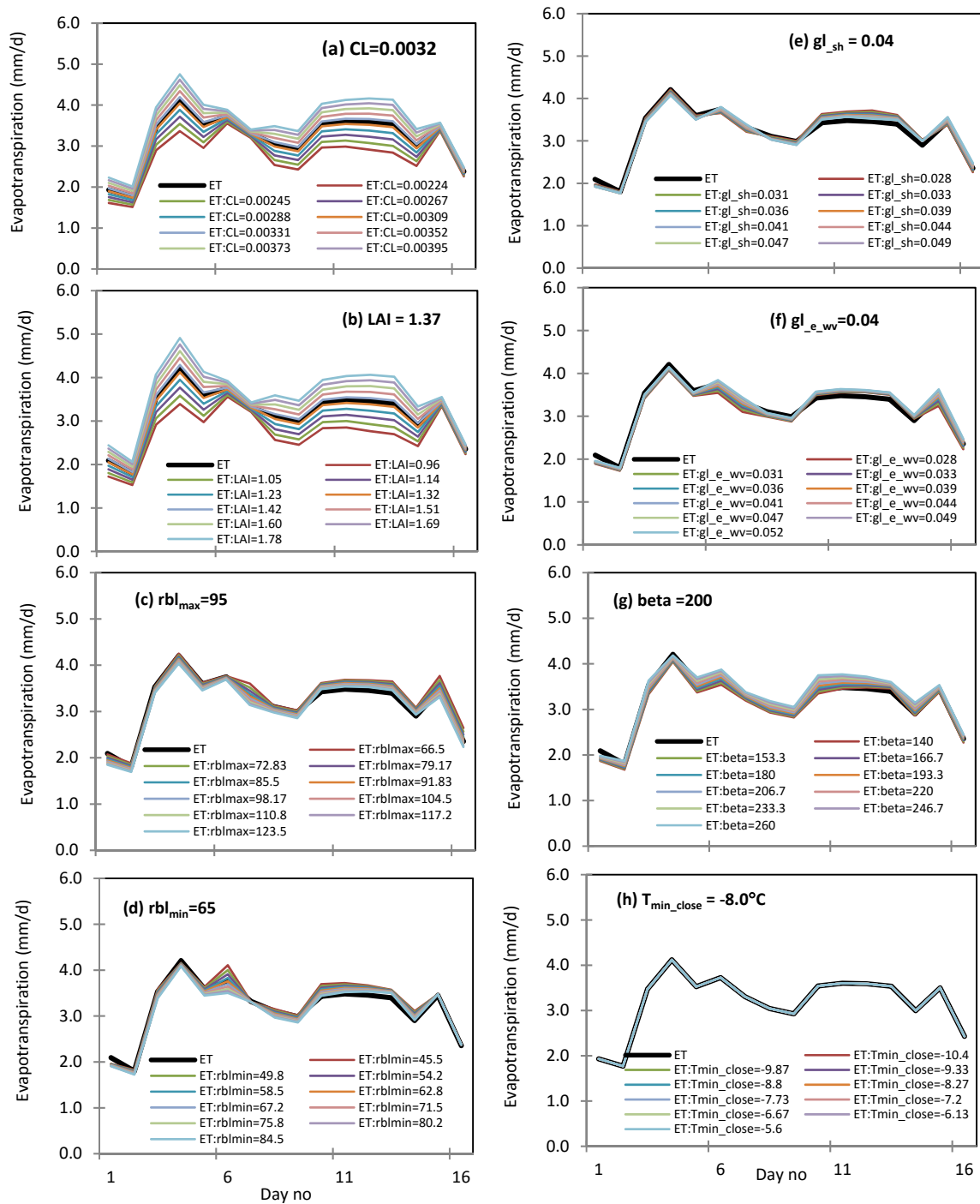


Figure 13. Sensitivity of MOD16 ET predictions to  $\pm 30\%$  changes in key parameters and variables namely the: (a) average stomatal conductance per unit leaf area – CL; (b) leaf area index – LAI (c) maximum boundary layer resistance –  $rbl_{max}$ ; (d) minimum boundary layer resistance –  $rbl_{min}$  (e) leaf conductance to sensible heat per unit LAI –  $gl_{sh}$ ; (f) leaf conductance to evaporated water per unit LAI –  $gl_{e\_wv}$ ; (g) power of the surface wetness fraction in the soil evaporation sub-model – beta, and (h) minimum air temperature for stomatal closure/opening –  $T_{min}$  (Dzikiti *et al.*, in review).

## 4.7 Groundwater recharge estimates

### 4.7.1 Available groundwater recharge data for the study area

Parsons and Wentzel (2007) define groundwater recharge as the addition of water to the zone of saturation either by the downward percolation of precipitation or surface water and/or the lateral migration of groundwater from adjacent aquifers. It is a key parameter that determines natural groundwater replenishment and level fluctuations. It is also the basis for the accurate quantification of groundwater resources for determining the modes of water allocation and groundwater resource susceptibility to climate change.

There is commonly a large degree of variability and consequently uncertainty, associated with reported groundwater recharge values. For example, various studies within the same physiographic area, e.g. quaternary catchment G21D in the Western Cape, have yielded strikingly different recharge estimates. Groundwater recharge in quaternary catchment G21D is estimated to be 81 mm a<sup>-1</sup> (Vegter, 1995). Bredenkamp and Vandoolaeghe (1982) estimated groundwater recharge in the Atlantis area, using a mass balance approach to be 25% of mean annual precipitation (MAP, 390 mm), i.e. 97 mm. DWAF (2006) estimated recharge in quaternary catchment G21D to be 15.4% of MAP (450 mm), i.e. 69 mm, using a chloride mass balance approach. DWAF (2006) also applied a generic, GIS based, groundwater recharge algorithm and estimated recharge in G21D to be 23.56 mm a<sup>-1</sup> or 5% of MAP. Woodford (2007) estimated groundwater recharge in the vicinity of Riverlands to be 13% of MAP (603 mm), i.e. 78 mm.

Groundwater recharge originates from local and regional precipitation and is highly variable across the Olifants-Doorn WMA. The highest groundwater recharge occurs in the mountainous areas where precipitation is high. For the remaining areas groundwater recharge is quite limited. DWAF (2006) estimated groundwater recharge in the vicinity of the study area to be less than 1 mm a<sup>-1</sup>. DWA (2012) estimated groundwater recharge in quaternary catchment E32E to be 0.13 mm a<sup>-1</sup>. This study, among other things, provides estimates of groundwater recharge before and after *Prosopis* invasions have been removed.

#### 4.7.2 Simulating groundwater recharge

Several methods for estimating groundwater recharge exist. However, choosing appropriate techniques is often difficult (Scanlon *et al.*, 2002) as various factors need to be considered, e.g. the space time/scales of the required recharge estimates, prevailing climatic conditions, etc. Small-scale differences in climate, geology, land use, topography and soil properties cause a high spatial and temporal variability of groundwater recharge making the assessment and predictions of recharge a challenge (e.g. Zagana *et al.*, 2007). Scanlon *et al.* (2002) subdivided techniques for estimating groundwater recharge on the basis of the hydrologic sources from which input data are obtained, i.e. surface water, unsaturated zone and saturated zone. Unsaturated zone techniques are applied mostly in semi-arid and arid regions, where the unsaturated zone is generally thick. Unsaturated zone techniques provide estimates of potential recharge based on drainage rates below the root zone (Scanlon *et al.*, 2002). However, in some cases drainage occurs laterally and does not reach the saturated zone.

Xu and Beekman (2003) reviewed commonly used recharge estimation methods in Southern Africa. The methods range from direct estimates with lysimetry and soil water fluxes to indirect estimates such as water balance equations and using tracers. Bredenkamp *et al.* (1995) used the chloride mass balance method to estimate recharge. Most of the groundwater recharge estimation methodologies are applicable at the large scale and in certain cases these ignore the influence of local scale processes. The successful prediction of groundwater recharge with models depends on the accuracy of the input data used and the correct representation of the system. For example, uncertainties still exist in the estimation of the ET component that would account for below/above-potential water use by vegetation and consequently affect recharge estimates.

This component of the study aims to quantify the impacts of *Prosopis* invasions on groundwater recharge. An unsaturated zone technique (Scanlon *et al.*, 2002) was applied, i.e. the process based model HYDRUS-1D (v 4.0, Simunek *et al.*, 2013). HYDRUS-1D utilizes climate data, soil physical properties and plant water use data, i.e. the transpiration rates associated with *Prosopis* invasions and *V. karroo* trees, to

quantify the potential downward fluxes from the unsaturated zone, i.e. groundwater recharge.

### 4.7.3 HYDRUS-1D

Unsaturated-zone modelling is used to estimate deep drainage below the root zone or groundwater recharge in response to meteorological forcing (Scanlon *et al.*, 2002). These methods may produce a wide range of recharge rates and thus it is required that the reliability of these methods be checked against field information, e.g. lysimeter data, soil water content data, etc. HYDRUS-1D has been used in several recent studies to estimate potential groundwater recharge.

HYDRUS-1D is a 1-dimensional physically based model, which can be used to estimate water fluxes, heat and solute transport in variably-saturated soil conditions. It uses Richards' equation for simulating variably-saturated flow and a Fickian-based advection-dispersion equation for heat and solute transport. In this study, only water flow was considered. The water flow equation incorporates a sink term to account for water uptake by plant roots (Feddes *et al.*, 1978). Potential transpiration and soil evaporation are inputs (time variable atmospheric boundary conditions). HYDRUS-1D v. 4.0 can be used to predict potential water flows in the vadose zone between the soil surface and the groundwater table. The graphical user interface includes data pre-processing and presentation of outputs. The pre-processing stage is used to specify inputs to discretize the soil profile into finite elements and to define vertical distribution of hydraulic parameters and root system. The output results are displayed in graphical format and written to output files at user-specified time intervals (Simunek *et al.*, 2013). For a detailed description of the model and the governing equations, the reader is referred to Simunek *et al.* (2013).

#### 4.7.3.1 Model Set-up

HYDRUS-1D was set-up to run from 01/08/2013 (day of simulation 0) to 31/07/2015 (day of simulation 730). The main processes simulated were water flow and root water uptake, i.e. the soil water balance (Figure 14), on a daily time step. The simulations were subjected to the following assumptions:

- the soil is homogenous and isotropic.
- the air phase does not affect liquid flow processes.

- that water flow due to thermal gradients is negligible.
- that no lateral flow occurs.

Conceptually, the model was set up as a one layered system, with a depth of 800 cm. The 800 cm is assumed to correspond to the depth of the unsaturated zone as the water strike at Borehole 1 occurred at this depth, i.e. the depth of the water table at the start of the simulation. The model requires potential evapotranspiration data, an estimate of the leaf area index (LAI) throughout the simulation and input parameters related to soil hydraulic properties and root water uptake. The boundary conditions of the model were:

- atmospheric upper boundary condition (precipitation, potential evapotranspiration)
- constant pressure lower boundary condition (0 cm to simulate the groundwater level)

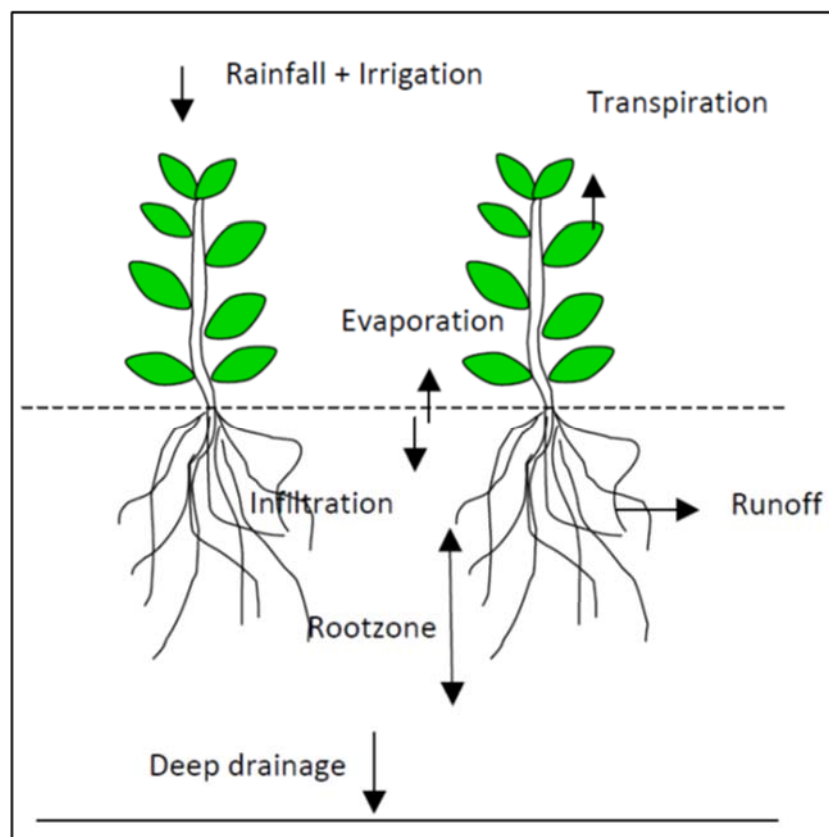


Figure 14. The soil water balance

The weather station installed at Brandkop was used to calculate the grass reference ET ( $ET_o$ ) according to the Penman-Monteith methodology (Allen *et al.*, 1998). The daily vegetation- or crop-specific potential evapotranspiration (PET, in mm/d) required by the model was calculated as:

$$PET = K_{cmax} \times ET_o \quad (10)$$

where  $K_{cmax}$  is the maximum value of the crop factor -Kc following rain (or irrigation), and was calculated as a function of weather data and vegetation height (Allen *et al.*, 1998).  $K_{cmax}$  was calculated as a function of the  $ET_o$  and the actual ET, measured with the eddy covariance method, during periods when water or energy limitations were minimum.  $K_{cmax}$  was estimated to be 0.74.

The LAI of both the *Prosopis* and *V. karroo* trees were measured during selected window periods, providing an estimate of seasonal changes in the LAI. The seasonal LAI associated with the *Prosopis* and *V. karroo* trees are presented in Table 5.

Table 5. The seasonal LAI associated with *Prosopis* and *V. karroo* trees

Season	Leaf Area Index	
	Prosopis	V. karroo
Summer	1.24	1.32
Autumn	1.3	1.01
Winter	0.71	0.23
Spring	1.41	0.88

A database of soil hydraulic parameters and root water uptake properties associated with various soil and vegetation types is included in the model. Soil hydraulic properties were not measured during this study and thus estimates were obtained from studies conducted in areas which exhibit similar soil types and climatic conditions. These estimates were used as initial values. HYDRUS-1D includes the functionality to automatically calibrate the soil hydraulic parameters. The parameters are adjusted within a user specified range and based on a comparison between the measured and simulated soil water content, the optimum parameter values are calculated. The initial values, the value range and the final values derived from the automatic calibration process are presented in Table 6.

Table 6. Parameters and values used in the HYDRUS-1D automatic calibration process

Parameter	Initial value	Value range	Final Value
Residual water content (Qr)	0.02	0-0.3	0.0822
Saturation water content (Qs)	0.35	0.3-0.6	0.3977
$\alpha$ of the soil water retention function	0.036	0.0001-0.6	0.01758
n of the soil water retention function	1.56	1.01-3	1.332
Saturated hydraulic conductivity (cm d <sup>-1</sup> )	15	5-100	8.354
l of the soil water retention function	0.5	-2-2	0.001822

Table 7. Summary of HYDRUS-1D inputs

Parameter	Input
Main processes	Water flow, root water uptake
Length units	cm
Number of materials and layers in the soil profile	1
Time units	Days
Initial Time	0 (1 August 2013)
Final time	730 (31 July 2015)
Initial time step	0.05
Minimum time step	1e-005
Maximum time step	0.5
Number of time variable boundary records	730
Initial condition	In the pressure head
Hydraulic model	Van Genuchten-Mualem
Hysteresis	No
Residual water content (Qr)	0.0822
Saturation water content (Qs)	0.3977
$\alpha$ of the soil water retention function	0.01758
$n$ of the soil water retention function	1.332
Saturated hydraulic conductivity (cm d <sup>-1</sup> )	8.354
$l$ of the soil water retention function	0.001822
Water uptake reduction model	Feddes
Potential evapotranspiration	Daily values calculated from weather data and vegetation characteristics
Vertical rectangular dimension (cm)	800
Root distribution	Relative distribution with the largest concentration (90%) from 0-150 cm and 600-800 cm
Atmospheric boundary condition	Top
Constant pressure boundary condition	Bottom
Initial pressure head	0 cm at the bottom with linear distribution to the top (- 10 000 cm)
Depth of observation nodes (cm)	50, 100 and 150

As HYDRUS-1D is mainly used for agricultural applications, the model database does not include root water uptake values for *Prosopis* and *V. karroo* trees, or even for similar vegetation types. The root water uptake parameters were therefore adjusted

based on observations between the simulated and observed root water uptake (transpiration).

Utilizing similar soil hydraulic properties, the potential groundwater recharge occurring from a profile planted with *Prosopis* and *V. karroo* trees will be estimated. Drainage from the bottom of the soil profile or bottom flux is assumed to be equal to the potential groundwater recharge. All input data used in the simulations are summarised in Table 7.

## 5 RESULTS AND DISCUSSION

### 5.1 Climatic conditions

The prevailing climate at the study site is known as a local steppe climate which is classified according to Köppen and Geiger as BSk which is characterized by hot and dry (often exceptionally hot) summers (Mucina and Rutherford, 2006). In this study daily total irradiance varied from less than  $8.0 \text{ MJ m}^{-2} \text{ d}^{-1}$  in mid-winter (July) to a peak of more than  $33.0 \text{ MJ m}^{-2} \text{ d}^{-1}$  during summer (late December) as shown in Figure 15a. More than 60% of the days were cloudless.

The annual average temperature during August 2013-July 2014 was  $18.7^\circ\text{C}$  compared with  $20.7^\circ\text{C}$  for the August 2014-July 2015 hydrological year. The maximum air temperature recorded during the study period was  $44.6^\circ\text{C}$  recorded in early January 2014 while the minimum temperature was  $-4.8^\circ\text{C}$  reached in July 2014 (Figure 15b). Maximum air temperature exceeded  $40^\circ\text{C}$  in six months of the year (November-April) in each of the hydrological years. Minimum relative humidity tended to be very low being less than 10% in the months except June and July 2015. Consequently, the vapour pressure deficit of the air was very high with peak values as high as 8.0 kPa during warm dry days (Figure 15c).

The study area is located at the boundary of the summer and winter rainfall regions of South Africa. For this reason the area received, albeit small amounts, of rainfall throughout the year but with most of the rain falling in winter (Figure 15d). Daily total reference evapotranspiration ( $\text{ET}_o$ ) was very high in summer reaching close to 8.0 mm/d during the December-January period. According to Allen *et al.* (1998), reference evapotranspiration is defined as evapotranspiration from a short grass that uniformly covers the ground and is actively growing and not short of water. This gives an indication of the atmospheric evaporative demand.

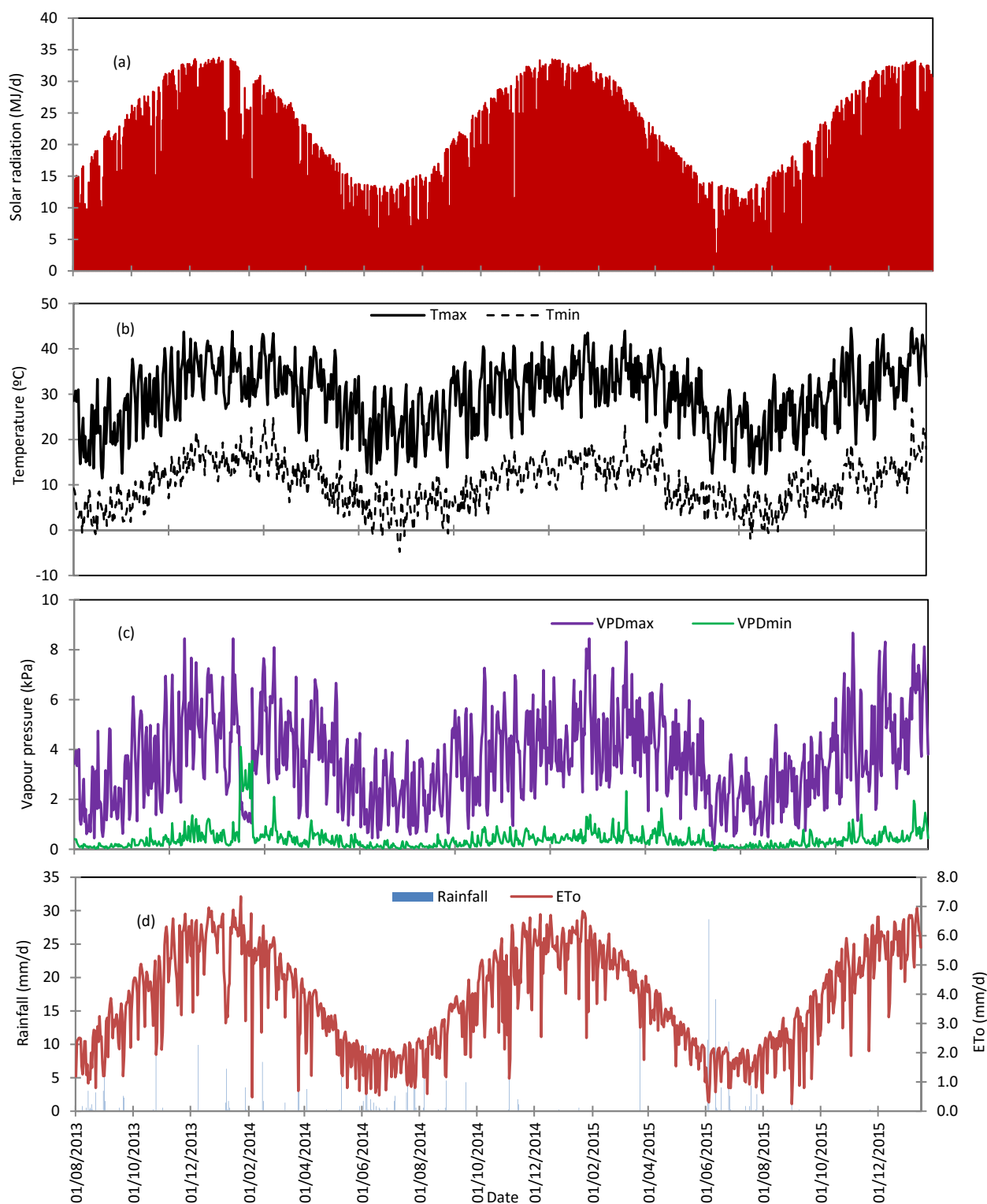


Figure 15. Seasonal changes in; a) the daily solar radiation, b) maximum and minimum air temperature, c) maximum and minimum vapour pressure deficit, and; d) daily rainfall and the reference evapotranspiration at Brandkop farm.

Table 8. Summary of the monthly weather conditions at Brandkop farm from August 2013 to January 2016.

Year	Month	Mean daily solar radiation (MJ m <sup>-2</sup> )	T <sub>max</sub> (°C)	T <sub>min</sub> (°C)	Rainfall (mm)	ET <sub>0</sub> (mm)	RH <sub>max</sub> (%)	RH <sub>min</sub> (%)	Average wind speed (m s <sup>-1</sup> )	
2013	Aug	13.4	33.3	-0.9	18.0	81.3	94.5	6.6	1.7	
	Sept	20.1	33.6	0.9	6.4	121.9	94.3	6.0	1.7	
	Oct	24.2	37.8	3.5	10.4	170.8	90.9	3.0	2.0	
	Nov	29.6	43.7	7.0	0.5	221.5	90.7	5.1	2.3	
	Dec	31.2	42.2	10.8	9.9	258.2	85.4	5.5	2.5	
2014	Jan	27.2	43.9	11.5	13.7	215.3	94.1	3.4	1.9	
	Feb	26.1	43.4	9.9	8.9	198.5	93.9	6.7	2.0	
	Mar	23.5	40.4	6.2	16.0	176.9	91.9	4.1	1.9	
	Apr	18.0	40.5	5.2	3.6	130.4	92.0	6.6	1.6	
	May	12.4	39.7	2.9	6.4	85.9	93.3	6.9	1.4	
	Jun	10.7	31.8	-1.5	21.3	61.5	94.9	10.1	1.5	
	Jul	11.5	32.2	-4.8	21.8	68.9	95.2	7.0	1.4	
	<b>Total</b>					<b>136.9</b>	<b>1 791.1</b>			
	2015	Aug	14.3	31.4	-0.7	13.2	94.6	94.2	5.6	1.6
		Sept	20.5	37.0	3.0	4.3	137.3	91.6	4.0	1.7
		Oct	25.2	40.5	3.2	0.0	197.4	85.5	4.0	2.2
		Nov	27.4	40.6	8.3	15.0	202.0	91.2	7.9	2.3
Dec		31.4	41.4	9.0	0.3	244.2	83.5	4.6	2.5	
Jan		29.9	43.5	8.9	0.5	244.4	87.6	3.8	2.3	
Feb		28.5	40.7	8.5	0.0	201.0	85.0	5.1	2.4	
Mar		23.3	27.1	9.8	12.5	186.0	87.9	6.9	1.8	
Apr		18.4	40.1	4.3	0.0	134.9	84.3	7.2	1.7	
May		13.8	37.9	1.7	0.0	92.9	89.3	7.6	1.1	
Jun		10.2	30.9	1.9	73.4	54.7	93.3	13.0	1.4	
Jul		10.7	30.2	-1.9	8.9	60.3	94.4	10.9	1.2	
<b>Total</b>					<b>128.1</b>	<b>1 849.7</b>				
2016	Aug	14.0	34.3	-0.6	7.1	88.0	94.7	7.3	1.3	
	Sept	17.6	34.3	2.6	0.3	126.2	91.6	8.8	1.9	
	Oct	25.0	44.6	3.8	0.0	199.5	84.2	6.1	2.0	
	Nov	28.2	42.1	5.1	0.3	212.7	90.4	3.0	2.4	
	Dec	30.0	44.6	8.2	0.0	239.5	81.7	8.2	2.2	

The annual  $ET_0$  from August 2013 to July 2014 of 1 791 mm and 1 850 mm from August 2014 to July 2015 was more than ten times higher than the rainfall of only 137 and 128 mm, respectively (Table 8). This rainfall was slightly higher than the average annual record for Brandkop which is around 120 mm. More than 50% of the total annual rainfall was received in three months in winter (June-August) with June and July being the wettest months. The monthly atmospheric evaporative demand, depicted by  $ET_0$ , varied from 54.7 mm in winter to a peak of 258.3 mm in summer.

Wind speed varied slightly between months with mean values ranging from 1.1 to 2.5 m s<sup>-1</sup>. Prevailing winds during the study period were south to south-westerly in August-October changing to south-easterly in the early summer months from November to January (data not shown). Wind direction was highly variable in the months February to July with no clear prevailing wind direction.

## 5.2 Water use by *Prosopis* and co-occurring *V. karroo* trees

### 5.2.1 Allometric relations

Processing of the heat pulse velocity sap flow data requires information on the sapwood area, wood density, wood moisture fraction and wounding widths to convert the raw HPV signals (in cm h<sup>-1</sup>) into volumetric sap flows (in L h<sup>-1</sup> or m<sup>3</sup> h<sup>-1</sup>). Wounding occurs due to the drilling and implantation of sensors into the trees which disrupts the normal flow of water through the xylem vessels. Estimating the size of the conducting sapwood area is particularly difficult as this often requires cutting down of the instrumented trees. In this section, we develop relationships between the sapwood depth and readily measurable plant attributes, e.g. the external bark-to-bark diameters at the stem, branch, and roots levels where sap flow sensors were installed in this study.

To achieve this, we felled nine *Prosopis* and four *V. karroo* trees in the size classes representative of the sap flow instrumented trees. We then cut the stems approximately 15 cm above the ground where stem sap flow sensors are installed. The tap roots were partially excavated and also excised about 15 cm below the base of the stem where the tap root sap flow sensors are installed. The sapwood-heartwood boundary was quite clear by visual inspection for *Prosopis* (Figure 16a) while the

heartwood of *V. karroo* was difficult to distinguish from the sapwood (Figure 16b). The brown portions in Figure 16a represent the heartwood while the light portions represent the conducting sapwood area where xylem vessels are actively involved in water transport in *Prosopis*. We injected methylene blue dye in the stem of the *V. karroo* trees and the blue trace in Figure 16b shows the extent of the sapwood.

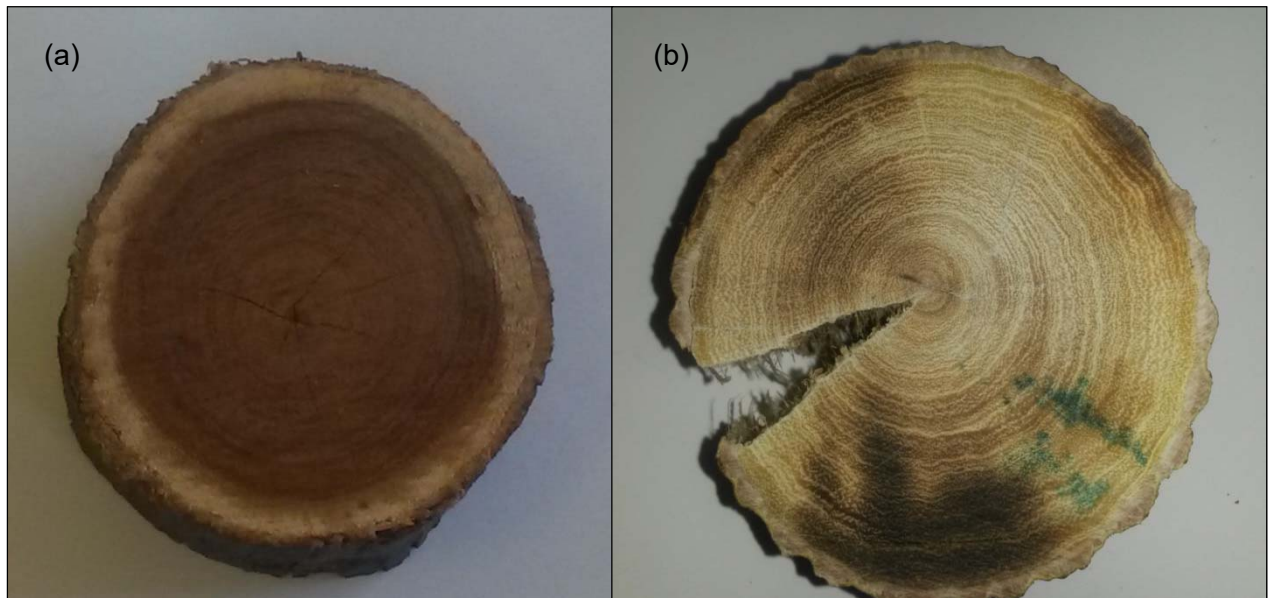


Figure 16. Sapwood-heartwood relationships for a (a) *Prosopis* and (b) *V. karroo* tree at Brandkop farm. The blue line in (b) depicts the trace of methylene blue dye indicating the extent of the sapwood depth.

The sapwood area and the bark-to-bark cross sectional area of both the stem and branches of *Prosopis* are related by quadratic functions (Figure 17 a & b). A similar relationship was observed by Dzikiti *et al.* (2013b) for the stem section of *Prosopis* in a study conducted near the town of Kenhardt in the Northern Cape. However, the sapwood-tap root cross sectional area relationship for *Prosopis* (Figure 17c) on the other hand is quite linear with a high coefficient of determination ( $R^2=0.97$ ). Similarly the tap root cross sectional area at 15 cm below the ground is also linearly related to the stem cross sectional area 15 cm above the ground (Figure 17d). The application of this data is that with measurements of the stem, branch and tap root bark-to-bark diameters, it is therefore feasible to estimate the size of the conducting sapwood area without cutting the trees. This information is also useful for estimating the sapwood

area index (m<sup>2</sup> of sapwood per m<sup>2</sup> of ground) for scaling up transpiration rates from individual trees to the stand level.

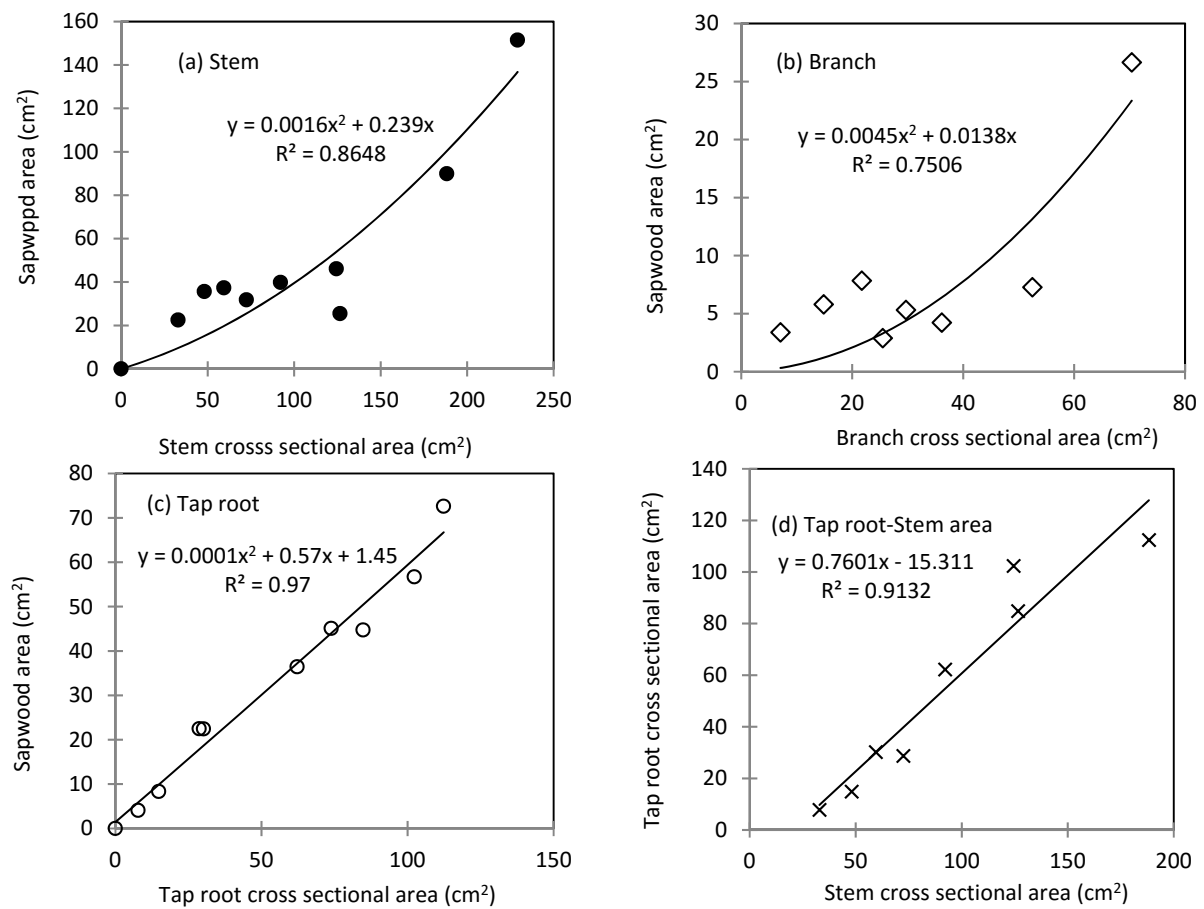


Figure 17. Allometric relationships between the size of the conducting sap wood area and (a) stem cross sectional area, (b) branch cross sectional area and (c) tap root cross sectional area for *Prosopis*. Graph (d) shows the tap root to stem cross sectional area relationship.

The sapwood to heartwood ratio of *Prosopis* was largest in the roots and smallest in the branches. For the nine excised *Prosopis* trees, Figure 18 shows that the sapwood area accounted for a maximum of 40% of the branch cross sectional area, 65% of the stem cross sectional area, and up to 80% for the tap root cross sectional area. This pattern implies that the hydraulic conductance is highest in the roots followed by the stems and lastly the branches. So *Prosopis* roots are therefore more efficient in facilitating water transport compared to the above ground organs.

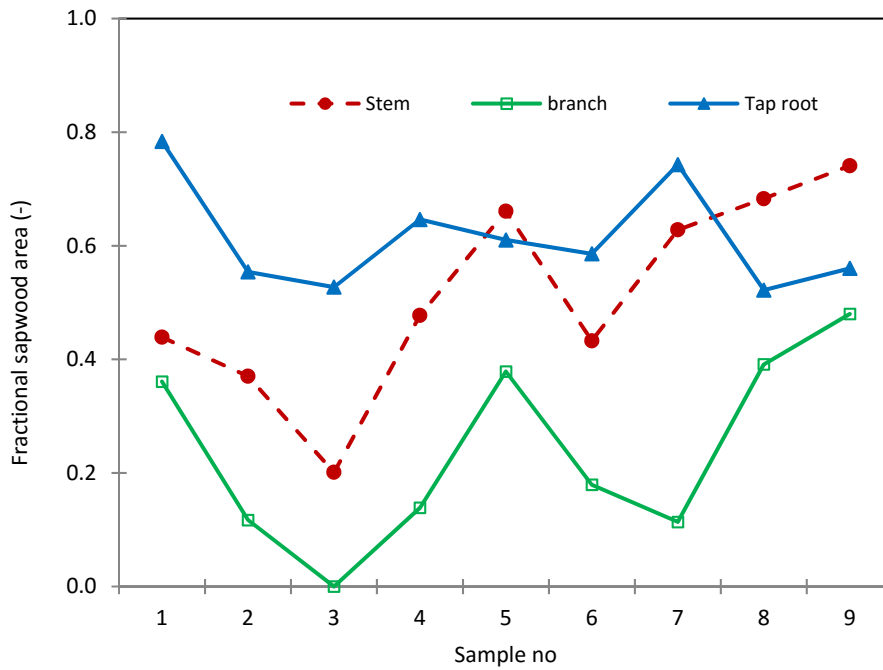


Figure 18 Sapwood as a fraction of the stem area for the tap root, stem and branches of *Prosopis* trees

In contrast to *Prosopis* the allometric relations for *V. karroo* showed strongly linear relationships between the sapwood and the stem cross sectional area (Figure 19a) and the tap root cross sectional area (Figure 19b). Fewer *V. karroo* trees were cut for this experiment given that they are indigenous species.

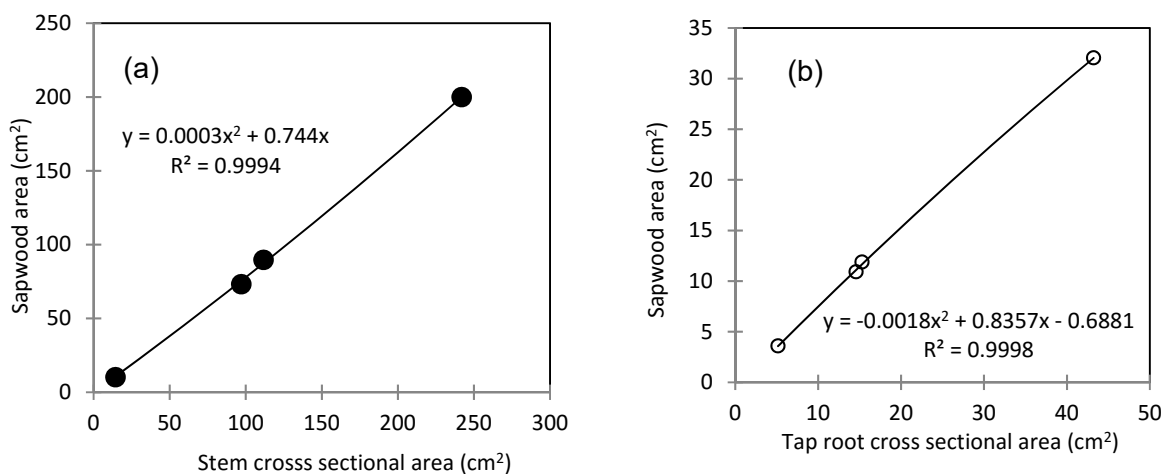


Figure 19. Allometric relations for *V. karroo* where (a) shows the sapwood area – stem cross sectional area relationship, and (b) sap wood area-tap root cross sectional area relationship

### 5.2.2 Tree transpiration rates

The actual volumes of water taken up by the invasions and the indigenous trees were calculated from the HPV data using the approach described by Burgess *et al.* (2001). Wounding corrections were applied according to the method by Swanson and Whitfield (1981). As expected, transpiration by both species peaked in summer when the LAI and atmospheric evaporative demand were highest (Figure 20). In Figure 20 we compare the typical daily water use by a *Prosopis* tree with peak LAI of 1.63 and that of a *V. karroo* tree with a peak LAI of about 0.93. The trees were growing less than 100 m apart.

Maximum water use by the *V. karroo* tree was approximately 58 L d<sup>-1</sup> compared to around 60 L d<sup>-1</sup> for a *Prosopis* tree (Figure 20). There was no statistical difference in the water use by the two species ( $p > 0.001$ ) over the one year period despite *V. karroo* having a small transpiring leaf area than *Prosopis*. The result suggests that at the individual tree scale, *V. karroo* had a higher transpiration rate per unit leaf area than *Prosopis* under similar conditions. The relatively low transpiration by individual *Prosopis* trees is likely an adaptation strategy to survive the dry conditions at the site. Some species sacrifice the active xylem converting the sapwood into heartwood to reduce the carbon cost of maintaining a large number of xylem vessels when photosynthesis is reduced, e.g. when water is not readily available.

Average tree density, determined from tree counts in five 20 m x 20 m quadrants located in different parts of the forest was 613 trees per hectare for *Prosopis* and 100 trees per hectare for *V. karroo*. Stand level transpiration by each species was calculated as the weighted sum of transpiration by trees in three stem size classes with the weighting functions being the number of trees in a particular stem size class per hectare.

At the stand scale, total transpiration from 02 August 2013 to 01 August 2014 was 634 mm. Of this amount, *Prosopis* contributed about 86% (543 mm) of the total compared to only 14% (90 mm) by *V. karroo* (Figure 21). Therefore even if the transpiration by individual trees appears to be higher for *V. karroo* than for *Prosopis*, *Prosopis* contributed up to six times more to the stand transpiration flux than *V. karroo* because of its higher plant density. In a review by Cavaleri and Sack (2010), they

noted that indigenous vegetation were equally likely to use as much water as the alien vegetation in some ecosystems, consistent with our observations here.

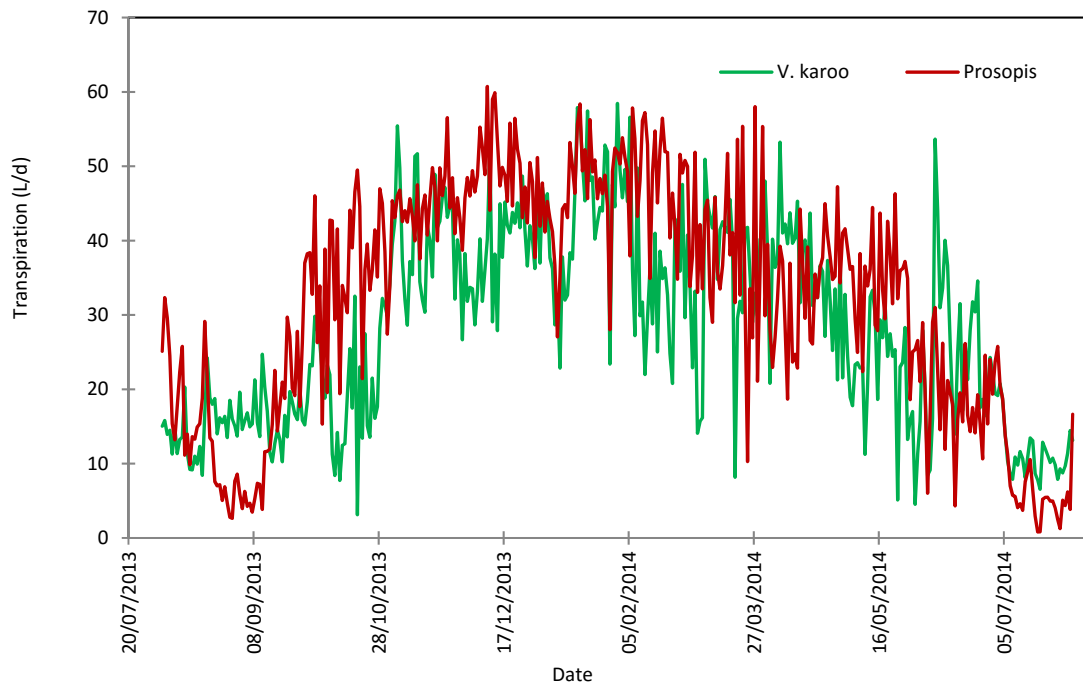


Figure 20. Comparison of daily transpiration by a *V. karoo* (LAI = 0.93) and a *Prosopis* tree (LAI ~ 1.63)

*Prosopis* transpiration at this site, where the groundwater level fluctuated between 4.0 and 8.5 m below the ground, was higher than that at another invaded site near the town of Kenhardt in the Northern Cape where annual transpiration was less than 100 mm and the groundwater level was much deeper varying between 10 and 12 m (Dzikiti *et al.*, 2013b; Fourie *et al.*, 2002). Trees at the Kenhardt site were also relatively smaller than the ones studied in the current project.

Soil water content in the root zone of both *Prosopis* and *V. karoo* hovered around 4% (Figure 22 a & b) although relatively heavy storms in June 2015 raised the soil water content to between 12 and 16%. This was the highest water content recorded throughout the monitoring period.

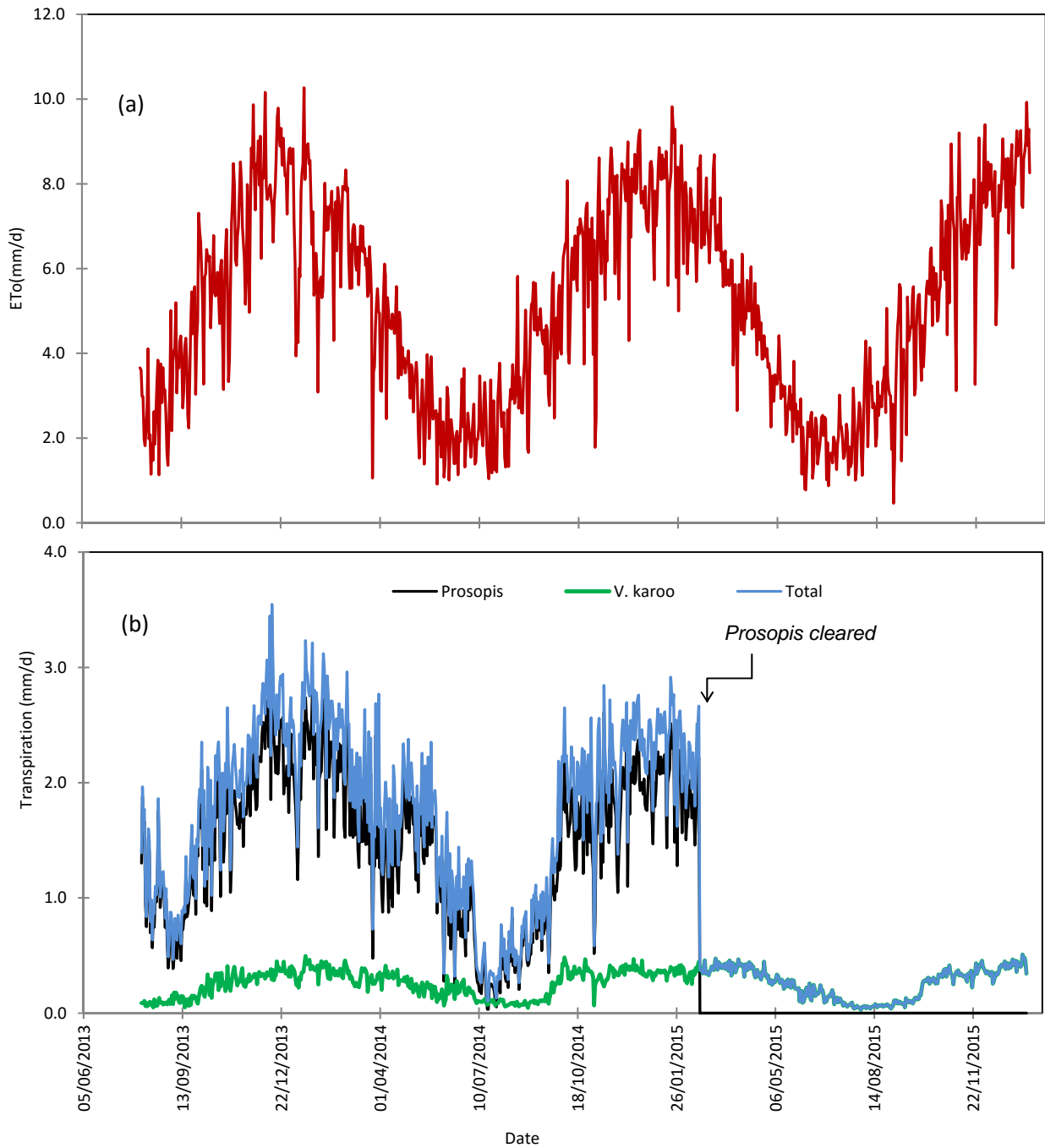


Figure 21. (a) Daily reference evapotranspiration from 02 August 2013 to 14 January 2016 at Brandkop farm. (b) Daily transpiration by *Prosopis* (black line), *V. karoo* (green line) and the total transpiration (*Prosopis* + *V. karoo* – blue line)

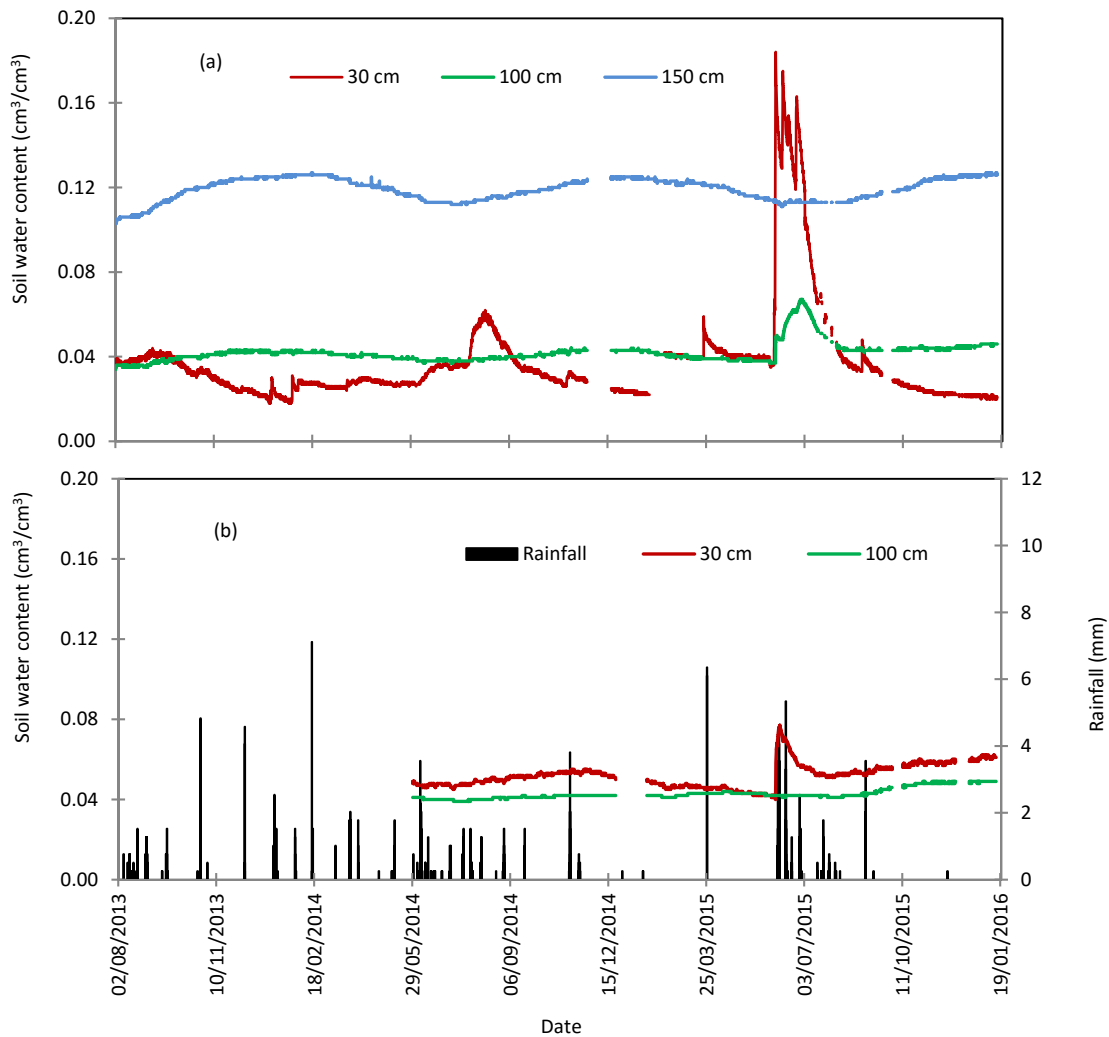


Figure 22. Variation in soil water content in the root zone of: (a) *Prosopis* and (b) *V. karroo* trees

Transpiration by both *Prosopis* and *V. karroo* was linearly related to the atmospheric evaporative demand- $ET_0$  (Figure 23). *Prosopis* transpiration on average translated to 27% of  $ET_0$  while that of *V. karroo* was only 5% of  $ET_0$ . These are equivalent to basal coefficients of 0.27 for *Prosopis* and 0.05 for *Prosopis* and *V. karroo* according to Allen *et al.* (1998). Cumulative rainfall over the entire data collection period from 02 August 2013 to 16 January 2016 (265 mm) was of a similar order of magnitude to the transpiration by the indigenous *V. karroo* (233 mm) (Figure 24). Water use by *Prosopis* on the other hand (845 mm) was three times higher than the rainfall over the same period.

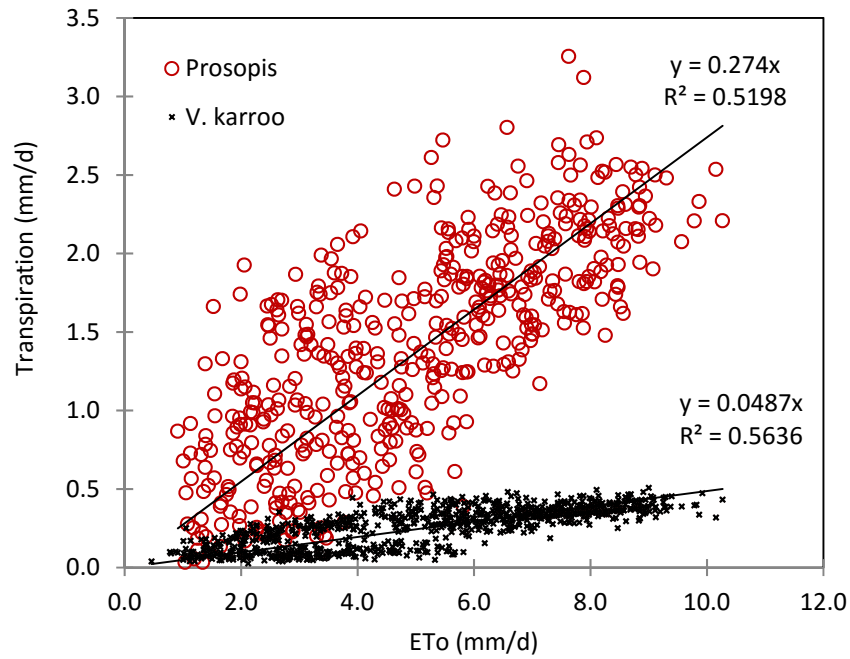


Figure 23. The basal coefficients of *Prosopis* (brown circles) and *V. karroo* (black stars) at Brandkop farm

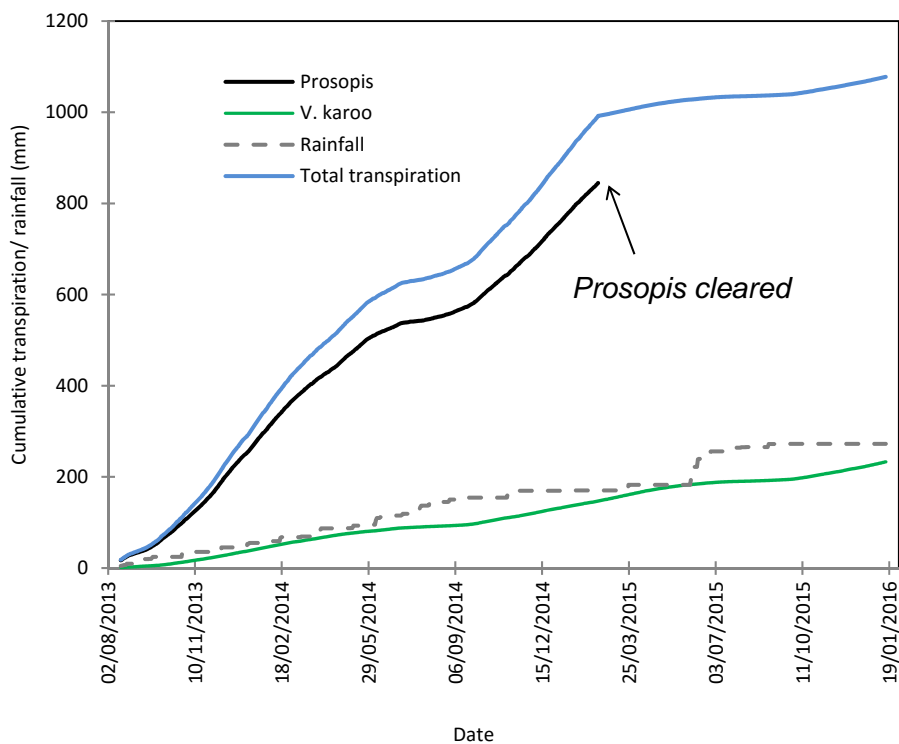


Figure 24. Cumulative rainfall (grey dotted line), cumulative transpiration by *Prosopis* invasions (black line) and the indigenous *V. karroo* (green line) from 02 August 2013 to 15 January 2016. The blue line depicts the cumulative total transpiration by the two tree species.

### 5.2.3 Root water uptake dynamics

The root water uptake patterns of *Prosopis*, but not *V. karroo* appeared to be influenced by the groundwater level depth. When the water table was high during February 2014, all the water taken up by *V. karroo* was transpired, i.e. positive sap flow towards the canopy (Figure 25 a & b). On the other hand, hydraulic redistribution (Figure 26 a & b) was apparent with *Prosopis*. Excess water taken up by the *Prosopis* tap roots was channelled towards the shallow soil layers by the lateral roots. The apparent increase in the soil water content in the 100 and 160 cm depths during periods of high water use in summer by *Prosopis* (Figure 22a) is likely a result of the redistribution phenomenon.

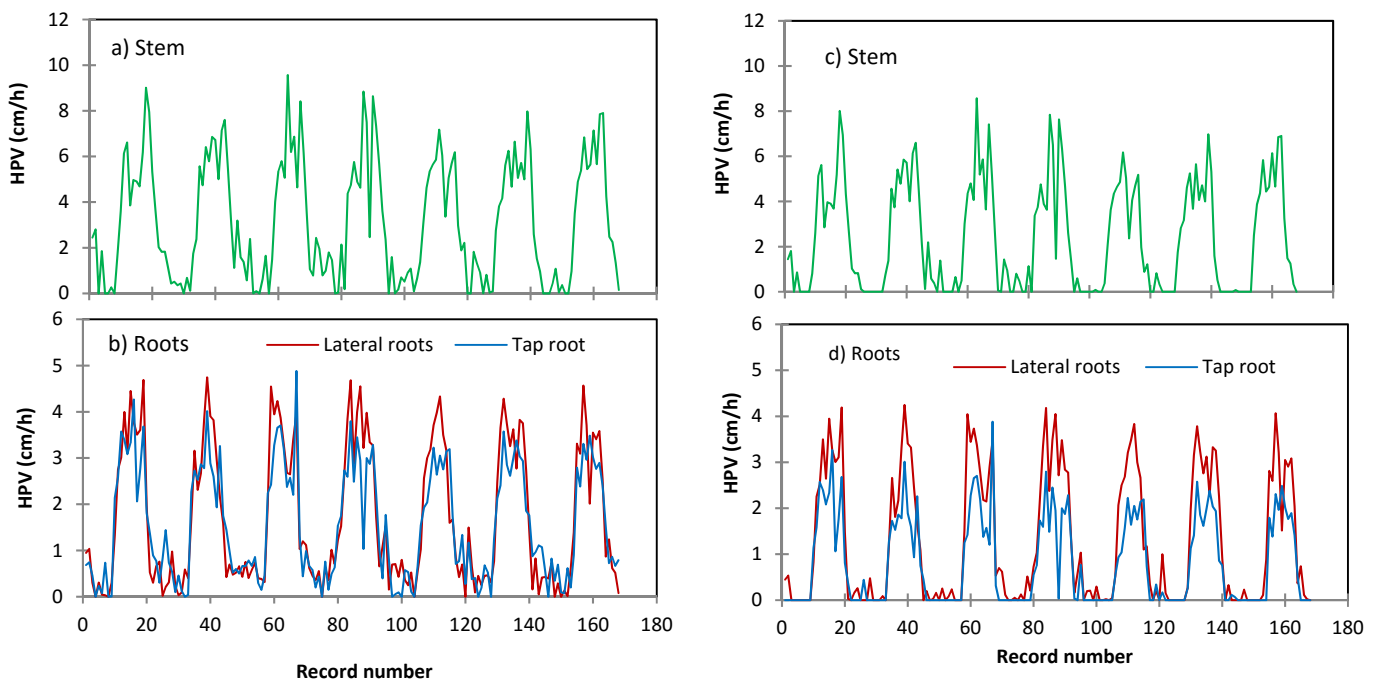


Figure 25. Water uptake patterns by a *V. karroo* tree when the groundwater level was high (~ 4 mbgl) after flooding on site with (a) showing the course of stem sap flow, and; (b) the tap and lateral root water uptake patterns from 20 to 26 February 2014. Sap flow dynamics of (c) the stem and (d) tap and lateral roots when the groundwater level was low (~ >8 mbgl deep) from 20 to 26 February 2015.

However, when the water table dropped to beyond 7 m below the surface in February 2015, still all the water taken up by *V. karroo* was transpired (Figure 25 c & d). Hydraulic redistribution in *Prosopis* ceased (Figure 26 c & d). Water taken up by both the tap and lateral roots was transpired. The changes in the root water uptake

patterns for *Prosopis* can be explained by the fact that, when groundwater level was shallow, the hydraulic path length and hence the hydraulic resistance for water transport from the saturated zone to the evaporating sites in the trees was small. Therefore the trees abstracted large quantities of water via the tap root.

Given the hydraulic limitations in the stem's sapwood for *Prosopis*, the excess water taken up by the tap roots was channelled away from the tree trunks. This was enhanced by a strong lateral water potential gradient given that *Prosopis*' lateral roots grow in very dry soil close to the surface. However, when the groundwater table dropped, the hydraulic resistance in the tap root likely increased such that water supply by the tap root alone was not sufficient to meet the tree's transpiration demand. Consequently, the hydraulically redistributed water stored in the shallow soil layers was also taken up to meet the trees' transpiration demand leading to a reversal in the lateral root water uptake patterns.

It is not clear why *V. karroo* trees growing right next to the *Prosopis* trees did not exhibit similar root water uptake patterns to *Prosopis*. A possible explanation is that, firstly the stem of *V. karroo* trees has a high sapwood to heartwood ratio than *Prosopis* (Ntshidi, 2015). This lowers the hydraulic resistance and high water volumes can therefore be transported at a given time than in *Prosopis*. Thus all the water taken up by *V. karroo*'s tap and lateral roots could be transpired. In addition, the lateral roots of *V. karroo* are steeply inclined into the soil (compared to those of *Prosopis*) so that the water potential gradient between the stem and the lateral roots is relatively small likely inhibiting hydraulic redistribution (Dawson, 1993).

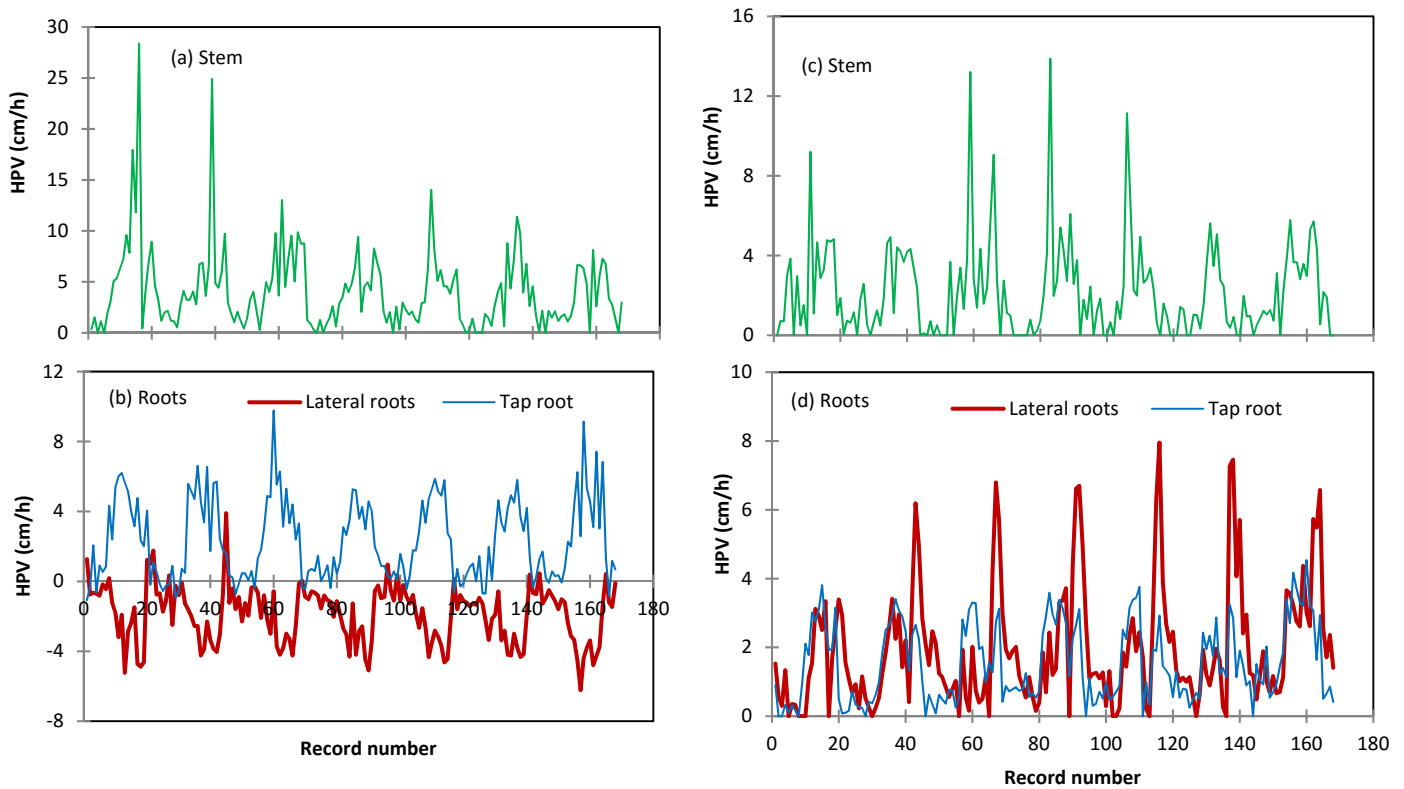


Figure 26. Water uptake patterns by a *Prosopis* tree when the groundwater level was high (~ 4 mbgl) after flooding on site with (a) showing the course of stem sap flow, and; (b) the tap and lateral root water uptake patterns from 20 to 26 February 2014. Sap flow dynamics of; (c) the stem and (d) tap and lateral roots when the groundwater level was low (~ >8 mbgl deep) from 20 to 26 February 2015.

There is abundant literature that supports the opportunistic behaviour of *Prosopis* regarding access to water (Schachtschneider, 2010; Schachtschneider and February, 2013). These studies show that *Prosopis* frequently switches between the soil and groundwater sources depending on the abundance of water in either source. This study therefore provides direct evidence of this phenomenon under different groundwater level regimes.

### 5.3 Site hydrogeology

The characteristics of the boreholes are presented in Table 9. The rotary percussion drilling method was used and boreholes were generally drilled to the depth at which shale was encountered as it is assumed that root activity would not continue beyond this depth. Borehole #4 was drilled deeper, i.e. to 30 m, to study the underlying geology and to investigate whether additional water strikes would occur within the shale.

The borehole specifications are:

- Solid PVC casing installed as required with slotted/perforated PVC casing at water strike depths
- Outer diameter of PVC casing = 160 mm
- Gravel pack was installed in the borehole annulus at depths corresponding to the slotted/perforated PVC casing. The rest of the annulus was backfilled.
- Boreholes were developed until all sand was removed and the water was clear (no sediment).
- Concrete slabs and lockable caps were installed at each borehole.
- The blow yield was measured with a V-notch weir after borehole development.

Images captured during borehole drilling are presented in Figure 27. The ground elevation and the elevation of the borehole collar was accurately surveyed on 3 May 2015.

Table 9. Borehole characteristics

BH ID	Date Drilled	Lat.	Long	Elev. (mamsl)	Depth (m)	Collar Height (m)	Blow Yield (L s <sup>-1</sup> )
Borehole #1	02/08/2013	-31.232539	19.20283	387.54	12.04	0.42	-
Borehole #2	08/10/2014	-31.230538	19.19964	386.75	9.02	0.49	0.3
Borehole #3	08/10/2014	-31.231709	19.20631	385.7	15.95	0.43	1.47
Borehole #4	09/10/2014	-31.235267	19.201998	388.68	30.30	0.38	1.71



Figure 27. Borehole drilling at Brandkop farm

During borehole drilling, samples (Figure 28) were collected at 1 m intervals. The samples were used to construct geological logs of the boreholes (Appendix B). A geological cross-section, for a transect line from Borehole #2 to Borehole #4 was also constructed (Figure 29). The borehole log and geological cross-section was drawn in the Excel-based software Borehole Logging v. 1.0 developed by H. Jia (University of Fort Hare) and Y. Xu (University of the Western Cape). The development of the software was funded by the Water Research Commission.

The geology of the specific site is generally characterised by Tertiary to recent (Quaternary) sand deposits which overly shales of the Van Rhynsdorp Group. At the interface of the overlying sand covering and underlying shales, a layer characterised by coarse sand and boulder chips/gravels commonly occurs. This interface layer of gravels is the water bearing horizon. This aquifer system may be described as an alluvial aquifer system, characterised by semi- to unconsolidated alluvial sands and gravels. These aquifer systems commonly occur along river courses. Borehole yields are reported to vary due to grain size and thickness of deposits, as well as the efficiency of borehole development (Titus *et al.*, 2002). Clay horizons also occur, however, these are not continuous across the site. The measured blow yields, i.e. 0.3-1.71 L s<sup>-1</sup> are within the range of values (0.1 and 2.0 L s<sup>-1</sup>) reported for intergranular and fractured aquifers (DWA, 2012).

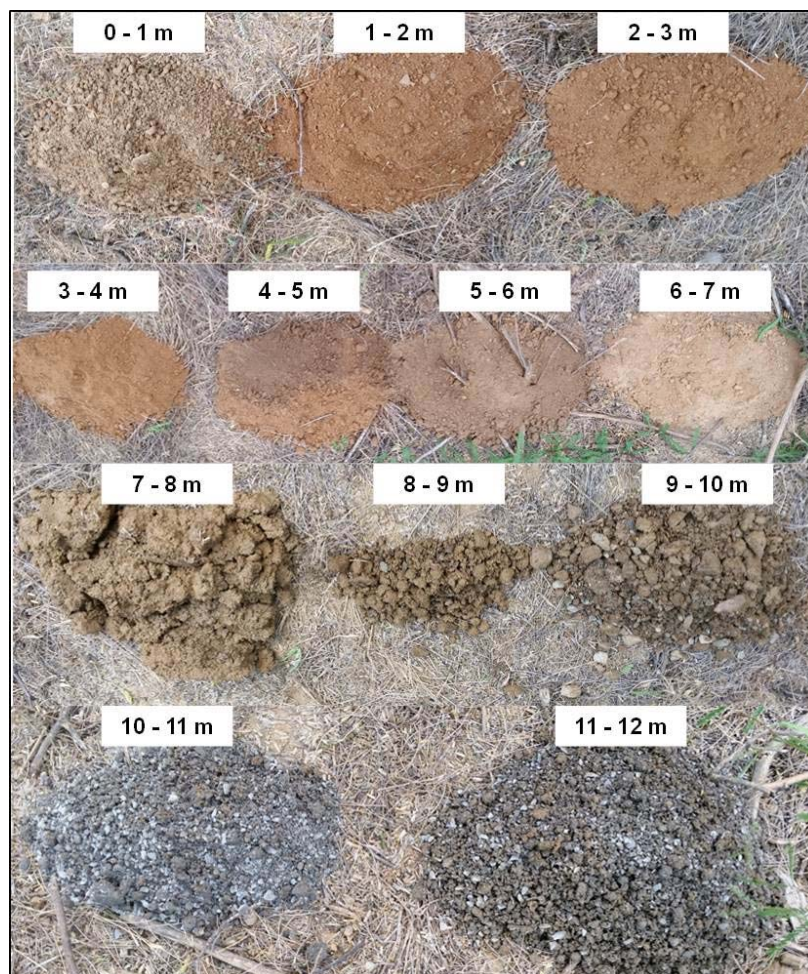


Figure 28. Samples collected during borehole drilling (Borehole #2)

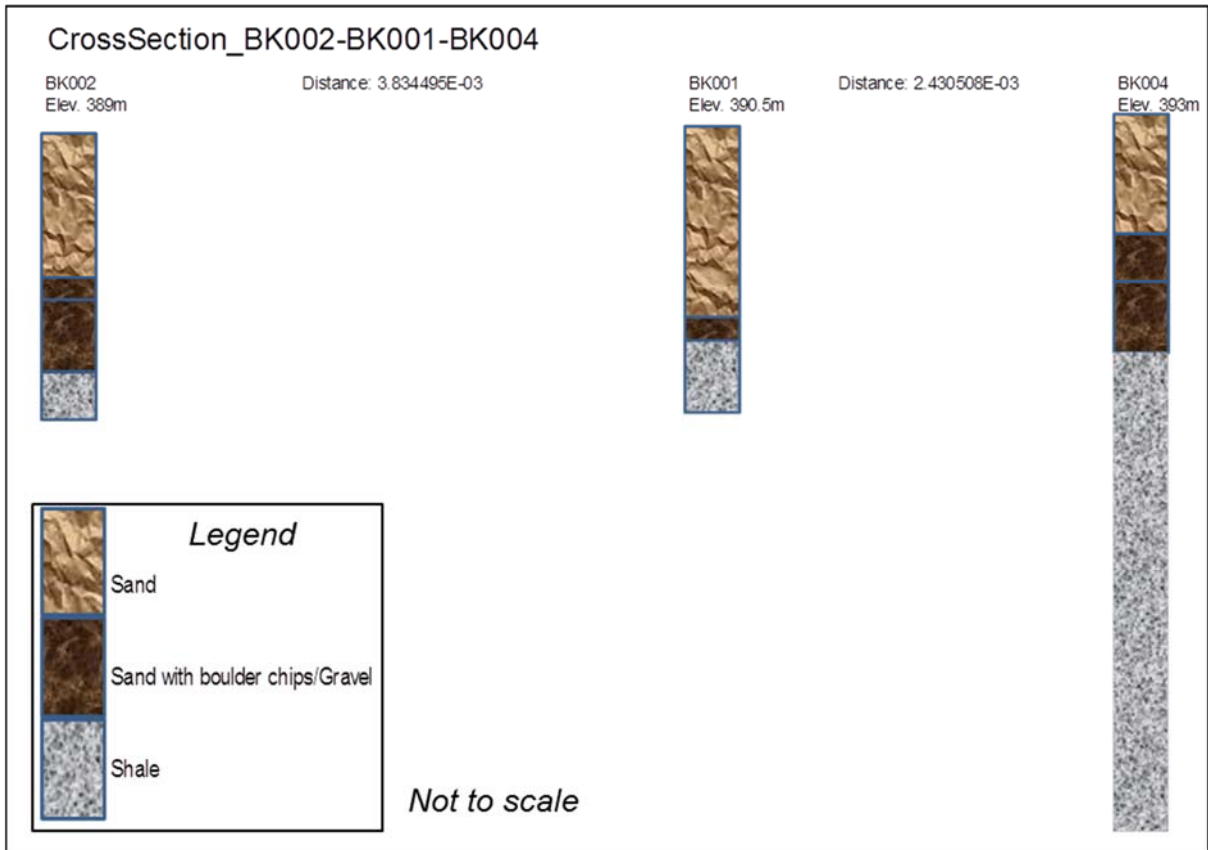


Figure 29. Geological cross section for the study site

### 5.3.1 Groundwater levels

Logged groundwater level data were frequently checked with manual measurements taken with a groundwater level dip meter. Generally, a good agreement existed between the two sets of measurements. The groundwater level data recorded at all four boreholes on the site are presented in Figure 30. The groundwater level at Borehole #1 fluctuated between 8.4 mbgl at the beginning of monitoring on 2 August to 3.85 mbgl on 1 September 2013. The pronounced rise in the groundwater level observed in late August 2013 was due to flooding that occurred at the site (see peaks in Figure 27). The flooding was a result of the Doorn River overflowing its banks after heavy rains upstream in the Nieuwoudtville area. But the study site itself received very little rainfall during this time (< 3 mm).

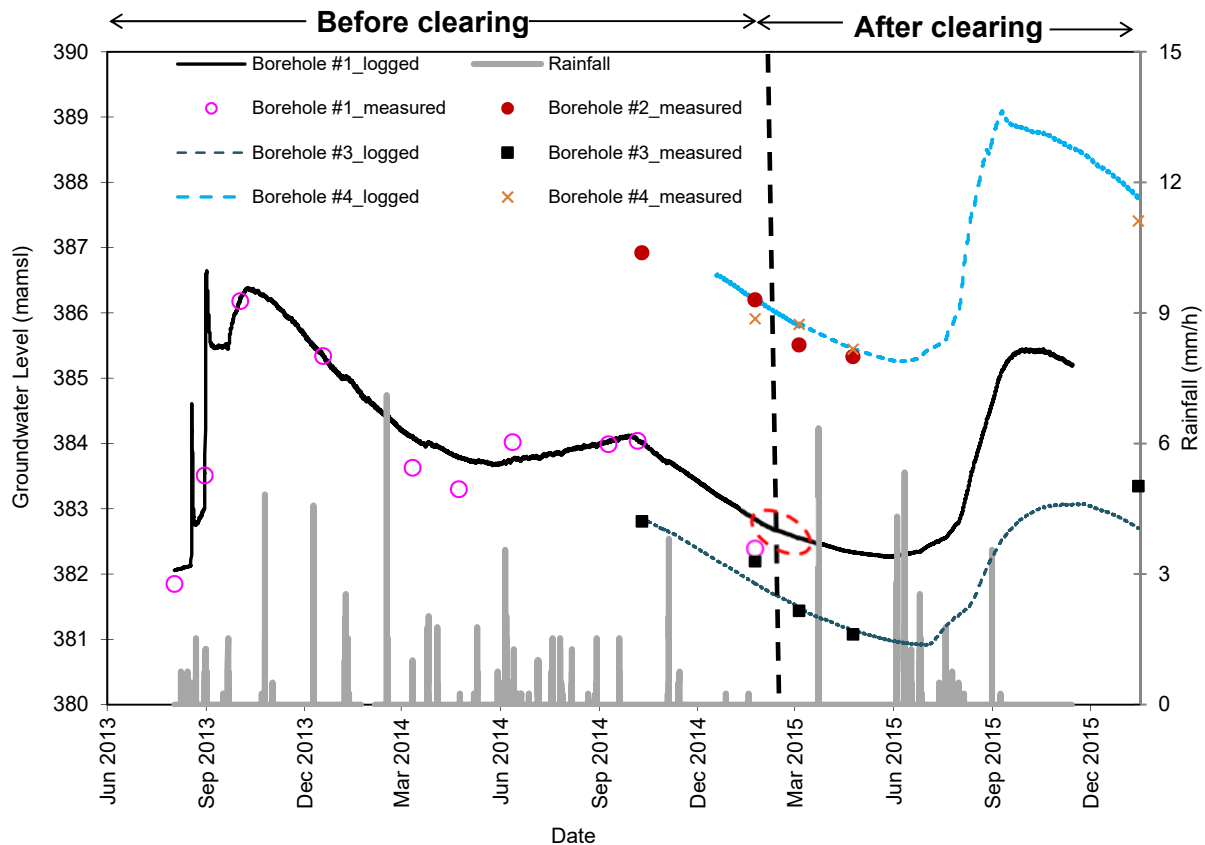


Figure 30. Changes in groundwater levels in four boreholes across the study site.

Borehole #1 (black line) has the longest record. There was no data logger in Borehole #2 (brown circles), while Borehole #3 (green dotted line) and Borehole #4 (Blue line) started logging in October 2014. The black dotted vertical line shows the period when *Prosopis* was cleared.

*Prosopis* invasions were cleared in an area about 80 ha (red circle in Figure 8) the week starting 9 February 2015. As expected the logged groundwater level exhibited signs of a seasonal oscillation. The flooding during 2013 produced a peak in the hydrograph which was not replicated in 2014. Another peak was observed after clearing in 2015, but we are uncertain whether any flooding occurred or not. The groundwater level at Borehole #1 showed a minimal seasonal oscillation during 2014. Also, the hydrograph did not exhibit a pronounced response to individual rainfall events. The length of the data record at Boreholes #3 and #4 does not allow for any extensive interpretation. The dynamics of the seasonal oscillation in 2014/2015 was however, similar to that observed at Borehole #1.

### 5.3.2 Spatial interpolation of groundwater levels

Groundwater level data collected on 24/4/2015 were used to interpolate a potentiometric surface across the study site as well as to calculate contours. This was achieved through the use of the Surfer modelling package. Surfer is a contouring, gridding and surface mapping software package. The results are presented in Figure 31. The potentiometric surface ranges between 377-384.5 mamsl. Groundwater flow is expected to occur perpendicular to equipotential lines. The interpreted direction of groundwater flow is therefore expected to occur in a north/north-easterly direction, which corresponds to the topographic gradient at the site.

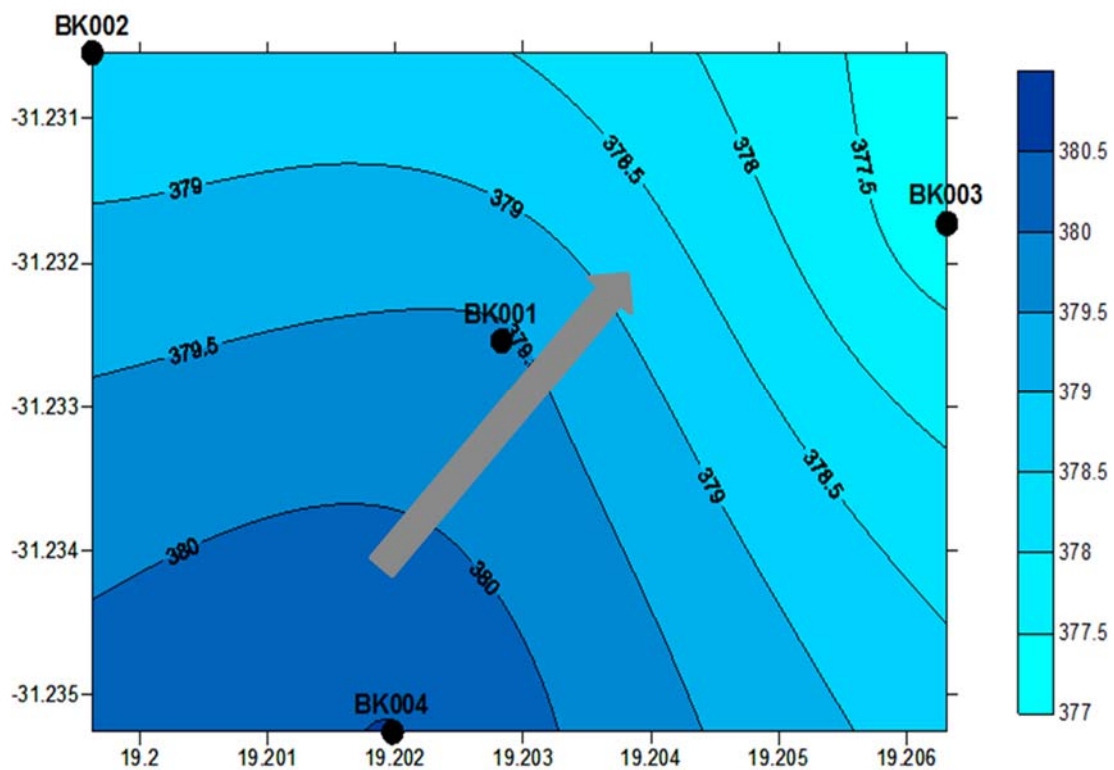


Figure 31. Potentiometric surface contours (mamsl) across the study site. BK001 is the code for Borehole #1, BK002, for Borehole #2, BK003 for Borehole #3, BK004 for Borehole #4. The interpreted direction of groundwater flow is also shown.

## 5.4 Vegetation-groundwater interactions

### 5.4.1 Effect of tree water uptake on groundwater levels

Diurnal changes in groundwater levels showed direct evidence of abstraction by the trees. In Figure 32, tree water uptake is represented by the heat pulse velocity signals

(HPV in cm/h) whose trend is similar to that of transpiration. It is apparent in Figure 32 (a & b) that groundwater levels increased during the night due to lateral recharge. The rate of increase slowed down at sunrise eventually stopping and beginning to fall at mid-morning around 1000. By midday, the water level was steeply falling as plant water uptake accelerated. The water level dropped throughout the day and stopped when plant water uptake was zero between 2000 and 2200 in the evening. Tree water uptake continued after sunset when transpiration had ceased to replenish the depleted trees' internal water reserves. A lower peak in groundwater level was reached between successive days indicating a net water loss from the aquifer (Figure 32) and a lowering of the groundwater level.

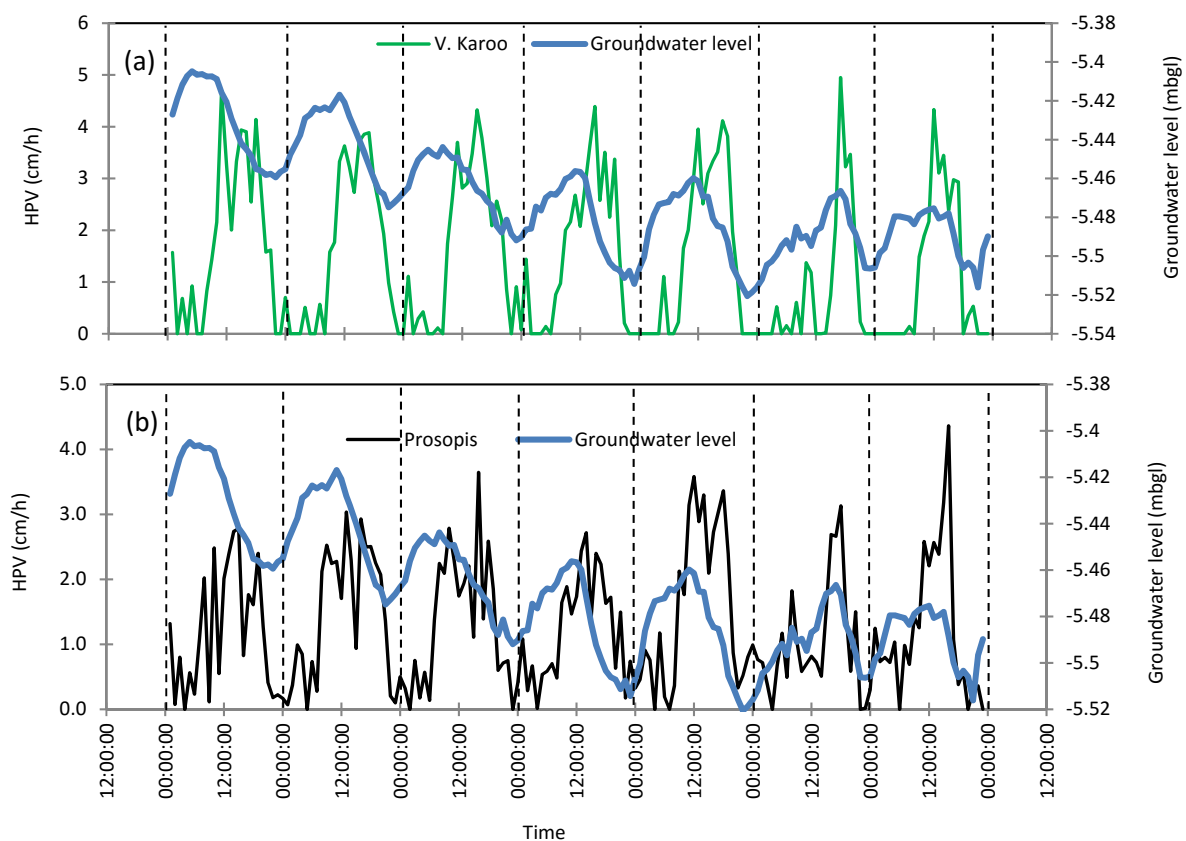


Figure 32. Direct impact of (a) *V. karroo* and (b) *Prosopis* on groundwater levels during clear days from 1-7 January 2014.

#### 5.4.2 Sources of water transpired by the trees

Both rain and groundwater stable isotope values fall along the Global Meteoric Water Line in Figure 33. Soil water showed a degree of evaporative enrichment, typical of arid areas, by plotting below the GMWL (Gat, 1996; Schachtschneider and February, 2010). The lowermost soil sample (-4.5‰  $\delta^{18}\text{O}$  and -66.7‰  $\delta^2\text{H}$ ) has  $\delta^2\text{H}$  isotope values similar to rainwater, suggesting that the top 50 cm of soil were infiltrated by rainwater and were also subject to evaporation (enriched  $\delta^{18}\text{O}$  isotope values relative to rainwater isotope values).

Water in the deeper soil layers (50-100 cm and 100-150 cm) was more similar to the groundwater isotope values. Given that the groundwater level was more than 7 m below the ground on most occasions, it is possible that hydraulically redistributed groundwater (rather than capillary rise) was responsible for the presence of groundwater in the 50-150 cm soil depths. All three *Prosopis* isotope samples plot close to groundwater and deeper soil water. *V. karroo* shows values similar to *Prosopis* and groundwater, as well as samples with more enriched  $\delta^{18}\text{O}$  isotope values.

The results suggest that shallow soil layers reflect some rainwater infiltration, while deeper soil layers corresponded more to groundwater isotope values. All six tree samples plot close to groundwater and deeper soil water, suggesting a dependence on deeper water sources, even at the end of the rainy season.

Given that the vegetation at this site had access to only two sources of water (i.e. groundwater and soil water), we applied a two compartment linear mixing equation proposed by Snyder and Williams (2000) to derive the proportion of plant xylem water derived from the two sources. If  $\delta\text{O}^{18}\text{x}$  is the isotope signature of the tree xylem water,  $\delta\text{O}^{18}\text{so}$  the isotope signature of the soil water source, and  $\delta\text{O}^{18}\text{gw}$  the isotope signature of groundwater, then the fraction ( $f$ ) of water derived from the shallow soil layers is given by

$$\delta^{18}\text{O}_x = f(\delta^{18}\text{O}_{so}) + (1 - f)\delta^{18}\text{O}_{gw} \quad (11)$$

Rearranging the equation gives

$$f = \frac{\delta^{18}O_x - \delta^{18}O_{gw}}{\delta^{18}O_{so} - \delta^{18}O_{gw}} \quad (12)$$

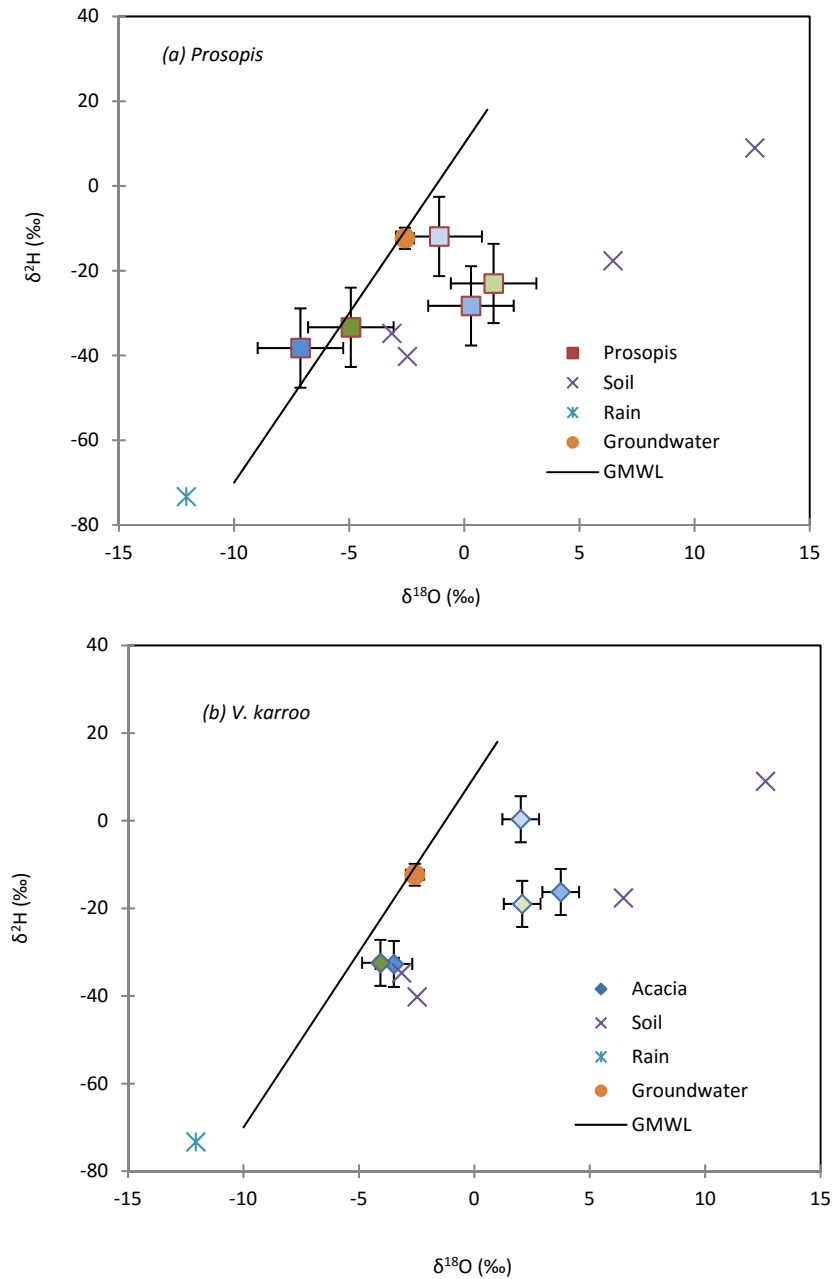


Figure 33. Comparisons of the O/H isotope signature of xylem water of: (a) *Prosopis*, and; (b) *V. karroo* with that of ground and soil water samples taken during winter, spring and summer seasons, respectively.

If “f” is the fraction of xylem water derived from the soil, then the fraction “1-f” is derived from the groundwater. According to Snyder and Williams (2000), the above method applies only when the plant  $\delta^{18}O$  is significantly different from that of groundwater. Table 10 shows the partitioning of the water sources at the site based on the above approach.

Table 10. Fraction of *Prosopis* and *V. karroo* xylem water derived from soil and groundwater sources, respectively

Month	Sample	$\delta O^{18}x$	$\delta O^{18}so$	$\delta O^{18}gw$	f	Groundwater fraction
Winter (Aug' 13)	Prosopis	-1.09	-2.48	-2.75	-	-
	V. karroo	2.01	-2.48	-2.75	-	-
Summer (Dec' 13)	Prosopis	0.29	9.17	-2.42	0.23	0.77
	V. karroo	3.74	9.17	-2.42	0.53	0.47
Autumn (Apr 2014)	Prosopis	-7.12	5.42	-1.64	-	-
	V. karroo	-3.49	5.42	-1.64	-	-

The partitioning of the xylem water between the soil and groundwater sources for the winter and autumn seasons were not realistic presumably because of the lack of contrast in the isotope signature of the plant xylem water and the groundwater. Data in Table 10 suggests that *Prosopis* derived about 23% of its water from the shallow soil layers and 77% from groundwater in summer although sap flow and rainfall data suggest that groundwater use maybe higher than the value presented here.

*V. karroo* on the other hand derived 53% of its water from the shallow soil layers and 47% from the saturated zone. The low proportion of water from the unsaturated zone for *Prosopis* could be a result of the fact that the lateral roots of this species form a dense mat close to the soil surface which is much drier (see Figure 10). The lateral

roots of *V. karroo* on the other hand are inclined at a steeper angle from the surface thereby accessing water from the less exposed parts of the soil.

If we assume that the proportion of water derived from soil and groundwater sources remains the same throughout the year, then *Prosopis* abstracted 418 mm from groundwater and only 125 mm from the unsaturated zone (Table 11). This translates to 4 180 m<sup>3</sup> (or 4.18 ML) groundwater abstracted by per hectare per year. This is equivalent to the quantity of groundwater that can potentially be released for each hectare of the invasions cleared. *V. karroo* on the other hand consumed much less water, i.e. 420 m<sup>3</sup> (or 0.42 ML) of groundwater per hectare per year. The total amount of groundwater consumed by both species at this site was approx. 4 600 m<sup>3</sup> per hectare per year.

Table 11. Amount of transpiration derived from the soil and groundwater sources by *Prosopis* and *V. karroo*, respectively

Species/stand	Variable	Quantity (mm/yr)	Duration
Prosopis	Total transpiration	543	Aug 2013-Jul 2014
Prosopis	Transpiration from soil	125	Aug 2013-Jul 2014
Prosopis	Transpiration from groundwater	418	Aug 2013-Jul 2014
V. Karoo	Total transpiration	90	Aug 2013-Jul 2014
V. Karoo	Transpiration from soil	48	Aug 2013-Jul 2014
V. Karoo	Transpiration from groundwater	42	Aug 2013-Jul 2014
Stand level	Total transpiration	633	Aug 2013-Jul 2014
Stand level	Transpiration from soil	167	Aug 2013-Jul 2014
Stand level	Transpiration from groundwater	466	Aug 2013-Jul 2014
	Reference ET	1 791	Aug 2013-Jul 2014

## 5.5 Groundwater level response to *Prosopis* removal

For this analysis, we use data from Borehole #1 which had the longest water level record. The response of groundwater levels to the removal of *Prosopis* is, to some extent, evident in Figure 30 (see red dotted ellipse). However, a clearer illustration is shown in Figure 34 where we compare the cumulative change in groundwater levels

for periods outside the rainy season in January to March 2014 (before clearing) and for the same months in 2015 (*Prosopis* cleared week starting 9 February 2015). The groundwater levels showed a steeper rate of decline in 2014 than in 2015 probably because of the higher water level in 2014 as a result of flooding late the previous year.

It is evident in Figure 34 that there was an immediate slowing down in the rate of drop in groundwater levels (orange line) soon after *Prosopis* was removed.

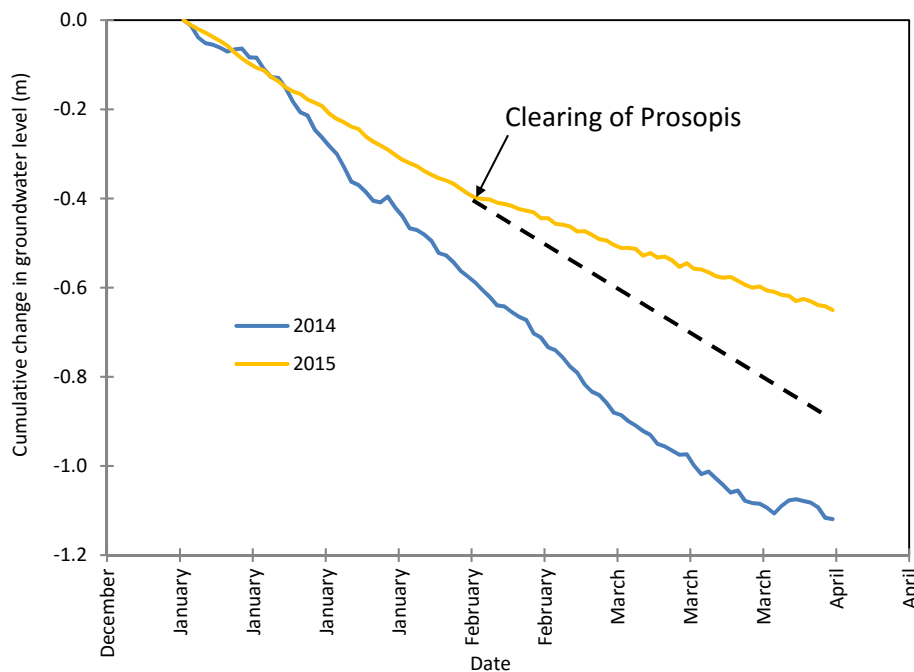


Figure 34. Comparison of the cumulative changes in groundwater levels over a three months period from January to March: a) before, and; b) after *Prosopis* invasions were cleared. Black dotted line depicts the possible trend in groundwater level in 2015 had the invasions not been cleared

The black dotted line in Figure 34 depicts the potential rate of fall in the water level had *Prosopis* not been removed. The water level would potentially have dropped by about 90 cm between January and March 2015 if *Prosopis* was present. However, the level actually fell by approximately 65 cm which was about 25 cm less than would have occurred if the invasions were present. The average rate of drop in the water level before *Prosopis* was cleared was about 9 mm/d. This decreased to approx. 5 mm/d after clearing.

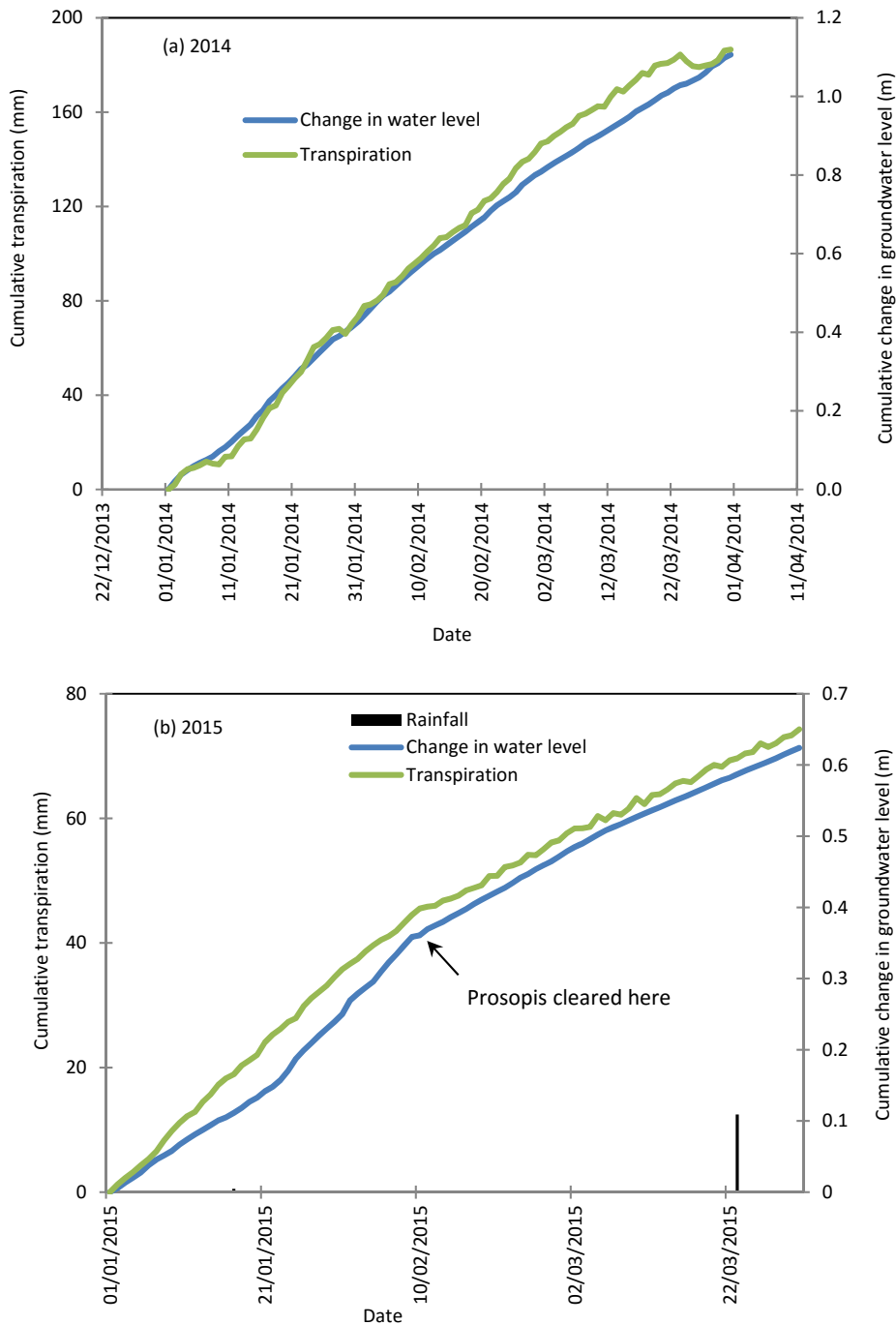


Figure 35. Relationship between cumulative tree water uptake and absolute changes in groundwater levels over a three months period from January to March (a) before (2014), and; (b) after *Prosopis* invasions were cleared in 2015

The continued drop in water level after clearing can be attributed to the uptake of groundwater by the remaining indigenous vegetation and water discharge from the aquifer as base flow away from the study area. The relationship between the

cumulative changes in stand transpiration with changes in groundwater levels are shown in Figure 35.

In January to March 2014, the cumulative rate of change of transpiration by the vegetation was linearly related to the cumulative change in groundwater level expressed as absolute values (both graphs had similar slopes). This trend was again confirmed in 2015 with the slopes of the two graphs changing by similar amounts after clearing (Figure 35b). This directly confirms a cause and effect relationship between changes in groundwater levels and tree water uptake rate.

## 5.6 Modelling evapotranspiration of a Prosopis invaded area

### 5.6.1 Site energy balance before clearing Prosopis

Removing the invasions has the effect of changing the surface energy balance of the site. On typical clear days, more than 50% of the available energy was converted to the latent heat flux (i.e. energy equivalent of evapotranspiration) before clearing (Figure 36).

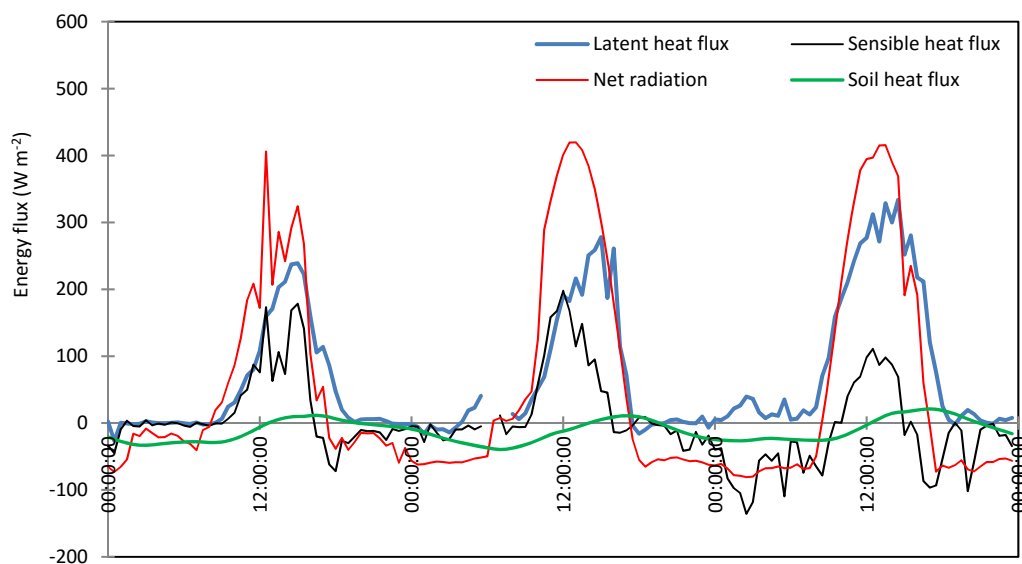


Figure 36. Energy balance of the study site before the invasions were cleared from 20-22 May 2014

A small proportion of the energy was converted into the sensible heat flux (used to heat the air). Evapotranspiration was fairly high exceeding 7 mm/d on some days (Figure 37) before clearing.

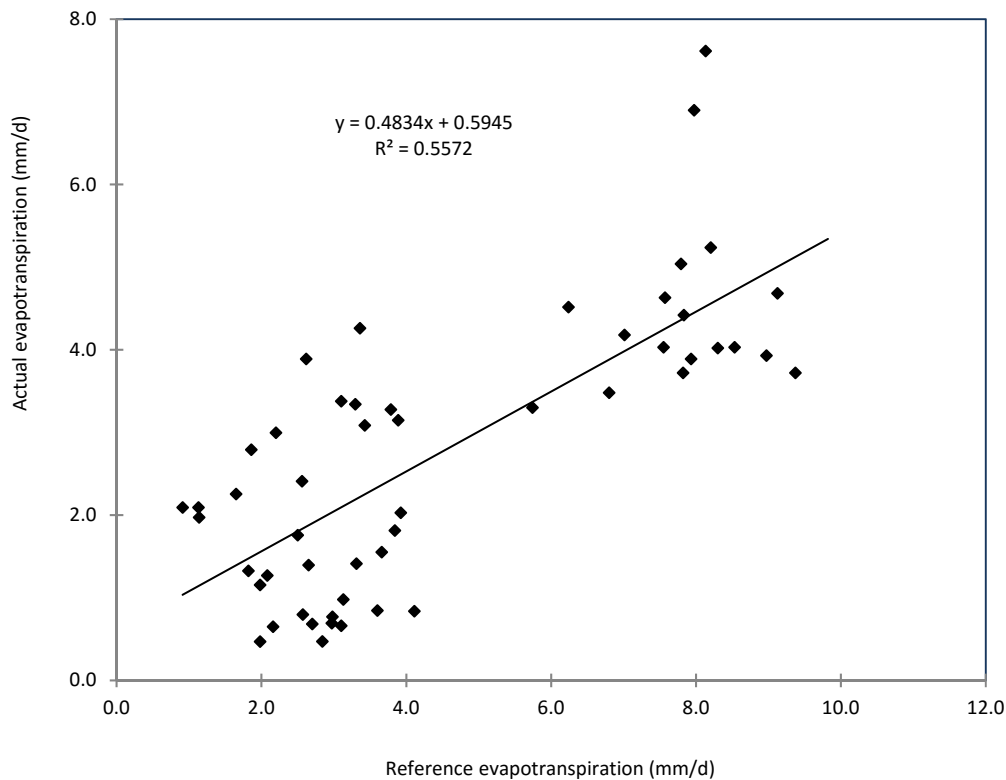


Figure 37. Effect of the atmospheric evaporative demand on evapotranspiration before *Prosopis* was cleared at Brandkop farm

### 5.6.2 Energy balance after clearing *Prosopis*

When *Prosopis* was cleared, it is apparent from Figure 38 that most of the available energy was instead converted into sensible heat. The latent heat flux was a fairly small proportion accounting for less than 20% of the available energy on typical clear days. As expected, this led to lower stand evapotranspiration rates (Figure 39) than before the invasions were cleared.

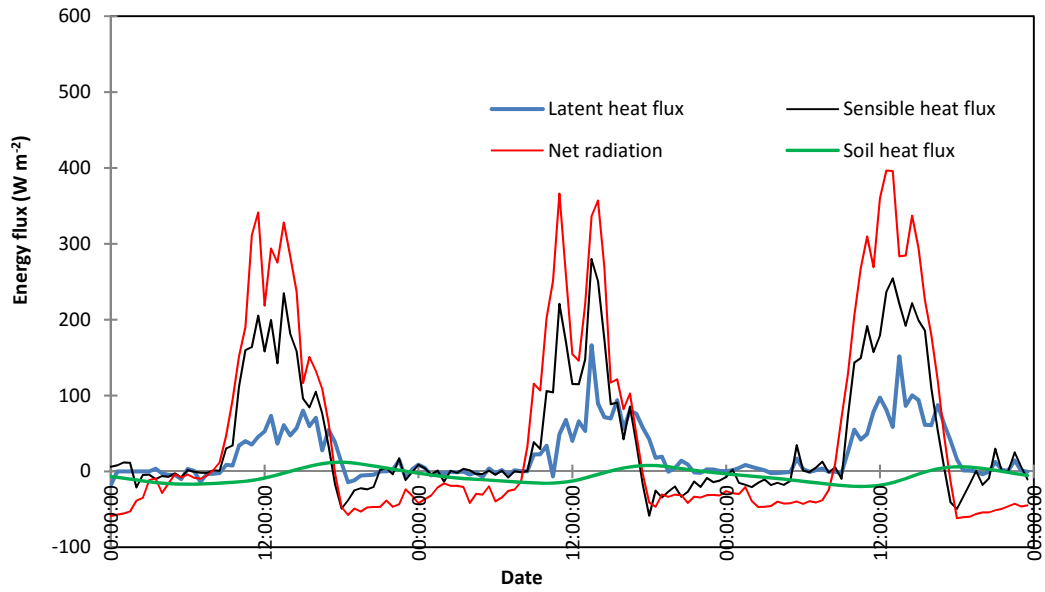


Figure 38. Energy balance of the study site after the invasions have been cleared from 14-16 May 2015

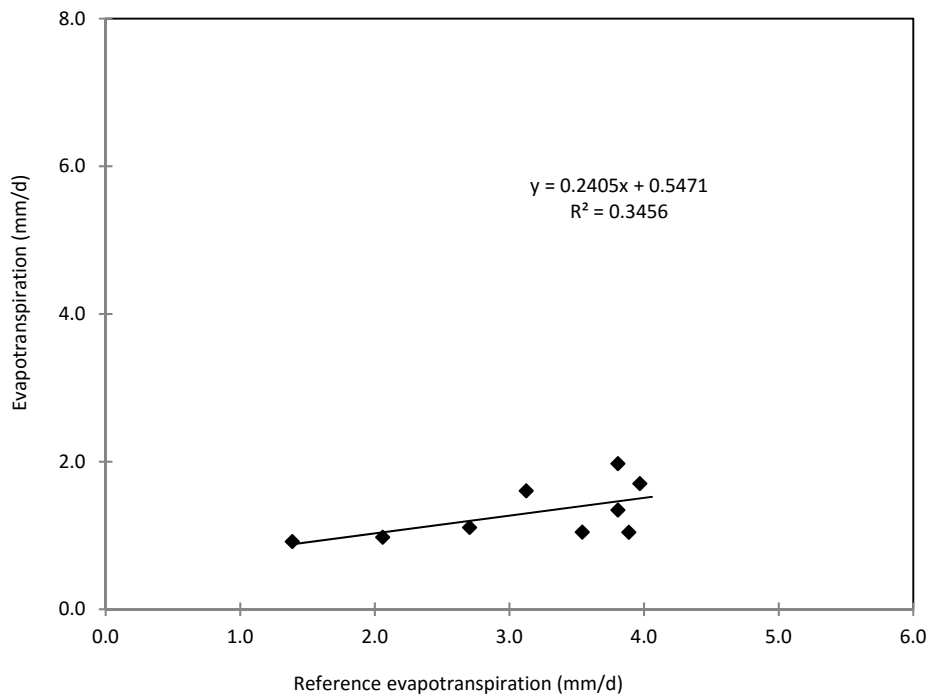


Figure 39. Effect of the atmospheric evaporative demand on evapotranspiration after *Prosopis* was cleared at Brandkop farm

### 5.6.3 Validation of the adapted MOD16 ET model

According to the biome information in the Look Up Table for MOD16 provided by Mu *et al.* (2011), the study site was characterized as a mixed forest. Default parameters for this biome were applied except for the specific parameters that were introduced in this study and these are summarized in Table 11. Measured evapotranspiration and stand transpiration data collected from 30 November to 4 December 2013 were used to optimize the model using the Marquadt iterative procedure within the ModelMaker software package (Cherwell Scientific, UK). According to this approach, parameter values that minimized the weighted sum of squared differences between the measured and modelled ET and transpiration were selected (Table 12). These new parameters meant that the following original MOD16 parameters were not required in the adapted model:  $VPD_{close}$ ,  $VPD_{open}$ ,  $T_{min\_close}$  and  $T_{min\_open}$ . So the proposed modifications replaced four parameters with only three new ones.

Table 12. New parameters for the adapted MOD16 model applied to the *Prosopis* invaded site.

Parameter	Value	Units
*CL	0.0057	$m\ s^{-1}/m^2$
$k_{d1}$	0.085	$Pa^{-1}$
$k_{s1}$	0.198	-
$k_{s2}$	0.450	-
* $\beta$	4.000	kPa

\* Parameters already present in MOD16 whose values were adjusted for the *Prosopis* invaded site.

Input data required to run the model at the daily time step are: 1) daily total solar radiation, 2) average daily temperature, 3) average day time temperature, 4) average day time relative humidity, 5) average night time relative humidity, 6) latitude, 7) altitude, 8) daily average soil water content, 9) leaf area index, 10) fractional vegetation cover, and; 11) surface albedo. The albedo was calculated from Landsat 8 bands 2 (Blue – 450-510 nm), 4 (640-670 nm), 5 (850-880 nm), 6 (1570-1650 nm), and 8 (2

110-2 290 nm) at the 30 m x 30 m resolution as described by Liang *et al.* (2000). The leaf area index was derived from the inversion of the PROSAIL (Prospect + SAIL) radiative transfer model (Cho *et al.*, 2014). The inversion was based on the Lookup table (LUT) using root mean square error (RMSE). The inversion solution was achieved when the minimum RMSE between the simulated and measured (image) spectra was reached. The parameterization of the PROSAIL model was based on Cho *et al.* (2014). The fractional vegetation cover was calculated from the fraction of the absorbed photosynthetically active radiation (FPAR) from LAI based on a simple equation using Beer's law (Ahl *et al.*, 2005; Turner *et al.*, 2005). Input weather data (solar radiation, air temperature and relative humidity) were obtained from the automatic weather station on site.

Validation of the adapted MOD16 model with the actual measured evapotranspiration before clearing was done from 24 April to 28 May 2014 and again from 19 December 2014 to 21 January 2015 for a total of 23 days. Data for validation after clearing was collected from 25 April to 18 May 2015 for a total of nine days. However, equipment failure and power outages led to substantial data losses. Only days with complete ET data were used in the validation and the results are shown in Figure 40.

Considering the pre-clearing data set only (dark dots in Figure 40), the predicted ET was within 12% of the measured values with a root mean square error of  $\pm 0.55$  mm/d. The dotted line in Figure 40 depicts the one to one line. However, including the post-clearing data set (open blue dots) increased the root mean square error to about  $\pm 0.77$  mm/d. The transpiration sub-model was validated using the measured transpiration data collected during the whole month of January 2014 (31 days). The predicted transpiration plotted very close to the 1:1 line being less than 5% of the measured values (Figure 41). The root mean square error was  $\pm 0.49$  mm/d.

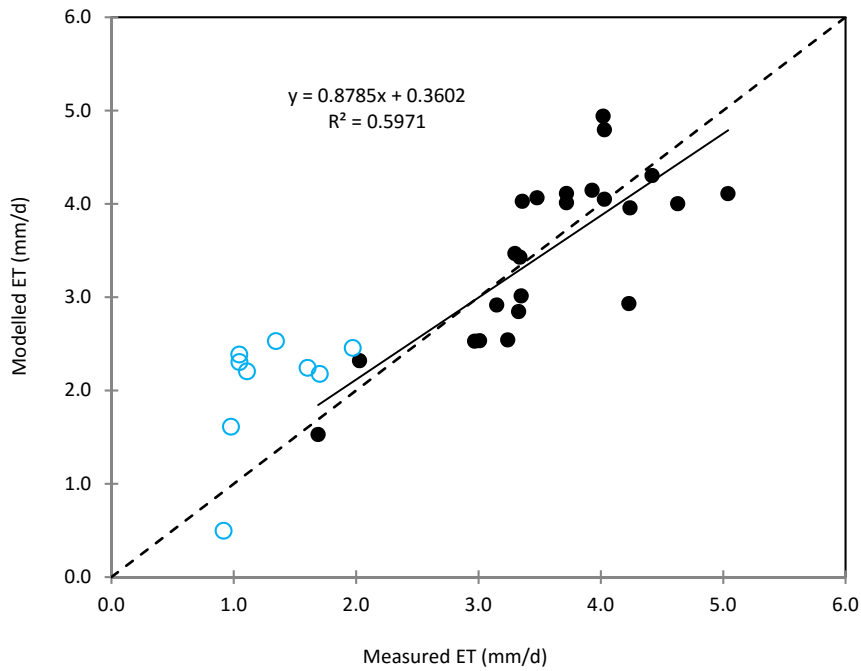


Figure 40. Comparison of the measured and modelled evapotranspiration for data collected during specific window periods before (black dots) and after (blue circles) *Prosopis* has been cleared

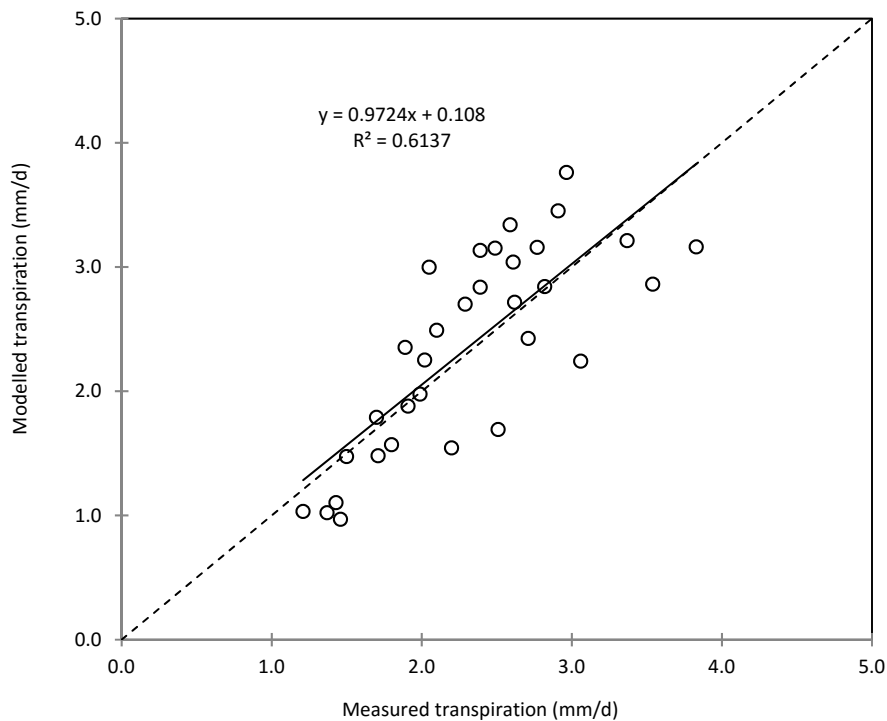


Figure 41. Comparison of the measured and modelled stand transpiration. Dotted line depicts the 1:1 line

As expected the day time fluxes contributed the bulk of the ET signal (Figure 42) with night time ET contributing less than 10% of the daily total evaporation. Transpiration from the *Prosopis* and *V. karroo* contributed more than 65% of the total ET on warm clear days (Figure 43). The balance of the fluxes came from the soil and undergrowth species whose water use was not measured due to equipment limitations.

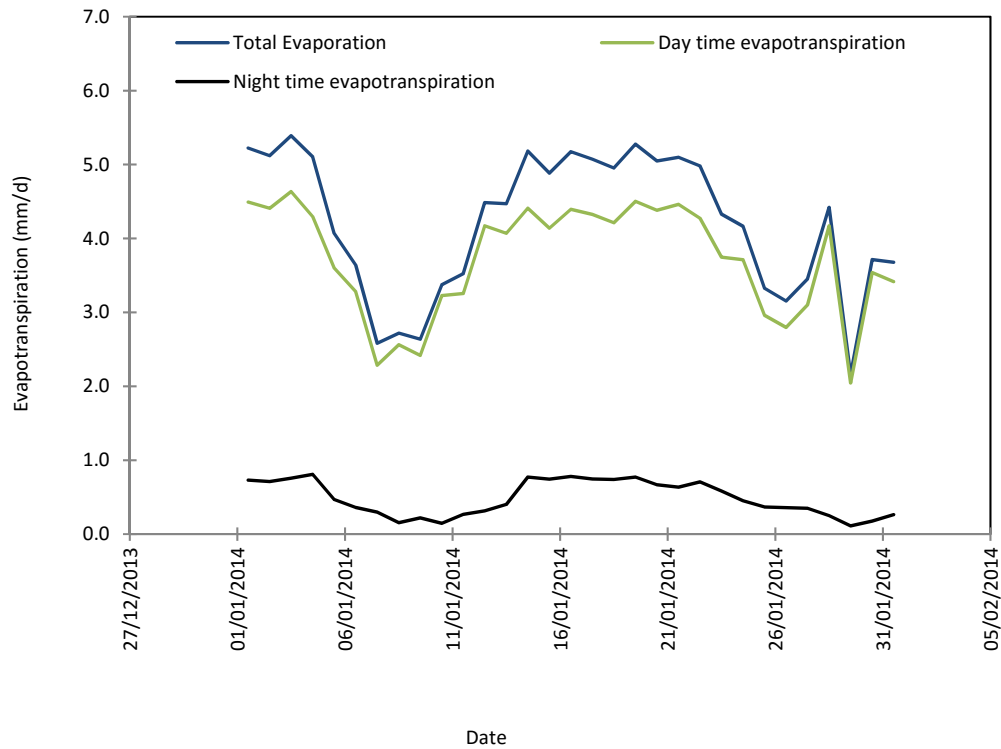


Figure 42. Partitioning of the modelled evapotranspiration between day time and night time fluxes. Total evaporation (blue line) is the sum of the day time (green) and the night time (black) fluxes.

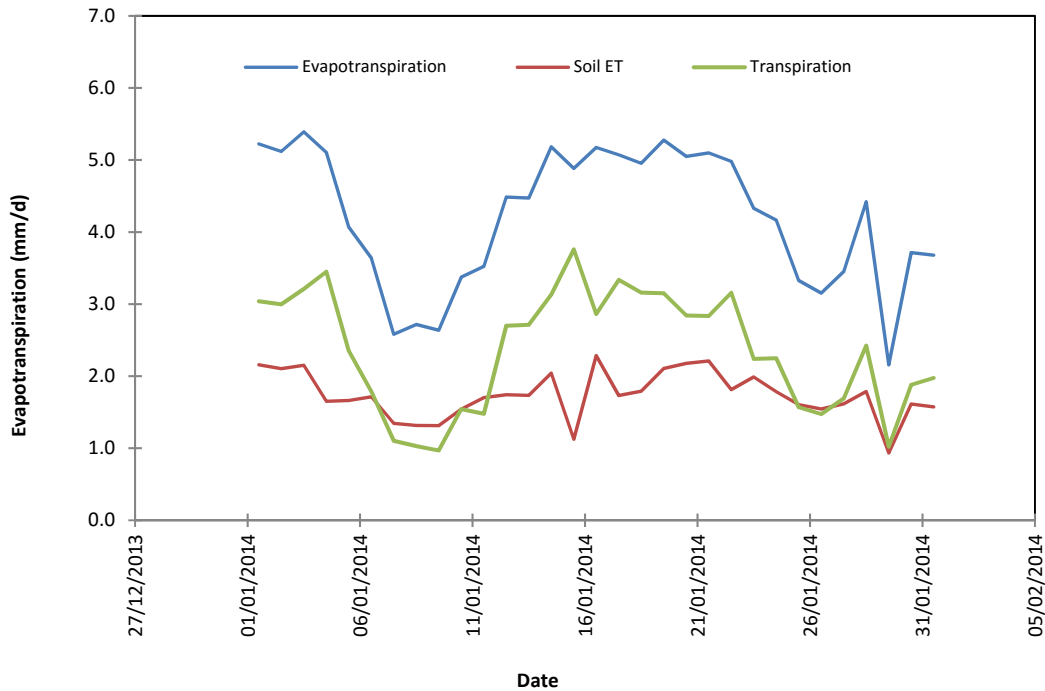


Figure 43. Partitioning of the modelled evapotranspiration (blue line) into the transpiration (green line) and soil evaporation (brown line) components

Spatial information on water use by invasive alien plants is important firstly because the area occupied by these plants is generally increasing in South Africa (Le Maitre *et al.*, 2015). Secondly this information is also useful for decision making, especially prioritizing and planning alien plant clearing activities. In this study we made the first attempt to refine and improve the MOD16 ET algorithm for application in an arid catchment as outlined above. We restricted our testing of the model to the *Prosopis* invaded area along the Doorn River (Figure 44) due to time constraints.

The adapted MOD16 ET code was developed using the MATLAB software (Matlab, 2015a, Mathworks, USA). Details of the changes made to the original code proposed by Mu *et al.* (2011) are explained in Section 4.6.2. Partitioning of the daily ET between the transpiration and soil evaporation components and between the day and night time ET are shown in Figure 45. We use simulations for a typical clear day on 14 April 2014 as an example. According to the model, soil evaporation accounted for a very small fraction of the daily ET (less than 5%). Although we did not measure soil evaporation, such low values are probable given the excessively dry soils (Figure 22) due to lack of rain.



Figure 44. *Prosopis* invaded area along the Doorn River near Brandkop and the neighbouring farms. The red circle depicts the area where detailed measurements were taken. Clearing of the *Prosopis* invasions was also done in the same area in February 2015.

Night time ET contributed up to 10% of the daily total evapotranspiration (Figure 45 c & d). The substantial night time ET was likely a result of the high VPD due to the low relative humidity especially during the summer months and possibly advection of warm air into the study area. The time series of the monthly total ET are shown in Figure 45 from January to December 2014. As expected high ET totals occurred during the summer and lower in winter. The poor quality of the remote sensing images in October accounted for the low quality in the ET simulations.

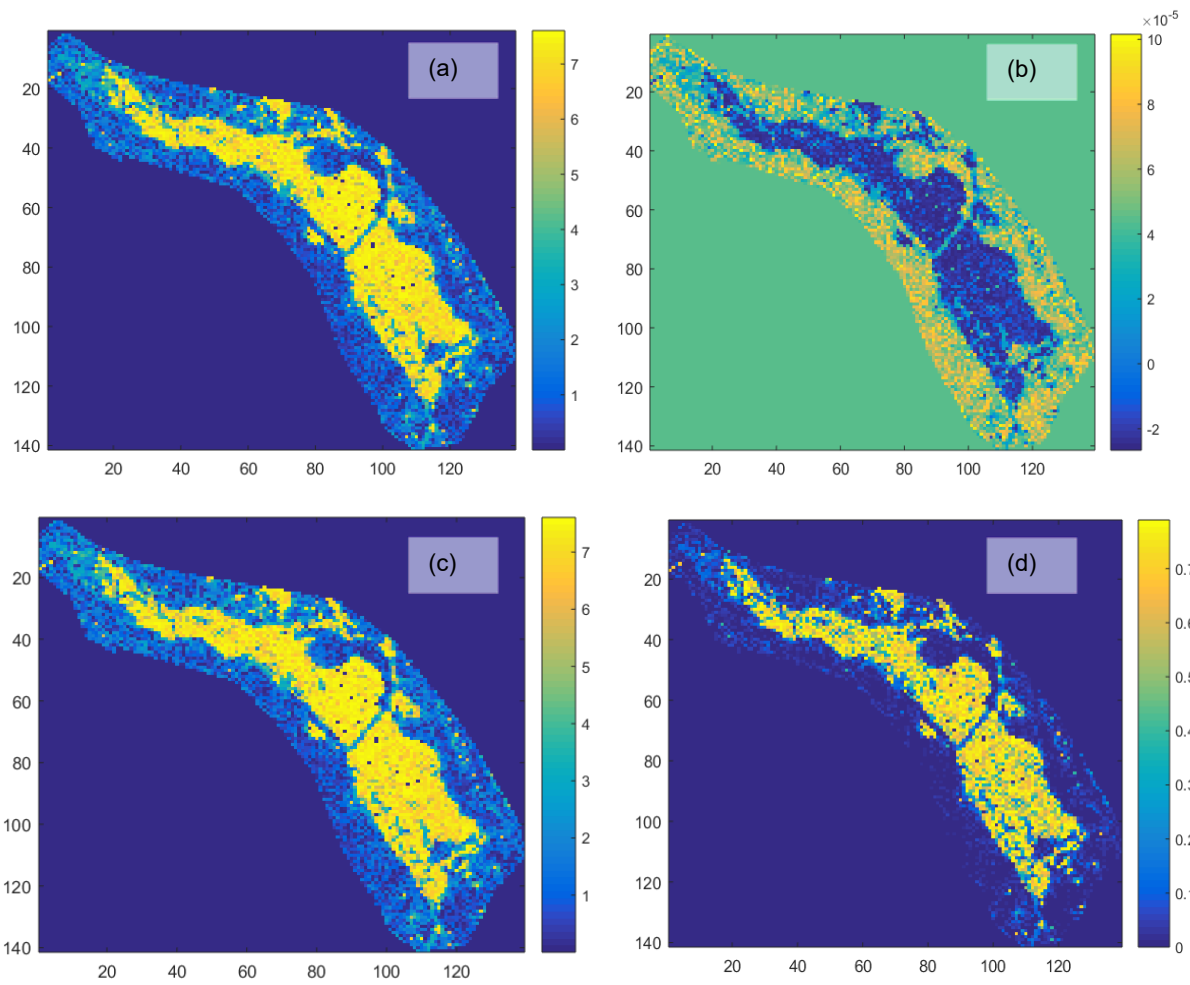


Figure 45. Partitioning of ET between transpiration (a) and evaporation from the forest floor (b) and between day time (c) and night time (d) ET values on 14 April 2014. The x and y-axes values represent the matrix for the remote sensing images.

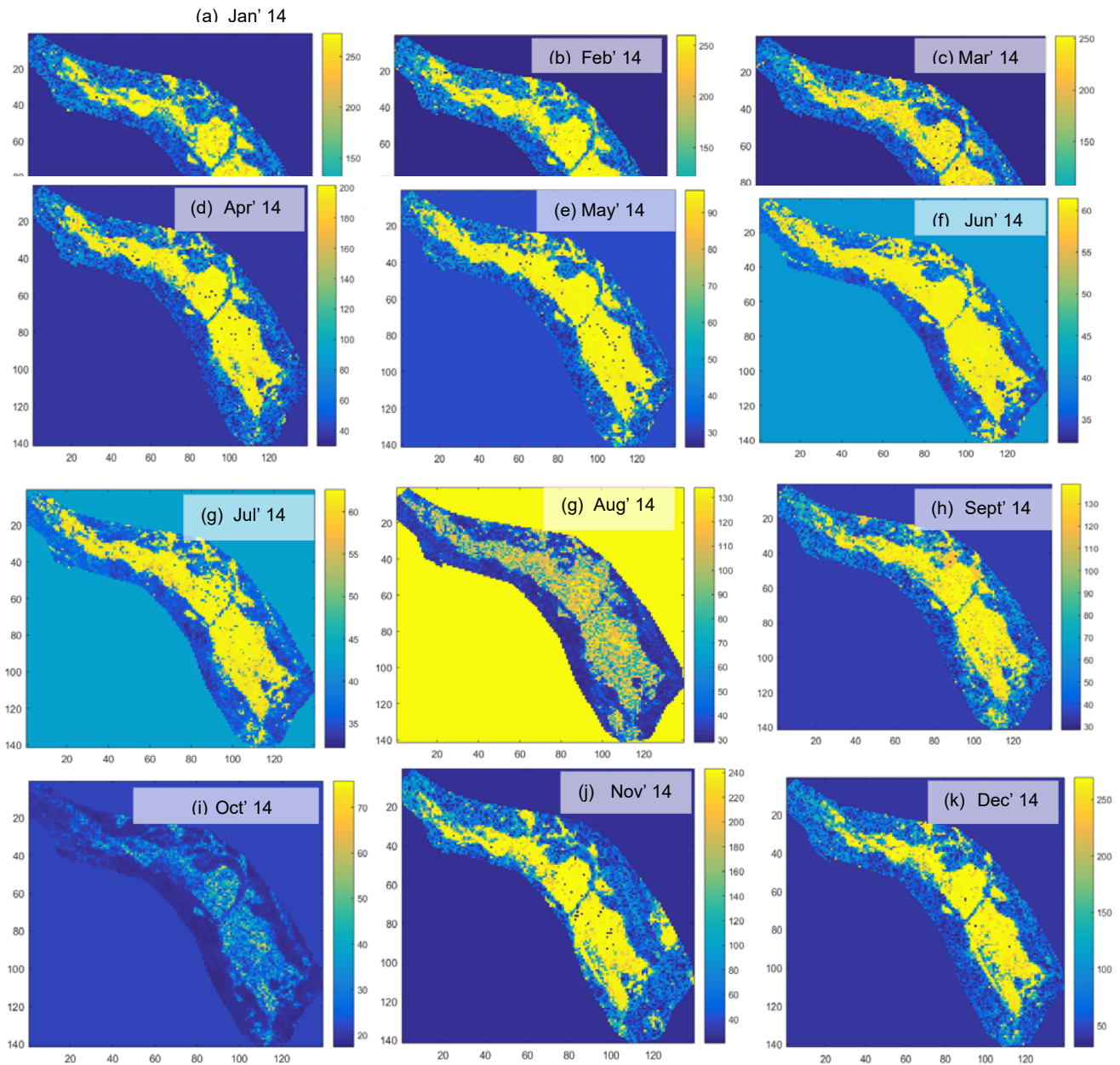


Figure 46. Monthly total ET at the *Prosopis* invaded site from January (a) to December 2014

### 5.7 Estimating groundwater recharge

The aim of applying HYDRUS-1D is to simulate the drainage out of the soil profile (groundwater recharge) and root water uptake (transpiration). This has been estimated for a soil profile planted with *Prosopis* trees and for a soil profile planted with *V. karroo* trees. The soil hydraulic properties were kept constant between the two simulations. However, the root water uptake parameters and the LAI (Table 5) were set-up to represent *Prosopis* and *V. karroo* trees, respectively.

Figure 47 shows the daily rainfall data recorded at Brandkop with the automatic weather station (top) and the flux produced with HYDRUS-1D at the atmospheric boundary (bottom). Negative HYDRUS-1D values represent fluxes which enter the profile, e.g. rainfall infiltration, and positive values represent fluxes leaving the profile, e.g. transpiration, deep drainage, etc. The total rainfall during the period of simulation was 26.52 cm. The data generally follows a similar pattern. The difference between the recorded rainfall (top) and the fluxes entering the soil profile (bottom) is a function of rainfall interception by vegetation, evaporation of rainfall, etc.

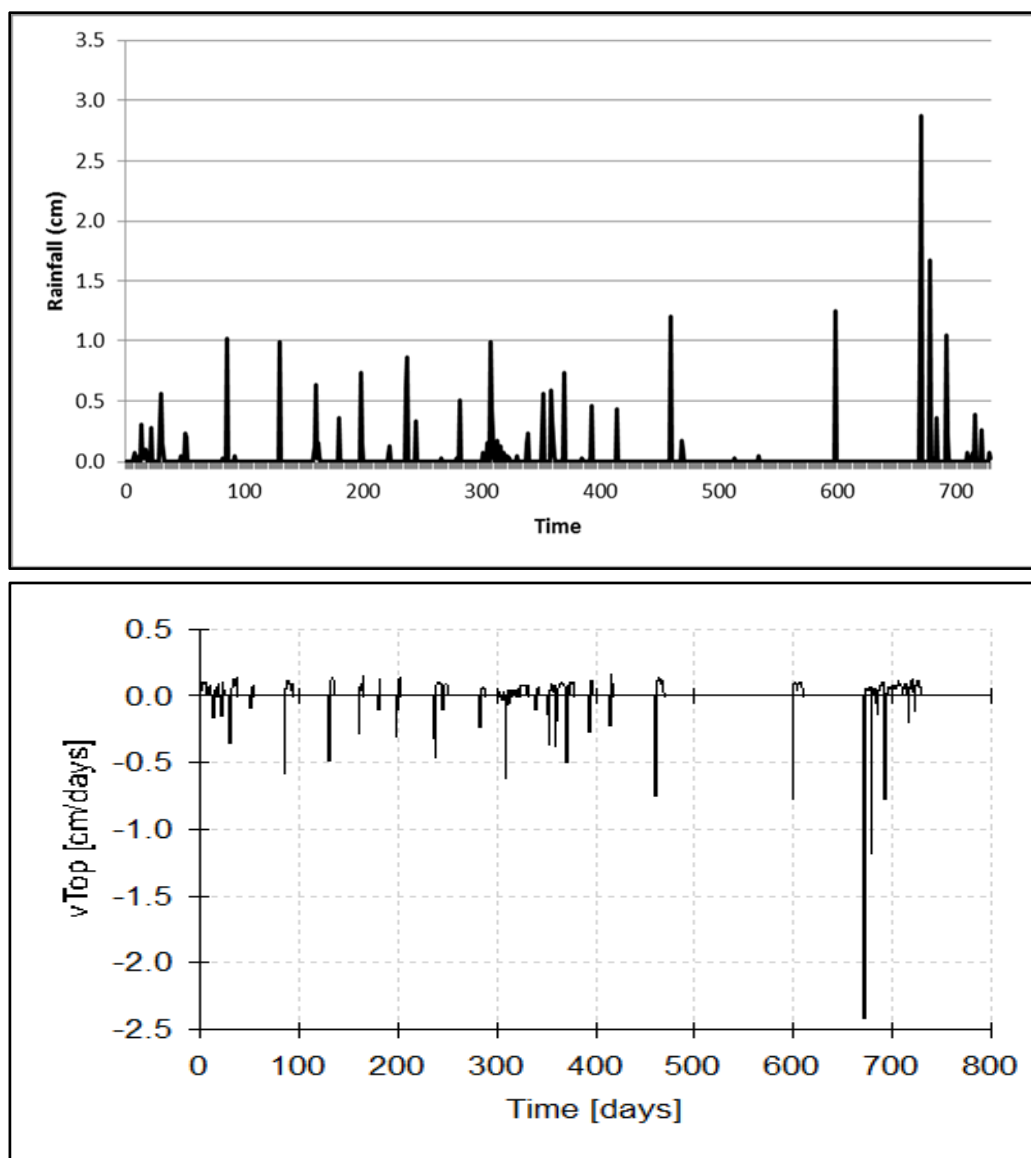


Figure 47. Daily rainfall data recorded at Brandkop (top) and simulated fluxes at the atmospheric boundary produced by HYDRUS-1D (bottom)

A comparison of the measured and simulated volumetric soil water (Figure 48) content is often used to assess the performance of unsaturated zone modelling packages such as HYDRUS-1D. The measured values were obtained from a soil moisture sensor installed at depths of 50, 100 and 150 cm. The measured soil water content generally ranged between 2-6% (50 cm and 100 cm) and between 10-13% (150 cm). The sensor installed at 50 cm soil depth exhibited a dramatic response to rainfall which occurred in June/July 2015. The simulated soil water content was generally of the order of 13%. Again, the observation node located at 50 cm soil depth exhibited dramatic response to rainfall which occurred in June/July 2015, with the simulated soil moisture at this depth increasing to 15.6%. The measured and simulated soil water compared well at 150 cm soil depth, however they exhibited minor deviations at shallower (50 and 100 cm) soil depths. Soil moisture is being monitored with CS616 sensors (Campbell Scientific, Inc., Logan UT, USA). These sensors are reported to generally exhibit an error margin of 3%. Gush *et al.* (in press) also reported that corrections (increases) of data collected with CS616 sensors are commonly required after comparisons with data which were obtained using gravimetric methods are made.

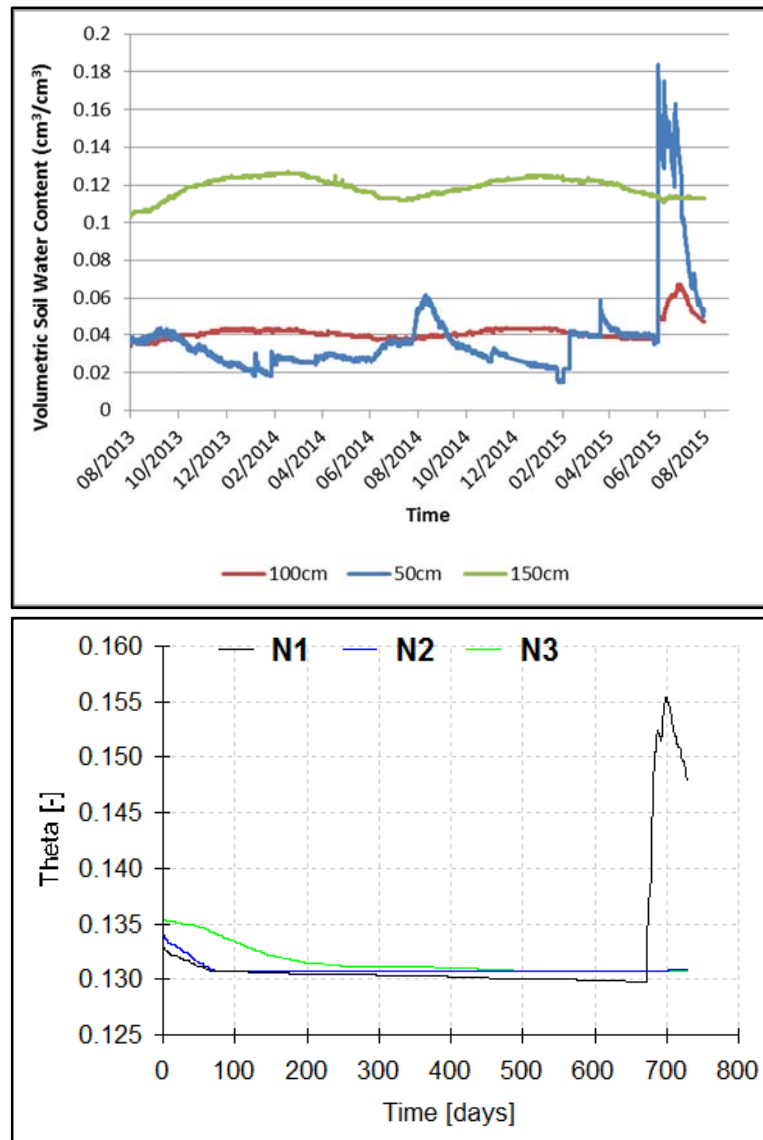


Figure 48. Volumetric soil water content data recorded at Brandkop (top) and simulated volumetric soil water content produced by HYDRUS-1D at 50 cm(N1), 100 cm (N2) and 150 cm (N3) soil depth (bottom)

A comparison of the observed and simulated root water uptake (transpiration) was used as a further measure to assess model performance (Figure 49 and 50). Figure 49 presents the HYDRUS-1D output graph of the cumulative actual root water uptake by *Prosopis* trees and the cumulative measured root water uptake. The *Prosopis* trees were cleared on 18/02/2015 (day of simulation 567) and thus only simulated data up to this day should be considered. The total measured root water uptake for *Prosopis* trees from 2/08/2013 to 17/02/2015 was 64 cm. The simulated root water uptake

during this same period was 57 cm. Thus, the simulated and observed root water uptake correlated fairly well, with a difference of only 11%.

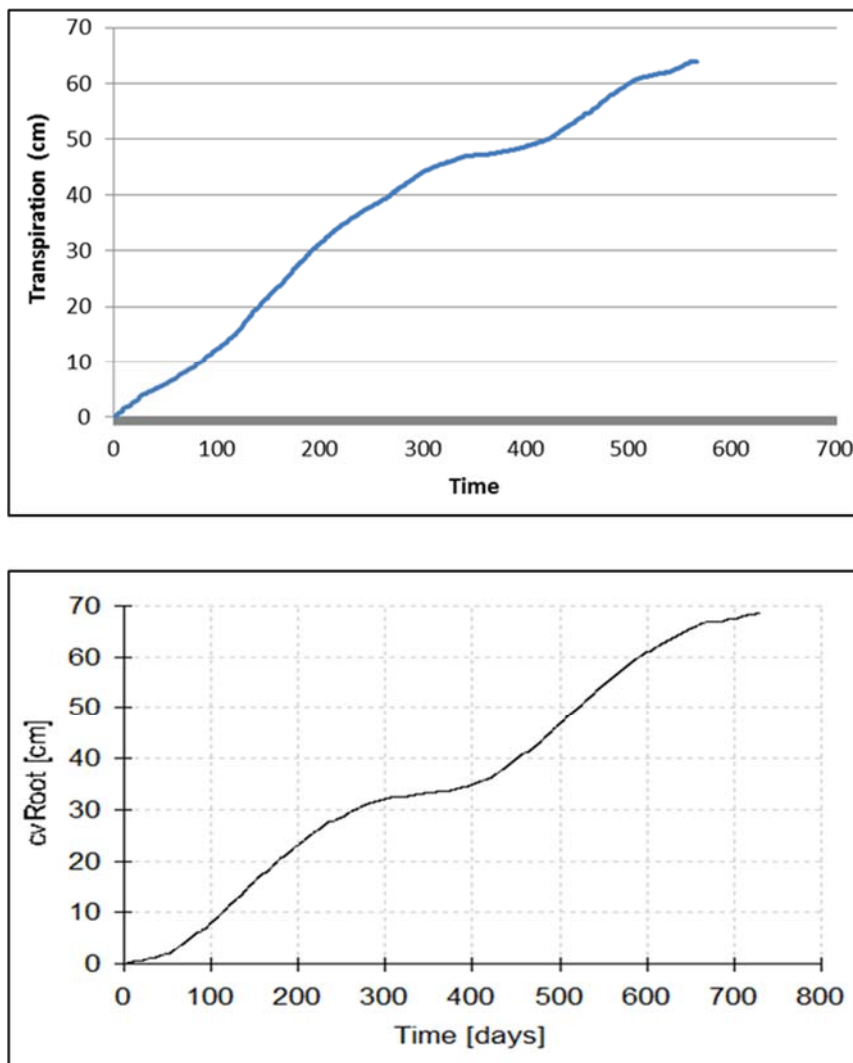


Figure 49. The cumulative measured (top) and simulated (bottom) root water uptake by *Prosopis* trees

Figure 50 presents the HYDRUS-1D output graph of the cumulative actual root water uptake by *V. karroo* trees and the cumulative measured root water uptake. The total measured root water uptake for *V. karroo* trees from 02/08/2013 to 3/07/2015 was 22 cm. The simulated root water uptake during this same period was 33 cm. Thus, a difference of approximately 33% is evident between the observed and simulated root water uptake. The model was therefore not able to accurately replicate the water use dynamics of the *V. karroo* trees, however it was able to replicate the reduced water use of the *V. karroo* trees when compared to the *Prosopis* trees.

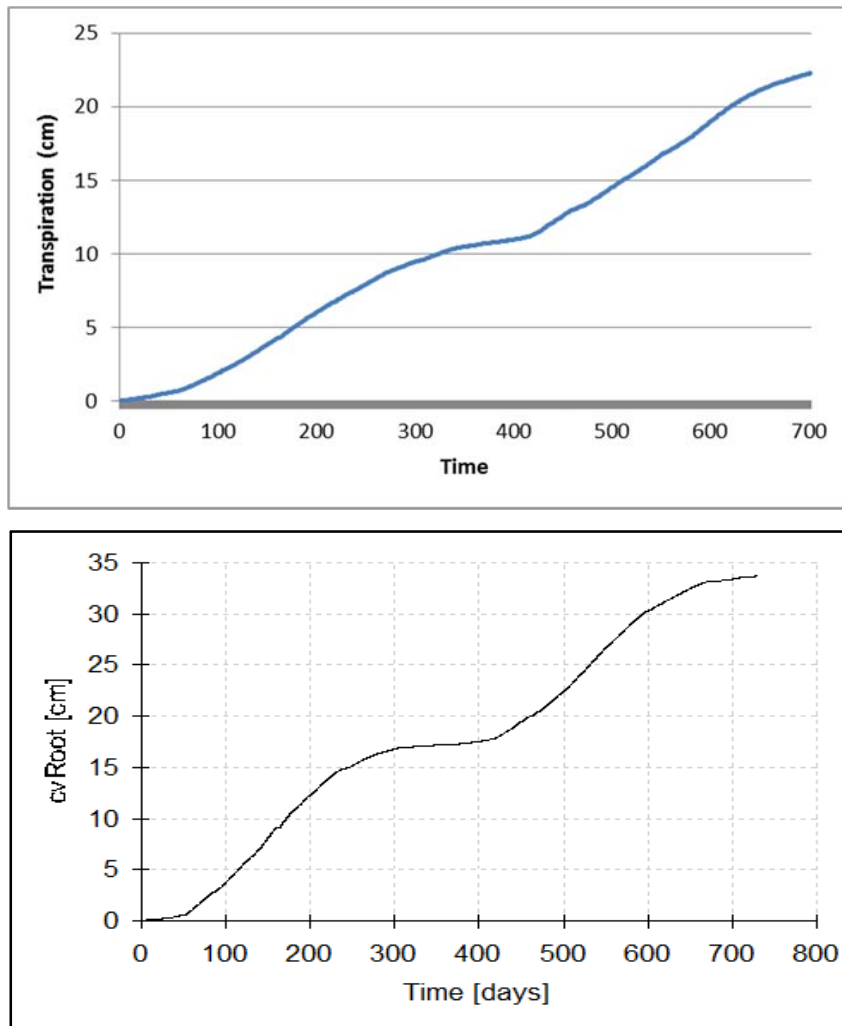


Figure 50. The cumulative measured (top) and simulated (bottom) root water uptake by *V. karroo* trees.

The difference between the rainfall (Figure 47) and the root water uptake (Figure 49 and Figure 50) during the simulation period already provides an indication that an alternative water source is being utilized to satisfy the water requirement of the *Prosopis* and *V. karroo* trees, i.e. groundwater. The magnitude of the difference between the rainfall and root water uptake suggests that minimal to no groundwater recharge occurs. This is in line with groundwater recharge estimates for the area, i.e.  $1 \text{ mm a}^{-1}$  (DWAF, 2006) and  $0.13 \text{ mm a}^{-1}$  (DWA, 2012). The simulated fluxes at the lower boundary of the soil profile is presented in Figure 51. These fluxes may either represent drainage/groundwater recharge (negative), root water uptake (positive), groundwater level rise (positive), capillary rise (positive), etc. From Figure 51 it is

evident that no negative fluxes occur and thus no vertical drainage/groundwater recharge occurred during the simulation period. The contrasting water use pattern of *Prosopis* and *V. karroo* trees is clearly evident in Figure 51.

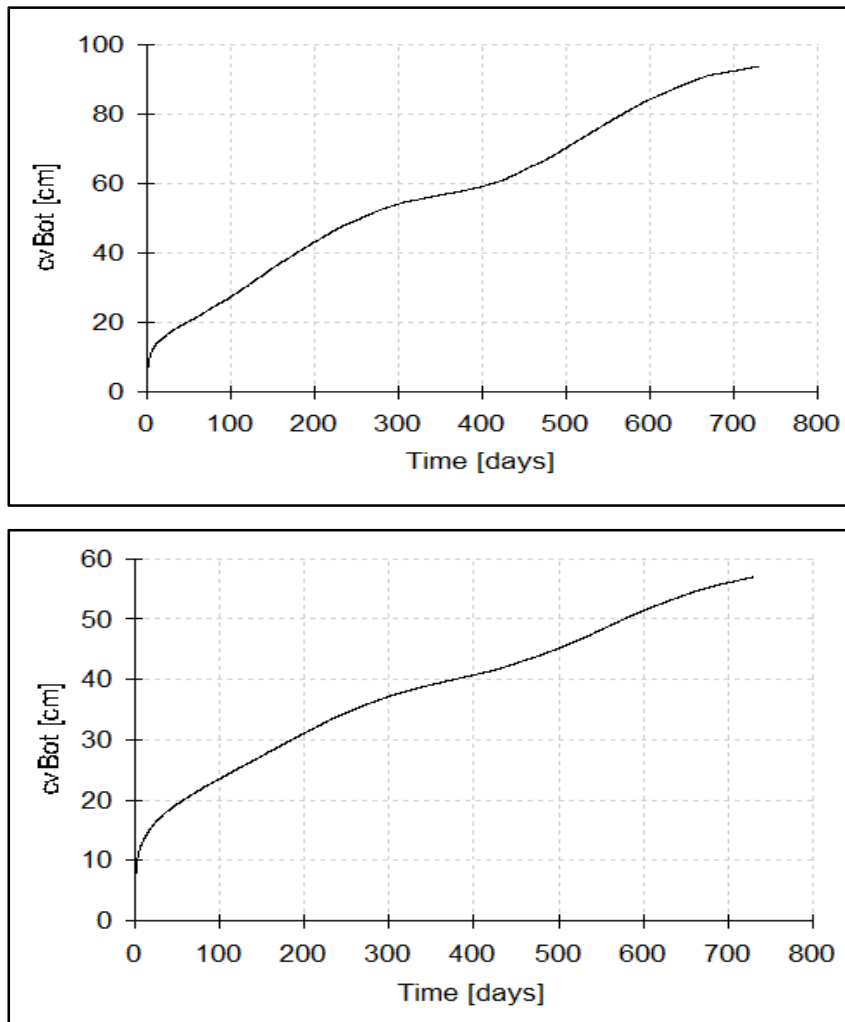


Figure 51. The HYDRUS-1D simulated cumulative fluxes observed at the lower boundary of the soil profile planted with *Prosopis* trees (top) and *V. karroo* trees (bottom)

HYDRUS-1D was able to replicate the soil water dynamics and water use patterns of *Prosopis* trees fairly well, while the simulation of root water uptake of *V. karroo* trees requires further improvement. The model showed that no vertical groundwater recharge occurred during the simulation period, which considered soil profiles planted with *Prosopis* trees and *V. karroo* trees. This is in line with recharge estimates available for the study area. Further validation for the simulation results is provided by the fact that the soil water content data collected during this study (Figure 48) shows

no evidence of a downward percolating wetting front, which may result in deep percolation and groundwater recharge.

It is therefore interpreted that the groundwater level fluctuations observed at the site (Figure 51) is not a result of downward percolation of precipitation, but rather a result of infiltration along the stream bed and the subsequent lateral migration of water across the site. Groundwater recharge processes like this are commonly observed in alluvial aquifer systems which occur along river courses. Flooding of the stream and the floodplain was observed during 2013 and 2014 which is a result of increased rainfall in the upstream parts of the catchment. The increased rainfall was not evident in the rainfall data records collected at the site. In 2013 the site was completely inundated with water. HYDRUS-1D is not able to account for this type of groundwater recharge process. Additionally, the tree water use data collected during this study suggests that the water uptake of *Prosopis* trees in particular exhibit fairly complicated behaviour which HYDRUS-1D is not able to represent, e.g. the phenomenon of hydraulic redistribution.

## 6 CONCLUSIONS

*Prosopis* invasions are a growing threat in many parts of the country and yet little information exists regarding their water requirements. This study sought to quantify the incremental water use by this invasive species over and above that used by the baseline indigenous vegetation and to establish the impacts on groundwater resources. This study revealed that *V. karroo* trees are equally likely to use as much or even more water than *Prosopis* at the individual tree scale. This observation is consistent with the findings from other studies (Dzikiti *et al.*, 2014; Cavalieri and Sack, 2010) where indigenous vegetation were reported to use large amounts of water.

The adverse impacts of *Prosopis* on groundwater arise from the ability of this species to form dense stands in the areas that they invade. Overall water use by *Prosopis* was more than three times higher than the rainfall received at the site. So to survive and thrive at this site the invasions were heavily dependent on groundwater. Water use by the indigenous *V. karroo* on the other hand was of the same order of magnitude as the rainfall although the species also used groundwater. Clearing one hectare of *Prosopis* at this site will potentially release at least 4.2 million litres of water per year. This amount of water is sufficient to irrigate one hectare of wheat or pasture which are the main economic activities in the Nieuwoudtville area. In contrast, *V. karroo* consumed a much smaller proportion of groundwater mainly because the trees were sparsely distributed across the site.

Groundwater levels showed pronounced seasonal oscillations characterized by periods of recharge and discharge. Clearly the trees were the main cause of groundwater abstraction and clearing the invasions led to an immediate reduction in the rate of decline of the groundwater level. However, direct recharge of the groundwater by rainfall was virtually non-existent because of the very low rainfall. Rather recharge, associated with base flows from the Doorn River whenever the river flowed appeared to be the main source of groundwater recharge.

Lastly, a promising multiple source ET model parameterized in an arid catchment was tested. This model still requires further testing beyond the current study area to establish its robustness.

## 7 RECOMMENDATIONS FOR FURTHER RESEARCH

The following are recommendations for future research:

### a) **Need for further monitoring post clearing**

In this study, monitoring of the recovery of groundwater levels following the clearing of *Prosopis* was done for a period of 11 months. To get a full understanding of the benefits of removing the invasions, a longer monitoring period covering a few seasons is needed. This will help improve our understanding of the drivers and factors that influence the actual volumes of water than can be recovered in practice.

### b) **Bush encroachment**

The fact that indigenous vegetation uses large quantities of water is a fact that is not often reported. On the other hand, bush encroachment by indigenous vegetation is fast becoming a problem in many parts of the country and yet little information exists to quantify its impact on the water resources. If individual *V. karroo* trees can use more water than *Prosopis*, for example, how much more water can dense stands of indigenous species use? What are the impacts on surface and groundwater resources? So the subject of bush encroachment in the context of groundwater preservation needs further research.

### c) **Clearing prioritization**

From an operational perspective, especially clearing of *Prosopis*, the results presented here suggest that clearing of the invasions should target areas with high densities of the invasions because the impacts on groundwater are greatest here. Alternatively, areas with low densities of the invasions, but with a high potential for being dense can also be targeted to prevent them from becoming fully established. The benefits of clearing *Prosopis* maybe small in areas where there are high densities of deep rooted indigenous trees like *V. karroo*.

### d) **Evaluation of ET model**

The remote sensing ET model has the potential to provide detailed information on the total evaporation and its partitioning between day and night and between various sources. However, more evaluations of the model are required in order to fully understand the advantages and limitations of using this product.

## 8 REFERENCES

- AHL, D.E., GOWER, S.T., MACKAY, D.S., BURROWS, S.N., NORMAN, J.M. and DIAK, G.R. 2005. The effects of aggregated land cover data on estimating NPP in northern Wisconsin, *Remote Sens. Environ.*, 97, 1-14, 2005.
- ALLEN, R.G., PEREIRA, L.S., RAES, D., SMITH, M. 1998. *Crop evapotranspiration*. FAO, irrigation and drainage paper 56. Rome.
- BARNES, R.D., FILER, D.L. and MILTON, S.J. 1996. *Acacia Karoo*. monograph and annotated bibliography. Tropical Forestry Papers 32. Oxford Forestry Institute, Oxford.
- BASTIAANSEN, W., WALTERS, R., ALLEN, R., TASUMI, M., TREZZA, R. 2002. *Surface energy balance algorithms for land – Advanced training and users' manual*. The Idaho Department of Water Resources, USA.
- BASTIAANSEN, W.G.M., CHEEMA, M.J.M., IMMERZEEL, W.W., MILTENBURG, I.J., PELGRUM, H. 2012. Surface energy balance and actual evapotranspiration of the transboundary Indus Basin from satellite measurements and the ETLook model. *Water Resour. Res.* 48, 1-16.
- BOSCH, J.M., HEWLETT, J.D. 1982. A review of catchment experiments to determine the effect of vegetation changes on water yield and evapotranspiration. *Journal of Hydrology* 55, 3-23.
- BREDENKAMP, D.B., BOTHA, L.J., VAN TONDER, G.J. and VAN RENSBURG, H.J. 1995. *Manual on the quantitative estimation of groundwater recharge and aquifer storativity*. WRC report no TT 73/95, Water Research Commission, Pretoria South Africa.
- BREDENKAMP, D.B., VANDOOOLAEGHE, M.A.C. 1982. *Die ontginbare grondwater potensiaal van die Atlantisgebied*, Department of Water Affairs and Forestry, Geohydrology, Technical Report No. Gh 3227, Pretoria, South Africa.
- BROMILOW, C. 2010. *Problem plants and alien weeds of South Africa*. Pretoria: Briza Publications.
- BRUTSAERT, W.H. 1975. On a derivable formula for long-wave radiation from clear skies, *Water Resour. Res.* 11, 742-744.
- BURGESS, S.O., ADAMS, M., TURNER, N., BEVERLY, C. 2001. An improved heat pulse method to measure low and reverse rates of sap flow in woody plants, *Tree Physiol.* 21, 589-598.
- BUSCH, D.E., INGRAHAM, N.L., SMITH, S.D. 1992. Water uptake in woody riparian phreatophytes of the South Western United States: a stable isotope study. *Ecological Applications* 2 (4), 450-459.

- CARRASCO, M., ORTEGA-FARIAS, S. 2007. Evaluation of a model to simulate net radiation over a vineyard cv. Cabernet sauvignon. *Chilean J. Agric. Res.* 68, 156-165.
- CAVALERI, M.A., SACK, L. 2010. Comparative water use of native and invasive plants at multiple scales: a global meta-analysis. *Ecology*. 91, 2705-2715.
- CHEW, M. 2009. The monsterring of Tamarisk: How scientists made a plant a problem. *J. Hist. Biol.* 42, 231-266.
- CHO, M.A., RAMOELO, A., MATHIEU, R. 2014. Estimation of leaf area index (LAI) of South Africa from MODIS imagery by inversion of PROSAILH radiative transfer model. 2014 IEEE International Geoscience and Remote Sensing Symposium (IGARSS), Quebec City, QC, Canada, 13-18 July 2014, pp 2590-2593.
- CLULOW, A.D., EVERSON, C.S., GUSH, M.B. 2011. The long-term impact of *Acacia mearnsii* trees on evaporation, stream flow, and ground water resources. Report No. TT 505/11, Water Research Commission, Pretoria.
- COLEMAN, M.L., SHEPHERD, T.J., DURHAM, J.J., ROUSE, J.E., MOORE, G.R. 1982. Reduction of Water with Zinc for Hydrogen isotope analysis. *Analytical Chemistry* 54, 993-995.
- CRAIG, H. 1961. Isotopic variations in meteoric waters. *Science*, 133: 1702-1703.
- DAWSON, T.E. 1993. Hydraulic lift and water use by plants: implications for water balance, performance and plant-plant interactions. *Oecologia* 95, 565-574.
- DAWSON, T.E., EHLERINGER, J.R. 1991. Streamside trees that do not use stream water. *Nature*. 350: 335-337.
- DAWSON, T.E., MAMBELLI, S., PLAMBOECK, A.H., TEMPLER, P.H., TU, K.P. 2002. Stable isotopes in plant ecology. *Annual Review of Ecology and Systematics* 33, 507-559.
- DEAN, W.R.J., ANDERSON, M.D., MILTON, S.J. and ANDERSON, T.A., 2002. Avian assemblages in native *Acacia* and alien *Prosopis* drainage line woodland in the Kalahari, South Africa. *Journal of Arid Environments* 51, 1-19.
- DOODY, T.M., NAGLER, P.L., GLENN, E.P., MOORE, G.W., MORINO, K., HUITINE, K.R., BENYON, R.G. 2011. Potential for water salvage by removal of non-native woody vegetation from dryland river systems. *Hydrol. Proc.* 25, 4117-4131.
- DWA. 2012. Olifants-Doorn WMA Classification Phase 3A – Groundwater Technical report, Department of Water Affairs, South Africa. Conrad J, Carstens, M, and Lasher C.
- DWAF. 2006. Groundwater Resource Assessment II – Task 3AE Recharge. Final Report Version 2. , Department of Water Affairs and Forestry, South Africa.

- DWAF. 2009. Water for growth and development in South Africa. Version 6. Department of Water Affairs and Forestry.
- DYE, P.J. 1996. Climate, forest and stream flow relationships in South African afforested catchments. *Comm. For. Rev.* 75, 31-38.
- DYE, P. 1996b. Response of *Eucalyptus grandis* trees to soil water deficits. *Tree Physiology* 16, 233-238.
- DYE, P., JARMAIN, C. 2004. Water use by black wattle (*Acacia mearnsii*): implications for the link between removal of invading trees and catchment streamflow response. *South African Journal of Science* 100, 40-44.
- DYE, P.J. and POULTER A.G. 1995. Field demonstrations of the effect on streamflow of clearing invasive pine and wattles trees from a riparian zone. *South African Forestry Journal* 173, 27-30.
- DZIKITI, S., GUSH, M.B., LE MAITRE, D.C., MAHERRY, A., JOVANOVIĆ, N.Z., RAMOELO, A., CHO, M.A. 2016. Quantifying potential water savings from clearing invasive alien *Eucalyptus camaldulensis* using in situ and high resolution remote sensing data in the Berg River Catchment, Western Cape, South Africa. *Forest Ecology and Management Journal*. 361, 69-80.
- DZIKITI, S., JOVANOVIĆ, N.Z., BUGAN, R., ISRAEL, S., LE MAITRE, D.C. 2014. Measurement and modelling of evapotranspiration in three fynbos vegetation types. *WaterSA*. 40, 189-198.
- DZIKITI, S., SCHACHTSCHNEIDER, K., NAIKEN, V., GUSH, M., LE MAITRE, D.C. 2013a. Comparison of water use by alien invasive pines growing in riparian and non-riparian zones in the Western Cape, South Africa. *For. Ecol. Man.* 293, 92-102.
- DZIKITI, S., SCHACHTSCHNEIDER, K., NAIKEN, V., GUSH, M., MOSES, G., LE MAITRE, D.C. 2013b. Water relations and the effects of clearing invasive *Prosopis* trees on groundwater in an arid environment in the Northern Cape, South Africa. *J. Arid. Environ.* 90, 103-113
- EFFENDI, I., 2012. Evapotranspiration in dry climate area: Comparing remote sensing techniques with unsaturated zone water flow simulation. Unpublished MSc dissertation, University of Twente, the Netherlands.
- EVANS, R.D., EHLERINGER, J.R. 1992. Water and nitrogen dynamics in an arid woodland. *Oecologia* 99, 233-242.
- FEBRUARY, E.C., HIGGINS, S.I., NEWTON, R., WEST, A.G. 2007(a). Tree distribution on a steep environmental gradient in an arid savanna. *Journal of Biogeography* 34, 270-278.

- FEBRUARY, E.C., WEST, A.G., NEWTON, R. 2007(b). The relationship between rainfall, water source and growth for an endangered tree. *Austral Ecology* 32 (4), 397-402.
- FEDDES, R.A., KOWALIK, P.J., ZARADNY, H. 1978. Simulation of field water use and crop yield. Pudoc, Centre Agric. Publ. Doc., Wageningen
- FISHER, J.B., TU, K.P., BALDOCCHI, D.D. 2008. Global estimates of the land-atmosphere water flux based on monthly AVHRR and ISLSCP-II data, validated at 16 FLUXNET sites. *Remote Sens. Environ.* 112, 901-919.
- FOURIE, F., MBATHA, K., VERSTER, H., VAN DYK, G. 2007. The effect of vegetation (*Prosopis* Sp) on groundwater levels in Rugseer river, Kenhardt, South Africa. Department of Water Affairs, South Africa.
- GARCIA, M., SANDHOLT, I., CECCATO, P., RIDLER, M., MOUGIN, E., KERGOAT, L., MORILLAS, L., TIMOUK, F., FENSHOLT, R., DOMINGO, F. 2013. Actual evapotranspiration in drylands derived from in situ and satellite data: Assessing biophysical constraints. *Remote Sens. Environ.* 131, 103-118.
- GAT, J.R. 1996. Oxygen and hydrogen isotopes in the hydrologic cycle. *Annual Review of Earth and Planetary Sciences* 24, 225-262.
- GUSH, M.B., MAPETO, T., DYE, P.J., NAIKEN, V. and GELDENHUYS, C.J., in press. Southern Cape Afrotropical tree species and *Pinus radiata* plantation at Saasveld. In: Gush, M.B. and Dye, P.J. (Eds). 2015. *Water Use and Socio-Economic Benefit of the Biomass of Indigenous Trees: Volume 2 (Site Specific Technical Report)*. WRC Report No 1876/2/15, Section 6. Water Research Commission, Pretoria, RSA.
- HARDING, G.B. 1987. The status of *Prosopis* as a weed. *Appl. Plant Sci.* 1, 43-48.
- HART, C.R., WHITE, L.D., MCDONALD, A., SHENG, Z.P. 2005. Saltcedar control and water salvage on the Pecos river, Texas, 1999-2003. *Jour. Environ. Man.* 75, 399-409.
- HAYS, K.B. 2003. Water use by salt cedar (*Tamarix* sp.) and associated vegetation on the Canadian Colorado and Pecos rivers in Texas. MS Thesis, Texas A&M University, College Station, TX.
- IMPENS, I., LEMEURE, R. 1969. Extinction of net radiation in different crop canopies. *Archiv fur Meteorologie, Geophysik und Bioklimatologie Serie B*, 17, 403-412.
- JACKSON, R.B., CANADELL, J., EHLERINGER, J.R., MOONEY, H.A., SALA, O.E., SCHULZE D.E. 1996. A global analysis of root distributions for terrestrial biomes. *Oecologia*, 108, 389-411.
- JARVIS, P.G. 1976. The interpretation of the variations in leaf water potential and stomatal conductance found in canopies in the field. *Phil. R. Trans. Soc. Lond. B* 273, 593-610

- LE MAITRE, D.C. 1999. *Prosopis* and groundwater: a literature review and bibliography. Report Number ENV-S-C 99077, Natural Resources and the Environment, CSIR, prepared for the Working for Water Programme, Department of Water Affairs and Forestry.
- LE MAITRE, D.C., GUSH, M.B., DZIKITI, S. 2015. Impacts of invading alien plant species on water flows at stand and catchment scales. AoB plants – early view DOI: 10.1093/aobpla/plv043
- LE MAITRE, D.C., FORSYTH, G.G., DZIKITI, S., GUSH, M.B. 2013. Estimates of the impacts invasive alien plants on water flows in South Africa. Report No CSR/NRE/ECO/ER/2013/006/B, Natural Resources and Environment, CSIR, Stellenbosch.
- LE MAITRE, D.C., VERSFELD, D.B. and CHAPMAN, R.A. 2000. The impact of invading alien plants on surface water resources in South Africa: a preliminary assessment. *Water SA* 26, 397-408.
- LIANG, S. 2000. "Narrowband to broadband conversions of land surface albedo I algorithms." *Remote Sensing of Environment* 76, 213-238.
- MARSHALL, M., TU, K., FUNK, C., MICHAELSEN, J., WILLIAMS, P., WILLIAMS, C., ARDO, J., BOUCHER, M., CAPPELLAERE, B., DE GRANDCOURT, A., NICKLESS, A., NOUVELLON, Y., SCHOLES, R., KUTSCH, W. 2013. Improving operational land surface model canopy evapotranspiration in Africa using a direct remote sensing approach. *Hydrol. Earth Syst. Sci.* 17, 1079-1091
- MCDONALD, A.K. 2010. Hydrologic impacts of saltcedar control along a regulated dry land river. PhD dissertation, Texas A&M University, College station, TX.
- MIDDLETON, B.J., BAILEY, A.K. 2008. Water resources of South Africa, 2005 study (WR2005): User's Guide (Version 1). WRC Report no. TT 381/08, Water Research Commission, Pretoria.
- MU, Q., HEINSCH, A.F., ZHAO, M., RUNNING, S.W. 2007. Development of a global evapotranspiration algorithm based on MODIS and global meteorology data. *Remote Sens. Environ.* 111, 519-536.
- MU, Q., ZHAO, M., RUNNING, S.W., 2011. Improvement to a MODIS global terrestrial evapotranspiration algorithm. *Remote Sens. Environ.* 115, 1781-1800.
- MUCINA, L., RUTHERFORD, M.C., 2006. The vegetation of South Africa, Lesotho and Swaziland. *Strelizia* 19. SANBI, Pretoria.
- NTSHIDI, Z., DZIKITI, S., MAZVIMAVI, D., BUGAN, R.B.H, LE MAITRE, D.C, GUSH, M.B., JOVANOVIĆ, N.Z. 2015. Comparative use of groundwater by invasive alien *Prosopis* spp and co-occurring indigenous *V. karroo* in a semi-arid catchment. Conference Proceedings: Paper presented at the 14th Biennial Ground Water Division Conference and Exhibition, 21-23 September 2015, Muldersdrift, South Africa.

- O'FARRELL, P.J., DONALDSON, J.S., HOFFMAN M.T. 2009. Local benefits of retaining natural vegetation for soil retention and hydrological services. *South African Journal of Botany* 75, 573-583.
- O'FARRELL, P.J., DONALDSON, J.S., HOFFMAN, M.T. 2007. The influence of ecosystem goods and services on livestock management practices on the Bokkeveld plateau, South Africa. *Agriculture, Ecosystems and Environment* 122, 312-324
- PARSONS, R., WENTZEL, J. 2007. Groundwater resource directed measures manual. WRC report no TT 299/07, Water Research Commission, Pretoria.
- PRINSLOO, F.W., SCOTT, D.F. 1999. Stream flow responses to the clearing of alien invasive trees from riparian zones at three sites in the Western Cape Province. *S. Afric. For. J.* 185, 1-7.
- RAMOELO, A., MAJOZI, N., MATHIEU, R., JOVANOVIC, N.Z., NICKLES, A., DZIKITI, S. 2014. Validation of global evapotranspiration product (MOD16) using flux tower data in the African Savanna, South Africa. *Remote Sen.* 8, 7406-7423.
- SCANLON, B.R., HEALY, R.W., COOK, P.G. 2002. Choosing appropriate techniques for quantifying groundwater recharge. *Hydrogeology Journal*, 10, pp. 18-39.
- SCHACHTSCHNEIDER, K., FEBRUARY, E.C. 2010. Water Sources for trees along the ephemeral Kuiseb River in Namibia differ for species and age groups, *Journal for Arid Environments*, 74: 1632-1637.
- SCHACHTSCHNEIDER, K., FEBRUARY, E. 2013. Impact of *Prosopis* invasion on a keystone species in the Kalahari Desert. *Plant Ecology* 214: 597-605.
- SCHULZE, R.E., MAHARAJ, M., WARBURTON, M.L., GERS, C.J., HORAN, M.J.C., KUNZ, R.P. and CLARK, D.J. 2008. South African Atlas of Climatology and Agrohydrology. WRC Report no. 1489/1/08, Water Research Commission, Pretoria.
- SCHWINNING, S., EHLERINGER, J.R. 2001. Water use trade-offs and optimal adaptations to pulse-driven arid ecosystems. *Journal of Ecology* 89, 464-480.
- SCOTT, D.F. 1999. Managing riparian zone vegetation to sustain streamflow: results of paired catchment experiments in South Africa. *Canadian Journal of Forest Research* 29, 1149-1157.
- ŠIMŮNEK, J., ŠEJNA, M., SAITO, H., SAKAI, M., and VAN GENUCHTEN, M. TH. 2013. The HYDRUS-1D Software Package for Simulating the One-Dimensional Movement of Water, Heat, and Multiple Solutes in Variably-Saturated Media. HYDRUS-1D vs 4.17. Dept. of Environmental Science, Univ. of California
- SNYDER, K.A., WILLIAMS, D.G. 2000. Water sources used by riparian trees varies among stream types on the San Pedro River, Arizona. *Agric. For. Meteorol.* 105, 227-240.

- SOCKI, R.A., KARLSSON, H.R., GIBSON, E.K. 1992. Extraction technique for the determination of Oxygen-18 in water using pre-evacuated glass vials. *Analytical Chemistry* 64, 829-831.
- STEENKAMP, H.E., CHOWN, S.L. 1996. Influence of dense stands of an exotic tree, *Prosopis glandulosa* Benson, on a Savanna dung beetle (Coleoptera: scarabaeinae) assemblage in southern Africa. *Biological Conservation* 78, 305-311.
- SWANSON, R.H., WHITFIELD, D.W.A. 1981. A numerical analysis of heat pulse velocity theory and practice. *J. Exp. Bot.* 32, 221-239.
- TITUS, R., ADAMS, S. and XU, Y. 2002. Groundwater situation assessment in Olifants Doorn Water Management Area (Version 1.0). Final draft prepared for Danced project of Department of Water Affairs and Forestry. Groundwater Group, Department of Earth Sciences, University of the Western Cape, South Africa.
- TURNER, D.P., RITTS, W.D., COHEN, W.B., MAIERSPERGER, T.K., GOWER, S.T., KIRSCHBAUM, A.A., RUNNING, S.W., ZHOA, M., WOFSY, S.C., DUNN, A.L., LAW, B.E., CAMPBELL, J.L., OECHEL, W.C., KWON, H.J., MEYERS, T.P., SMALL, E.E., KURC, S.A. and GAMON, J. A. 2005. Site-level evaluation of satellite based global terrestrial gross primary production and net primary production monitoring, *Glob. Change Biol.* 11, 666-684, doi:10.1111/j.1365-2486.2005.00936.
- VAN DEN BERG, E.C. 2010. Detection, quantification and monitoring *Prosopis* spp. in the Northern Cape Province of South Africa using Remote Sensing and GIS. Masters Dissertation, North-West University, Potchefstroom.
- VEGTER, J.R. 1995. An Explanation of a Set of National Groundwater Maps, Water Research Commission, Report No. TT74/95, Pretoria, South Africa.
- VILÀ, M., ESPINAR, J.L., HEJDA, M. 2011. Ecological impacts of invasive alien plants: a meta-analysis of their effects on species, communities and ecosystems. *Ecology Letters* 14, 702-708.
- WHITE, J.W.C, COOK, E.R., LAWRENCE, J.R., BROECKER, W.S. 1985. The d/h ratios of sap in trees: implications for water sources and tree ring d/H ratios. *Geochimica Cosmochimica Acta* 49, 237-246.
- WISE, R.M., VAN WILGEN, B.W. and LE MAITRE, D.C. 2012. Costs, benefits and management options for an invasive alien tree species: The case of mesquite in the Northern Cape, South Africa. *Journal of Arid Environments* 84, 80-90.
- WOODFORD, A.C. 2007. Preliminary assessment of supplying Eskom's Ankerlig power station with water from local groundwater resources, SRK Consulting, Report No. 374624, Cape Town, South Africa.
- XU, Y., BEEKMAN, H.E. 2003. Groundwater recharge estimation in Southern Africa. UNESCO IHP Series No. 64, UNESCO Paris, Cape Town.

YUAN, W., LIU, S., YU, G., BONNEFOND, J., CHEN, J., DAVIS, K., DESAI, A., GOLDSTEIN, A.H., GIANELLE, D., ROSSI, F., SUYKER, A.E., VERMA, S. 2010. Global estimates of evapotranspiration and gross primary production based on MODIS and global meteorology data. *Remote Sens. Environ.* 114, 1416-1431.

ZAGANA, E., KUELLS, C., UDLUFT, P., CONSTANTINO, C. 2007. Methods of groundwater recharge estimation in eastern Mediterranean – a water balance model application in Greece, Cyprus and Jordan. *Hydrological Processes*, 21, 2405-2414.

ZHANG, H., SIMMONDS, L.P., MORISON, J.I.L., PAYNE, D. 1997. Estimation of transpiration by single trees: comparison of sap flow measurements with a combination equation. *Agric. For. Meteorol.* 87, 155-169.

## **DATA STORAGE**

All the data generated in this study are safely stored at:

CSIR, Natural Resources and Environment

11 Jan Cilliers Street

Stellenbosch

7600

South Africa

## APPENDIX A. CAPACITY BUILDING AND TECHNOLOGY EXCHANGE

### STUDENTS TRAINING

Three students were trained in the project. These include:

- 1) Ms Zanele Ntshidi who completed an MSc in Environmental Science at the University of Western Cape in September 2015;

Thesis title: A comparative assessment of the quantity and sources of water used by alien invasive *Prosopis* spp and indigenous *Acacia* karroo in the Northern Cape Province

- 2) Mr Lumko Ncapai did his Honours degree project in Environmental Science at the University of Western Cape.

Project title: Estimating evapotranspiration from groundwater level information at a *Prosopis* invaded site in Niewoudtville, Northern Cape

- 3) Miss Yonela Mkunyané also completed her Honours degree project in Environmental Science at the University of Western Cape.

Project title: Estimating water savings by clearing invasive alien plants at a site dominated by *Prosopis* spp and deep rooted indigenous trees

### PUBLICATIONS

The following publications were produced in this project:

#### Peer reviewed journal articles

- a) **Dzikiti S.**, Ntshidi Z., Le Maitre DC., Bagan RDH., Mazvimavi D., Schachtschneider K., Jovanovic NZ., Pienaar HH. 2017. Assessing water use by *Prosopis* invasions and *Vachellia* karroo trees: Implications for groundwater recovery following alien plant removal in an arid catchment in South Africa. **Forest Ecology and Management. 398, 153 -163**

### **Non-peer reviewed publications**

- a) Van Vuuren L (2015). Do invasive alien plants really use more water? Study investigates. *WaterWheel*. Jan/Feb 2015, 14 (1).
- b) Mahomed R., Dziki S. (2015). Groundwater dependent alien invasive species. *Quest*. 11 (5) 16-19.

### **Conference proceedings**

- a) Ntshidi, Z., Dziki S., Mazvimavi, D., Bugan R.D.H., Le Maitre D.C., Jovanovic N.Z. (2015). Comparative use of groundwater by invasive alien *Prosopis* spp and co-occurring indigenous *V. karroo* in a semi-arid catchment. Conference Proceedings: Paper presented at the 14th Biennial Ground Water Division Conference and Exhibition, 21-23 September 2015, Muldersdrift, South Africa.
- b) Ntshidi, Z (2015). A comparative assessment of the quantity and sources of water used by alien invasive *Prosopis* spp and indigenous *Vachellia Karoo* in the Northern Cape Province. MSc thesis, University of Western Cape.

## **PRESENTATIONS**

Presentations made as part of this project can be summarized as follows:

- a) **17<sup>th</sup> SANCIAHS National Hydrology Symposium, held at the University of Western Cape from 01-03 September 2014 (oral)**

**Title:** Comparison of water use by deep rooted alien invasive *Prosopis* and indigenous *Acacia Karroo* trees in the Northern Cape Province.  
Z. Ntshidi\*, S. Dziki, R. Bugan, DC Le Maitre, N. Jovanovic, D Mazvimavi

- b) **14<sup>th</sup> Biennial Groundwater Conference: From Theory to Action (GWD), held from 21-23 September 2015 in Muldersdrift, South Africa (oral)**

**Title:** Comparative use of groundwater by invasive alien *Prosopis* spp and co-occurring indigenous *V. karroo* in a semi-arid catchment

Z. Ntshidi\*, S. Dzikiti, D. Mazvimavi, R. D. H. Bugan, D. C. Le Maitre, N. Jovanovic, M. B. Gush

**c) National Management, Research and Planning Forum 2015 of the Department of Environmental Affairs, held from 13 to 15 October 2015 at False Bay Nature Reserve, Zeekoevlei, Cape Town (invited presentation)**

**Title:** Impact of *Prosopis* on groundwater

**S Dzikiti\***, RDH Bugan., DC Le Maitre., Z Ntshidi., NZ Jovanovic

## **APPENDIX B. RESISTIVITY INTERPRETATION: BRANDKOP, NIEUWOUDTVILLE**

Prepared by Louise Soltau: GEOSS – Geohydrological and Spatial Solutions

### **A1. INTRODUCTION**

The CSIR approached GEOSS – Geohydrological and Spatial Solutions International (Pty) Ltd to analyse and interpret resistivity data that were acquired at Brandkop farm near Nieuwoudtville in the Northern Cape. The objective of the resistivity survey was to delineate the depth to the groundwater table.

### **A2. GEOLOGICAL SETTING**

From the geological log of the borehole drilled near the resistivity profiles, it is clear that the area is underlain by shale of the Malmesbury Group.

### **A3. FIELD WORK**

Resistivity is a non-invasive geophysical tool that can provide cost-effective solutions to geological questions. The bulk resistivity of different geological units varies mostly because of changes in either water saturation, salinity of the pore fluid or changes in porosity (Telford et al., 1990). The resistivity tomography method was used for delineating the drilling positions. The Lund imaging system is a completely automated resistivity tomography data acquisition system. The resistivity tomography method provides a pseudo-section of change in electrical properties in the subsurface along a specified profile line. Two multi-core cables with 32 electrode take-outs every 2 m were used. These cables were laid out on the ground end to end in a straight line (where possible). An electrode (metal stake) is inserted into the ground next to every electrode take-out on the cable. The electrode take-out is then connected to the electrode with a short cable jumper. The multi core cables are connected to the ABEM electrode selector ES464 that controls the measurement sequence. The electrode selector is connected to the ABEM Terrameter SAS1000 that takes the apparent resistivity measurements. The data were collected using a standard protocol with the Wenner array. All data were acquired for  $n = 1$  to 8 and 10, 12, 14 and 16 where “n” is the electrode separation multiplication factor.

The apparent resistivity data acquired in the field were inverted using the RES2DINV software (Loke and Barker, 1996) to provide a true-depth resistivity section. The only pre-processing done was to erase obviously erratic data points (minimal). The elevation along

the profiles and very flat and no elevation corrections were applied. The resulting true resistivity pseudo-sections are used for the interpretation.

#### A4. RESULTS AND DISCUSSION

The resistivity data were acquired along 2 profile lines at Brandkop. The location of these profile lines was overlain on a Google Earth image for the area in Map A1. The borehole is also indicated (Bh).



Map A1. Google earth image of the Brandkop site with the location of the resistivity profiles and borehole overlain.

The inverted resistivity data for profile line BK001 is shown in Figure 1. The resistivity profile shows a shallow (0-2.0 m) low resistivity (<10 ohm.m) layer, which is underlain by an intermittent layer, varying in thickness from absent to 6 m with relatively high resistivity (>50 ohm.m). This in turn is underlain by an extensive, intermediate resistivity layer (10-50 ohm.m) with a thickness of 5-10 m. This is underlain by another relatively high resistivity layer up to depth. There is good correlation with the borehole log; the image of the log has been rescaled to the depth scale of the resistivity image and added to the resistivity profile in Figure 1. The borehole log indicates alluvial material, consisting of coarse brown sand with boulder chips, up to a depth of about 5 m and this correlates with the upper higher resistivity layer. The low resistivity shallow layer is likely indicative of water saturated (it did rain shortly

before the acquisition of the resistivity profile) or clay rich alluvial material. The alluvial material is underlain by clay (weathered shale), which correlates with the intermediate resistivity layer. The bedrock shale then correlates with the higher resistivity at depth. §BK stands for **Brandkop** – just a descriptor for the profile lines.

The groundwater level was at 8.19 m at the time of the acquisition of the resistivity profile. The approximate water level is indicated on the small log with an “upside down triangle”. The water level occurs within the clay sediments underlying the alluvium and overlying bedrock. It is important to note that the resolution is not sufficient to define the water table exactly. This can be the result of a number of factors or a combination of some of these:

- The clay layer forms a confining layer and the aquifer is thus confined – the resistivity method cannot delineate piezometric surfaces, only water table surfaces.
- The difference in resistivity between the overlying clay layer and the water saturated clay and boulder chips is not significant enough to be able to define the groundwater surface accurately.
- The resolution at this depth is not sufficient to define the water table surface accurately.

The inverted resistivity data for profile line BK002 is shown in Figure 2. The resistivity distribution along this profile is similar to that of profile BK001, with a more extensive shallow (0-2.0 m) low resistivity (<10 ohm.m) layer. The higher resistivity layer corresponding to the alluvial material occurs mostly along the south-eastern half of the profile. The underlying lower resistivity layer corresponding to the clay layer is extensive; and this is underlain by the higher resistivity bedrock layer. A bedrock high occurs to the northwest at depth.

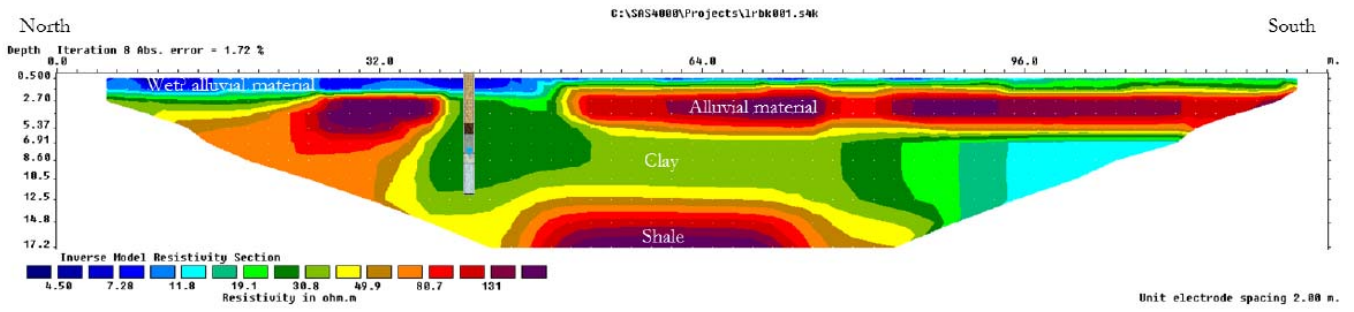


Figure 1: Inverted resistivity data profile: BK001, showing drilling log and water level.

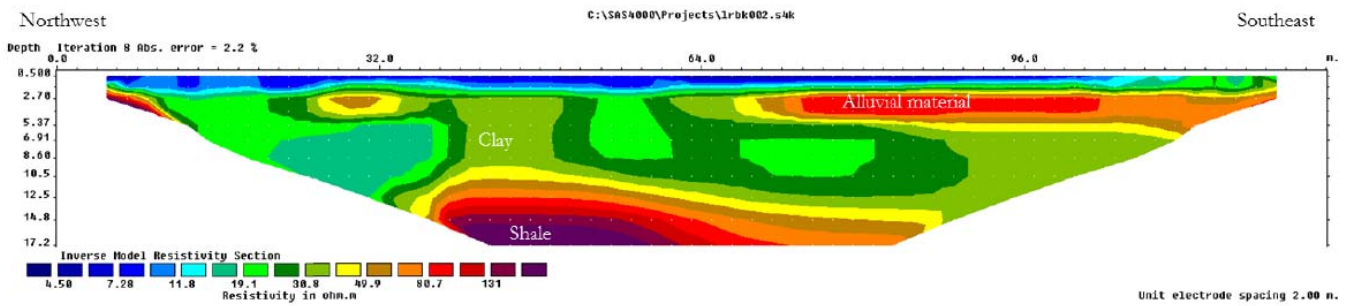
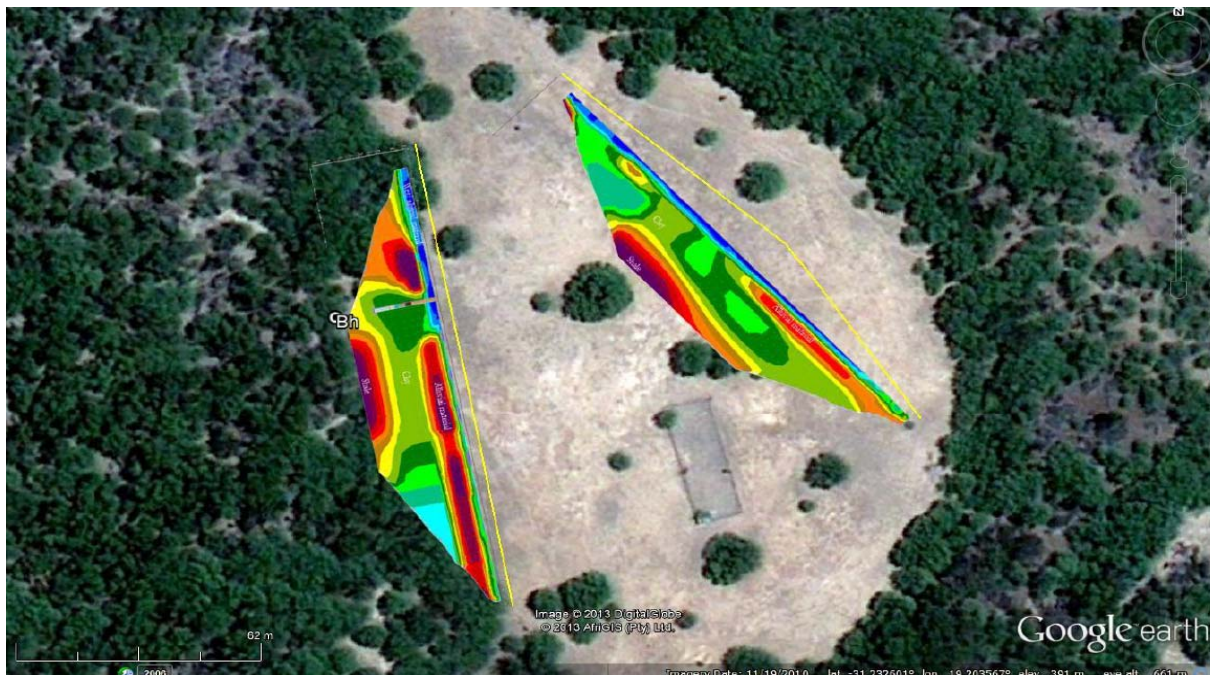


Figure 2: Inverted resistivity data profile: BK002

The inverted resistivity profiles have been overlain on the Google Earth image in Map A2. The image shows the intermittent alluvial cover. It should be noted that this could also indicate a change in the character of the alluvium, for example, more clay rich in areas of lower resistivity. There is also no clear indication of water level on either of the two profiles.



Map A2. Google earth image with resistivity profiles overlain.

## **A5. CONCLUSIONS AND RECOMMENDATIONS**

Resistivity data were acquired along 2 short profiles (128 m) at Brandkop near Nieuwoudtville in the Northern Cape, with the aim of delineating the water table. However, the water table is not indicated by a clear interface and this can be for a number of reasons or a combination of them:

- The clay layer forms a confining layer and the aquifer is thus confined – the resistivity method cannot delineate piezometric surfaces, only water table surfaces.
- The difference in resistivity between the overlying clay layer and the water saturated clay and boulder chips is not significant enough to be able to define the groundwater surface accurately.
- The resolution at this depth is not sufficient to define the water table surface accurately.

The resolution at depth can potentially be improved by using a smaller spacing between the electrodes (for example 1 m). However, the depth of investigation will be much less and the bedrock will not be visible on the resistivity profile. Also, the water level might then still not be visible.

## **A6. REFERENCES**

Loke M.H. and Barker R.D., 1996. Rapid least-squares inversion of apparent resistivity pseudo-sections by a quasi-Newton method. *Geophysical Prospecting*, Volume 44, Issue 1, pp 131-152.

Telford W.M., Geldart L.P. and Sheriff R.E., 1990. *Applied Geophysics: Second Edition*. Cambridge University Press.

## APPENDIX C. BOREHOLE LOGS.

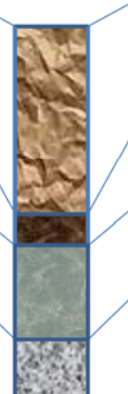
### Key

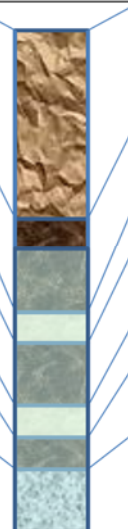
BK001 – Borehole 1

BK002 – Borehole 2

BK003 – Borehole 3

Well ID	Well Log: Lithology and Construction						
	Brandkop (Nieuwoudtville)						
Drilling method:	Rotary Percussion			Contract No.			
Coordinate	X	19.20288		Scale	H	20	
	Y	-31.23257			V	200	
Surface Elevation (m)	390.5			Diameter (mm)	160		
Well depth (m)	12.5			Commencing date	20130801		
Casing depth (m)	11			Ending date	20130801		
Layer No.	Strata	Thick (m)	Elev. (m)	Depth (m)	Column map	Lithology	Remark
1	Q	8	382.5	8		Fine to medium brown sand. Some clay observed	Quaternary deposits
2	Q	1	381.5	9		Fine sand with boulder chips.	Water strike
3	Sn	3	378.5	12		Grey/blue Shale	Medium fragments

Well ID	BK002	Well Log: Lithology and Construction					
		Brandkop (Nieuwoudtville)					
Drilling method:		Rotary Percussion			Contract No.		
Coordinate		X	19.19961		Scale	H	20
		Y	-31.23057			V	200
Surface Elevation (m)		389			Diameter (mm)		160
Well depth (m)		12			Commencing date		20141008
Casing depth (m)		10			Ending date		20141008
Layer No.	Strata	Thick (m)	Elev. (m)	Depth (m)	Column map	Lithology	Remark
1	Q	6	383	6		Light to dark brown fine sand	Quaternary deposits
2	Q	1	382	7		Coarse sand with boulder chips (fine to medium)	
3	Q	3	379	10		Coarse sand with large boulder chips	Water strike
4	Sn	2	377	12		Grey/blue Shale	Fine to medium fragments

Well ID	BK003	Well Log: Lithology and Construction					
		Brandkop (Nieuwoudtville)					
Drilling method:		Rotary Percussion			Contract No.		
Coordinate		X	19.2063		Scale	H	20
		Y	-31.23172			V	200
Surface Elevation (m)		387			Diameter (mm)		160
Well depth (m)		16			Commencing date		20141008
Casing depth (m)		16			Ending date		20141008
Layer No.	Strata	Thick (m)	Elev. (m)	Depth (m)	Column map	Lithology	Remark
1	Q	6	381	6		Light brown fine sand	Quaternary deposits
2	Q	3	378	9		Coarse sand with boulder chips	Water strike
3	Q	1	377	10		Clay	
4	Q	2	375	12		Gravel (very coarse boulder fragments)	Water strike
5	Q	1	374	13		Clay	
6	Q	1	373	14		Gravel (medium boulder fragments)	Water strike
7	Sn	2	371	16		Grey/blue Shale	Fine to medium fragments